General Disclaimer

One or more of the Following Statements may affect this Document

- This document has been reproduced from the best copy furnished by the organizational source. It is being released in the interest of making available as much information as possible.

- This document may contain data, which exceeds the sheet parameters. It was furnished in this condition by the organizational source and is the best copy available.

- This document may contain tone-on-tone or color graphs, charts and/or pictures, which have been reproduced in black and white.

- This document is paginated as submitted by the original source.

- Portions of this document are not fully legible due to the historical nature of some of the material. However, it is the best reproduction available from the original submission.

X-481-71-108
PREPRINT

NASA TM X- 63490

ATTITUDE-CONTROL PERFORMANCE OF THE IMPROVED TELEVISION INFRARED OBSERVATION SATELLITE (ITOS 1)

MARCH 1971

GSFC

GODDARD SPACE FLIGHT CENTER
GREENBELT, MARYLAND

ATTITUDE-CONTROL PERFORMANCE OF THE IMPROVED TELEVISION INFRARED OBSERVATION SATELLITE (ITOS 1)

William M. Peacock
TOS Project

March 1971

GODDARD SPACE FLIGHT CENTER
Greenbelt, Maryland

ATTITUDE-CONTROL PERFORMANCE OF THE IMPROVED TELEVISION INFRARED OBSERVATION SATELLITE (ITOS 1)

William M. Peacock
TOS Project

ABSTRACT

The National Aeronautics and Space Administration (NASA), Goddard Space Flight Center (GSFC) has deployed a new-generation meteorological satellite called Improved Television Infrared Observation Satellite (ITOS 1) on an operational basis. A single ITOS 1 performs the functions of two TOS's (TOS/AVCS and TOS/APT), and carries secondary sensors and experiments as required. The dynamic and attitude-control subsystem incorporates many similar principles and much of the same hardware as the TOS satellite, although the satellite configuration is entirely different. A single rotating flywheel provides the gyroscopic stability and the required momentum interchange to keep one side of the satellite facing the earth. Magnetic torquing against the earth's magnetic field eliminates the requirement for expendable propellants which would limit satellite life in orbit.

CONTENTS

ILLUSTRATIONS

ILLUSTRATIONS (continued)

ILLUSTRATIONS (continued)

TABLES

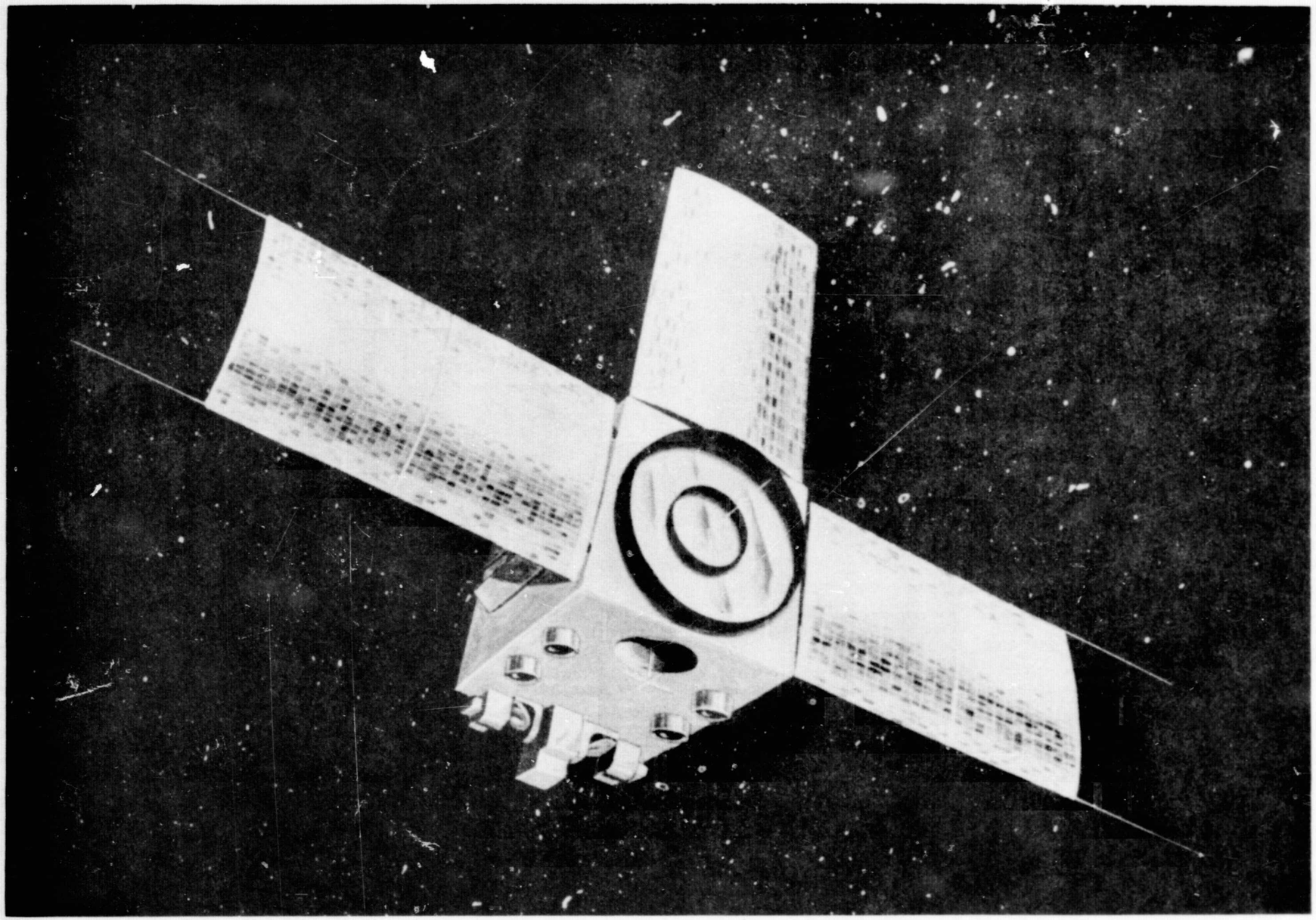

Frontispiece—Artist's Conception of ITOS

ATTITUDE-CONTROL PERFORMANCE OF THE IMPROVED TELEVISION INFRARED OBSERVATION SATELLITE (ITOS 1)

INTRODUCTION

ITOS 1 is a research and development flight-prototype satellite that evolved from the Television and Infrared Observational Satellite (TIROS). The ITOS satellite differs markedly in appearance from the TOS satellite. Figure 1 is a comparison of the TOS and ITOS configurations. To compare weather coverage of the two satellites, TOS provides only daytime coverage of the entire earth and its cloudcover; ITOS provides day and night coverage of the entire earth and its cloudcover. ITOS also measures the amount of heat radiated into space by the earth, and the earth's proton and electron environment.

ITOS 1, weighing 682 pounds, was launched from the Air Force Western Test Range (AFWTR) at Vandenberg Air Force Base, California, on January 23, 1970, and has successfully provided thousands of high-quality daytime and nighttime pictures of the earth, sea, and cloudtops.

ITOS 1 is a dual-spin satellite which exhibits dynamic characteristics between those of the single-spin satellite (early TIROS) and the three axes control satellites (Orbiting Geophysical Observatory (OGO), Orbiting Astronomical Observatory (OAO), etc.). ITOS 1 has performed excellently.

On June 15, 1970, NASA turned over control of ITOS 1 to the National Oceanic and Atmospheric Administration (NOAA), formerly ESSA, for operational use.

Figure 2 shows the primary axes of the satellite. Figure 3 shows the geometry of the sun-synchronous orbit. A list of the nominal orbital parameters before launch and the parameters obtained after launch on January 24, 1970, and July 29, 1970, follows:

- Nominal orbital elements for ITOS 1

Semimajor axis	007840.40 km
Eccentricity	0.00023
Inclination	101.739 degrees
Mean anomaly	291.047 degrees
Argument of perigee	068.262 degrees
Motion minus	01.9182 degrees per day
Right ascension of ascending node	339.615 degrees
Motion plus	00.9842 degree per day

TOS

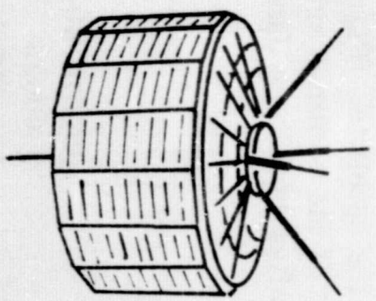

	TOS/AVSS	TOS/APT
FLIGHT WEIGHT	≃347 lb	≃299 lb

NOTE: THE DYNAMICS FOR TOS/AVCS AND TOS/APT IS THE SAME.

ITOS-1

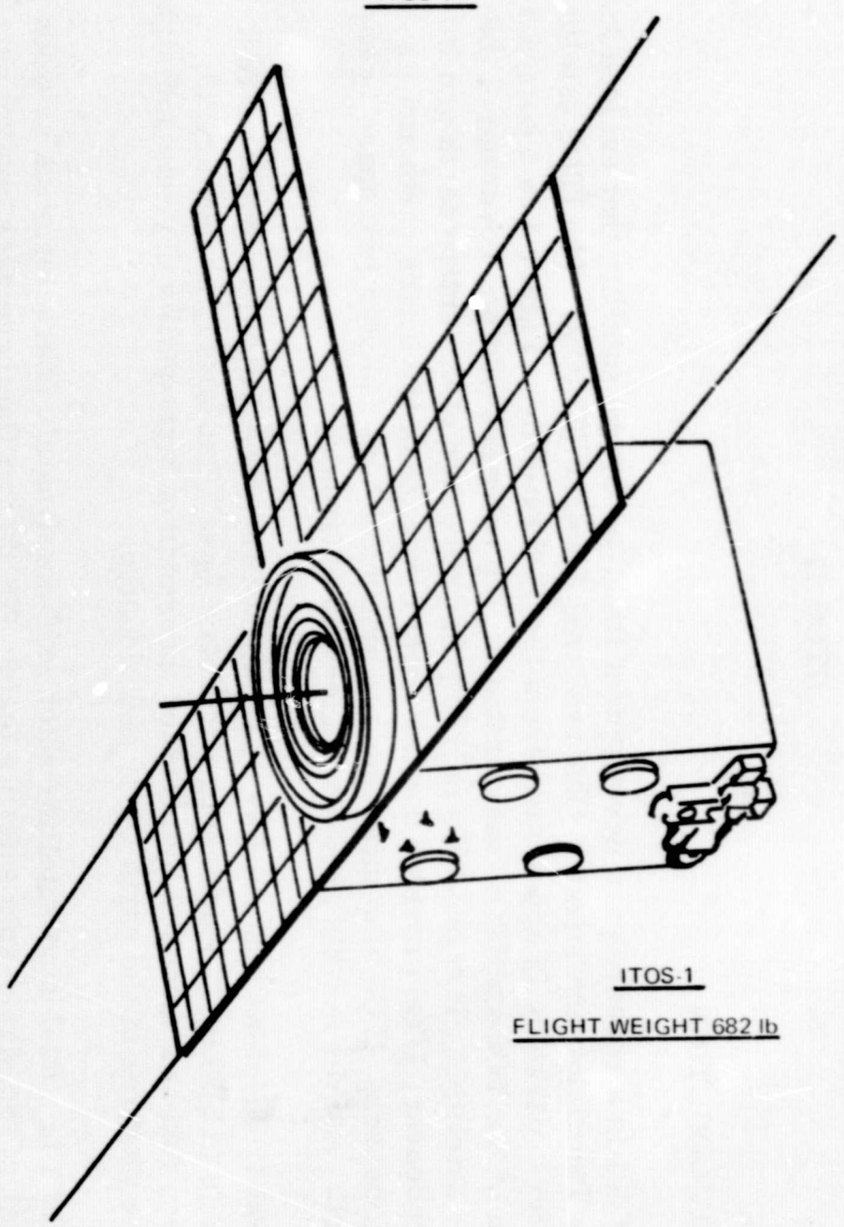

ITOS-1

FLIGHT WEIGHT 682 lb

Figure 1. Size and Appearance of TOS and ITOS

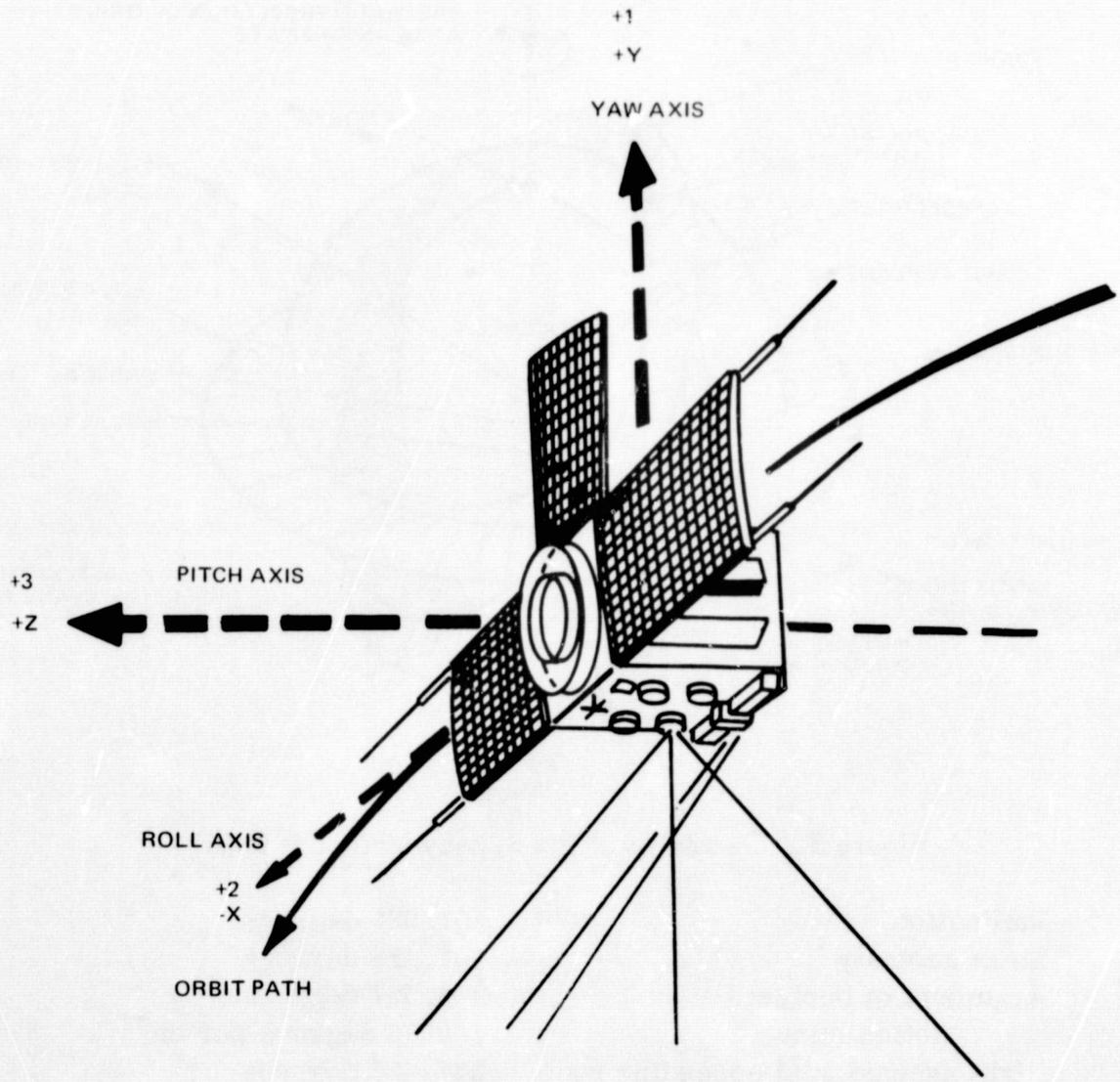

Figure 2. ITOS Mission Mode

Anomalistic period	0115.15023 minutes
Motion plus	0.00000 minute per day
Height of perigee	001460.43 km
Height of apogee	001464.04 km
Velocity at perigee	025675 km per hour
Velocity at apogee	025663 km per hour
Geocentric latitude of perigee	65.431 degrees

- Brouwer mean-orbital elements for ITOS 1 (1-24-70)

Semimajor axis	7833.78 km
Eccentricity	0.002917

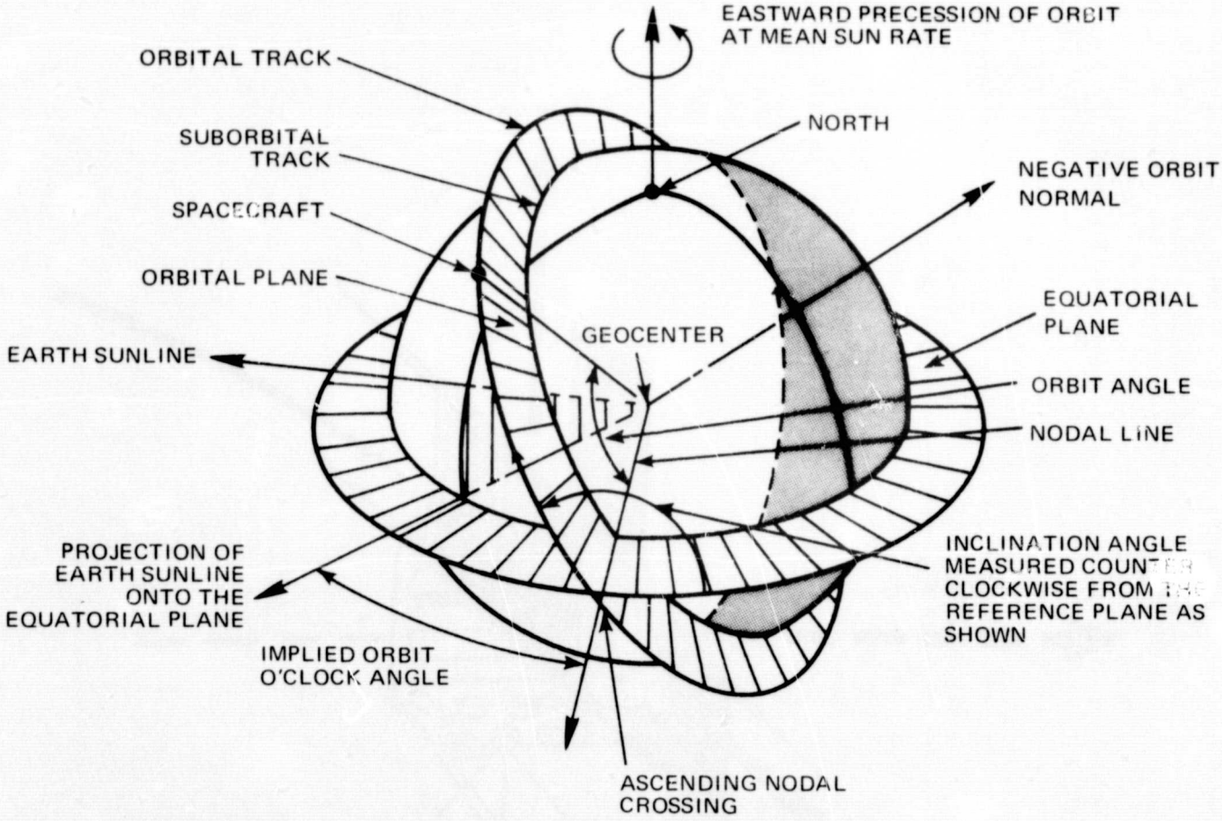

Figure 3. Geometry of the Sun-Synchronous Orbit

Inclination	101.990 degrees
Mean anomaly	101.428 degrees
Argument of perigee	262.527 degrees
Motion minus	1.9025 degrees per day
Right ascension of ascending node	347.428 degrees
Motion plus	1.0079 degrees per day
Anomalistic period	115.00437 minutes
Height of perigee	1432.76 km
Height of apogee	1378.46 km
Velocity at perigee	25755 km per hour
Velocity at apogee	25605 km per hour
Geocentric latitude of perigee	75.901 degrees

- Brouwer mean-orbital elements for ITOS 1 (7-29-70)

Semimajor axis	7833.792 km
Eccentricity	0.002397
Inclination	102.009 degrees
Mean anomaly	172.627 degrees

Argument of perigee	276.352 degrees
Motion minus	1.9009 degrees per day
Right ascension of ascending node	171.155 degrees
Motion plus	1.0095 degrees per day
Anomalistic period	115.00469 minutes
Period dot	0.0 minute per day
Height of perigee	1432.93 km
Height of apogee	1478.32 km
Velocity at perigee	25754 km per hour
Velocity at apogee	25605 km per hour
Geocentric latitude of perigee	76.437 degrees

The ITOS 1 dynamics subsystem is based on the fundamental simplicity of gyroscopic stability and the principle of magnetic interaction torques pioneered on the TIROS and TOS series of satellites. The attitude control of ITOS 1 has demonstrated precision control of direction and magnitude of the momentum vector in space.

Figure 4 identifies the elements of the dynamics subsystem for ITOS 1 by approximate location on the satellite and describes the sequence of events during attitude acquisition. Figure 5 is a simplified block diagram of the dynamics subsystem. The subsystem consists of:

- Redundant nutation dampers
- Redundant momentum-control coils (MCC)
- Functionally redundant roll/yaw-axis control by the quarter-orbit magnetic attitude-control (QOMAC) coil
- Magnetic-bias control (MBC) coil including horizon sensors
- Nonredundant digital solar-aspect sensor (DSAS)
- Redundant pitch-control electronics (PCE)
- Momentum-wheel assembly (MWA)

FOLDOUT FRAME

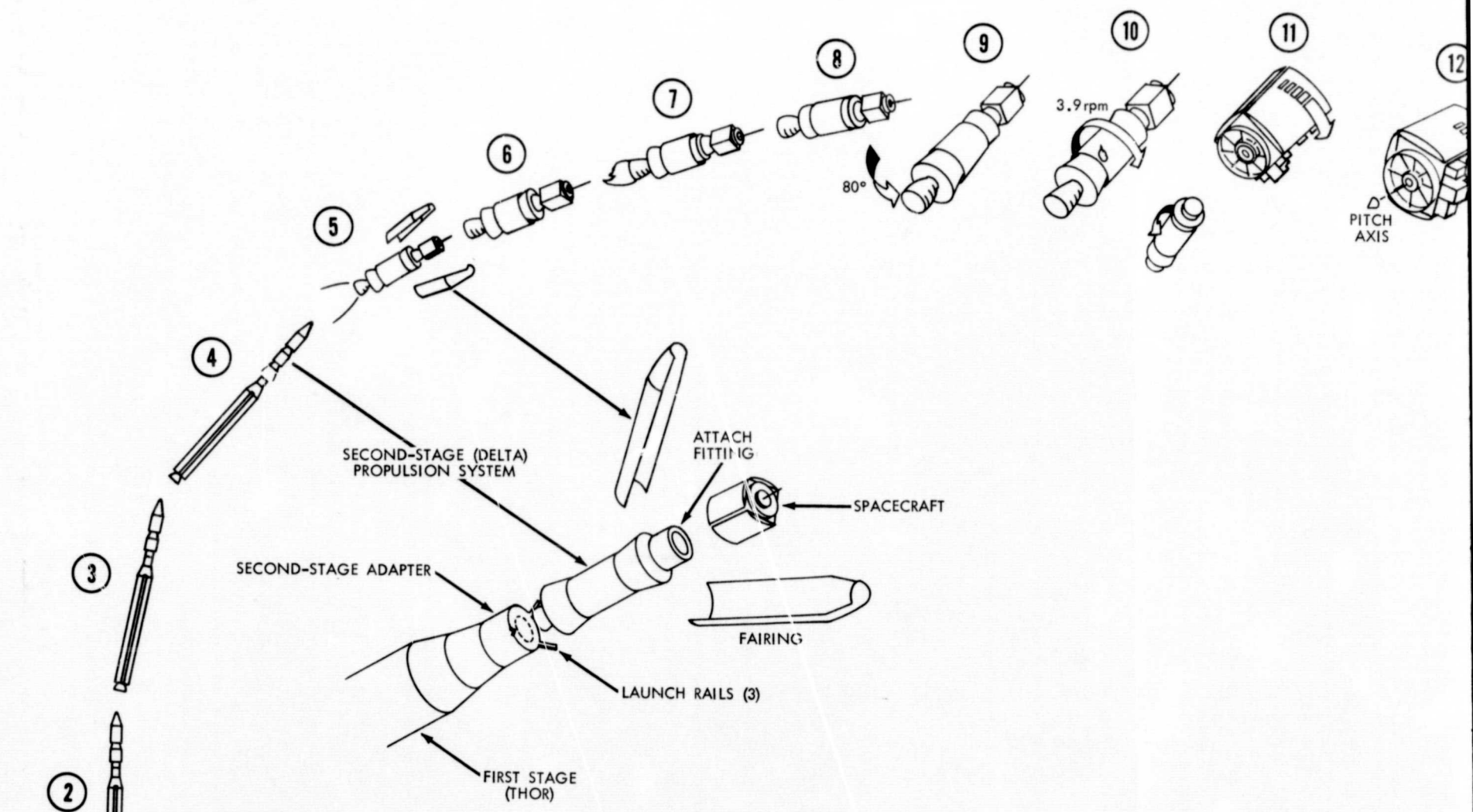

NO.	EVENT	TIME (sec)
1	First-stage igrition and liftoff	T+0
2	Jettison the solid rockets	T+90
3	First-stage cutoff	T+220.548
4	First-to-second stage explosive bolts firing and second-stage ignition	T+224.548
5	Jettison the fairing	T+239.548
6	Second-stage initial cutoff and coast phase	T+589.640
7	Second-stage reignition	T+3662.548
8	Second-stage final cutoff	T+3676.204
9	Begin 80-degree yaw maneuver of second stage	T+3695.548
10	Roll jets operate and spin up second stage and ITOS to about 3.9 rpm	T+3915.548
11	Roll jets cutoff; ITOS separates from second stage and second stage retros to preclude collision with ITOS	T+3926.548

NO.	EVENT
12	Upon separation from the second stage, the satellite axis at a rate of about 3.9 rpm.
13	Two nutation dampers begin a damping action to re (nutation) of its pitch axis to an angle less then ±0.
14	At the instant of separation, the pitch-control loop separation switches, accelerates the momentum flyw about 30 seconds. This transfers momentum from the wheel and reduces the satellite's spin rate from 3.9
15	During the satellite's initial orientation maneuver, satellite's spin rate and the angle between the satel axis (nominally 45 degrees). CDA stations use this over the 136.77-MHz beacon/telemetry transmitter sensor and pitch-index pulse information to correct
16	If the satellite's roll or yaw angles exceed ±3 degre mand the QOMAC coil to move the satellite in the reduce the angle to less than ±1 degree.

FOLDOUT FRAME 2

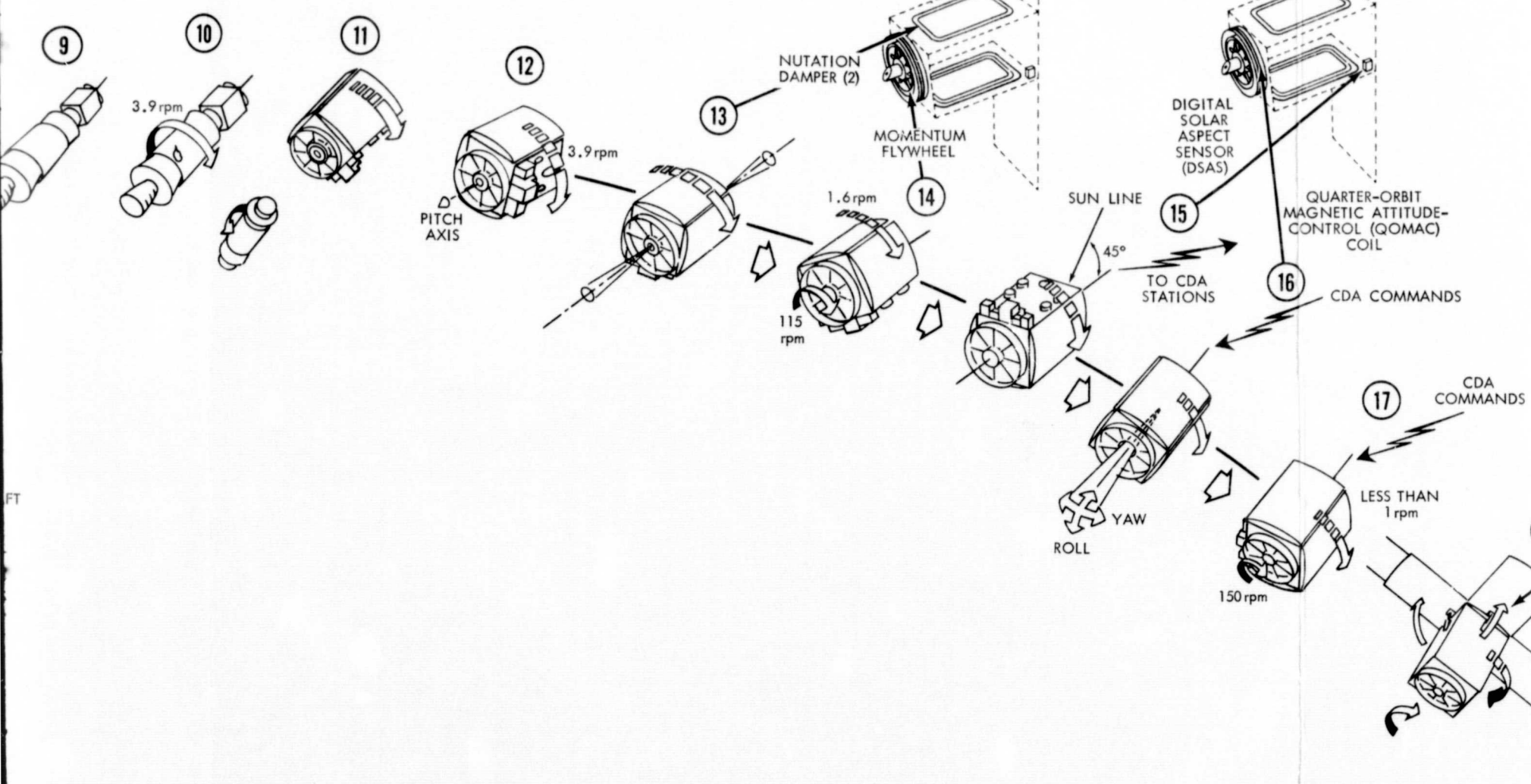

NO.	EVENT
12	Upon separation from the second stage, the satellite spins about its pitch axis at a rate of about 3.9 rpm.
13	Two nutation dampers begin a damping action to reduce satellite wobble (nutation) of its pitch axis to an angle less then ±0.3 degree.
14	At the instant of separation, the pitch-control loop motor, operated by separation switches, accelerates the momentum flywheel to 115 rpm in about 30 seconds. This transfers momentum from the satellite to the flywheel and reduces the satellite's spin rate from 3.9 rpm to about 1.6 rpm.
15	During the satellite's initial orientation maneuver, the DSAS measures the satellite's spin rate and the angle between the satellite-sun line and pitch axis (nominally 45 degrees). CDA stations use this information transmitted over the 136.77-MHz beacon/telemetry transmitter along with roll-horizon sensor and pitch-index pulse information to correct the spin rate.
16	If the satellite's roll or yaw angles exceed ±3 degrees, CDA stations command the QOMAC coil to move the satellite in the direction required to reduce the angle to less than ±1 degree.

NO.	EVENT
17	CDA stations command the pitch-control loop motor to accelerate the momentum flywheel to its normal operating mode of 150 rpm. This reduces the satellite's spin rate from 1.6 rpm to less than 1 rpm.
18	CDA stations command deployment of the three solar panels.
19	If the satellite's spin rate is not within the range of -0.1 and +0.5 rpm, the CDA stations command two momentum coils to move the satellite in the direction required to adjust the spin rate to this range. When this is achieved and the flywheel is rotating at 150 ±10 rpm, CDA stations command the pitch-control loop into operation.
20	CDA stations command the MBC coil to continuously correct for minor roll-yaw attitude changes throughout the orbit by moving the satellite in the direction required to maintain the pitch axis perpendicular to the orbit plane. This procedure also keeps the angle between the sun and the solar panels constant.
21	ITOS is completely oriented and stabilized within ±1 degree about the pitch, yaw, and roll axes so that the TV cameras and infrared sensors face the earth continuously as the satellite orbits the earth.

Figure 4. Sequence
Subsystem

2

FOLDOUT FRAME 3

PRECEDING PAGE BLANK NOT FILMED

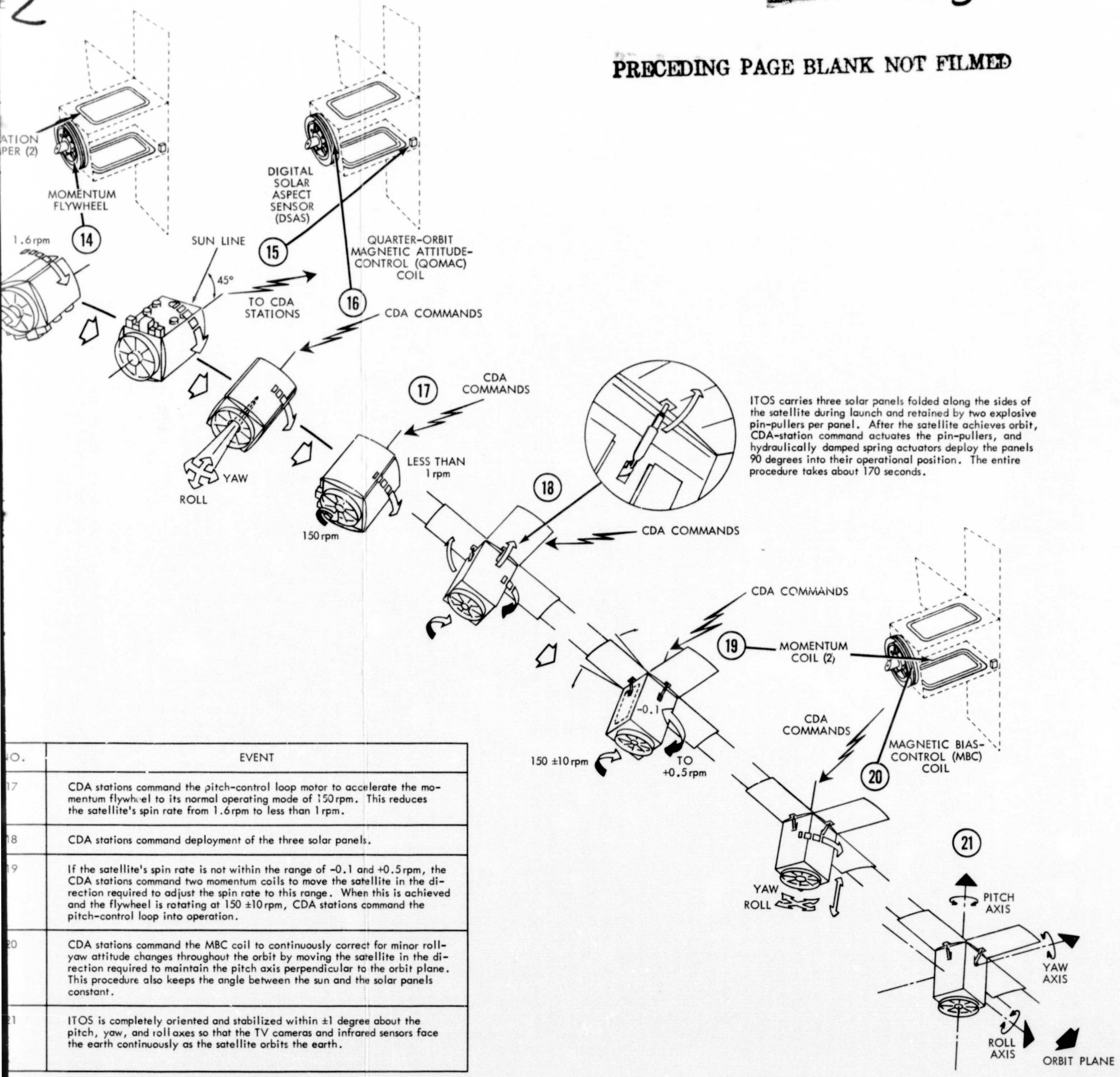

ITOS carries three solar panels folded along the sides of the satellite during launch and retained by two explosive pin-pullers per panel. After the satellite achieves orbit, CDA-station command actuates the pin-pullers, and hydraulically damped spring actuators deploy the panels 90 degrees into their operational position. The entire procedure takes about 170 seconds.

O.	EVENT
17	CDA stations command the pitch-control loop motor to accelerate the momentum flywheel to its normal operating mode of 150 rpm. This reduces the satellite's spin rate from 1.6 rpm to less than 1 rpm.
18	CDA stations command deployment of the three solar panels.
19	If the satellite's spin rate is not within the range of -0.1 and +0.5 rpm, the CDA stations command two momentum coils to move the satellite in the direction required to adjust the spin rate to this range. When this is achieved and the flywheel is rotating at 150 ±10 rpm, CDA stations command the pitch-control loop into operation.
20	CDA stations command the MBC coil to continuously correct for minor roll-yaw attitude changes throughout the orbit by moving the satellite in the direction required to maintain the pitch axis perpendicular to the orbit plane. This procedure also keeps the angle between the sun and the solar panels constant.
21	ITOS is completely oriented and stabilized within ±1 degree about the pitch, yaw, and roll axes so that the TV cameras and infrared sensors face the earth continuously as the satellite orbits the earth.

Figure 4. Sequence of Events—Attitude Acquisition Showing Dynamics Subsystem Element Locations on the Satellite

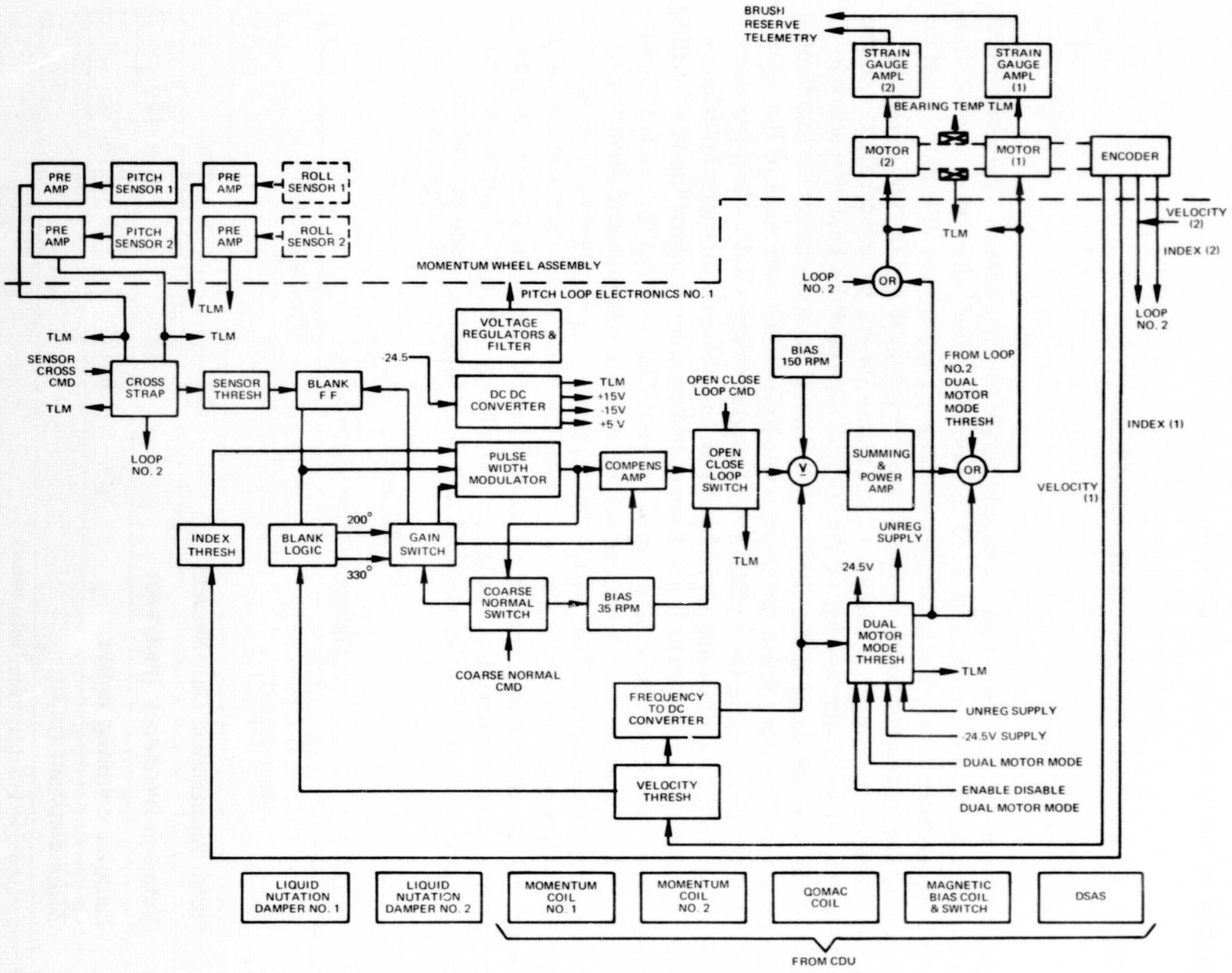

Figure 5. Vehicle Dynamics Subsystem Block Diagram

To describe attitude maneuvers by observing the righthand rule: when viewing the satellite from behind its flight path, grip the arrow with the right hand and point the thumb in the direction of the arrow head. The fingers will point in the direction of positive motion (Figure 2).

ELEMENTS OF THE DYNAMICS SUBSYSTEM

NUTATION DAMPERS

The nutation dampers are round aluminum tubes (1-inch outside diameter) which are toroid shaped (39.5 inches by 31.3 inches) and filled with low-viscosity fluid (Dow Corning type 200). Each damper contains an expansion chamber to act as a void trap for gases and to allow for thermal expansion of the fluid. During nutation, transverse angular accelerations cause the oil to move relative to the toroid walls. The kinetic energy of rotation is expended as heat through the action of the viscous drag of the fluid. The loss of kinetic energy is manifested as a momentum transfer from the transverse axis to the spin axis of the spacecraft, thereby decreasing the nutation cone angle towards null. Damper performance at small nutation angles is based on the absence of vapor bubbles in the fluid. Bubbles could form in the tube at temperatures below the fluid-filling temperature. Bubbles in the tube would prevent fluid inertial forces from overcoming surface tension for small angular excursions which would result in a nutation-angle threshold. The expansion chamber prevents the formation of bubbles by allowing fluid volume to vary with temperature. Figure 6 shows the damper and its expansion chamber. Table 1 lists the damper time constants during two modes of operation: solar panels closed with the wheel at 115 rpm and solar panels open with the wheel at 150 rpm, mission mode operation.

Table 1

Damper Time Constants

Parameter	Dynamic Mode	
	1*	2**
Total momentum (in.-lb-sec)	235	212
Nutation frequency (rad/sec)	0.181	0.183
Damper coupling factor	0.17	0.17
Time constant (min)	51	111

*Flywheel speed at 115 rpm; folded solar panels
**Mission mode (locked pitch loop)

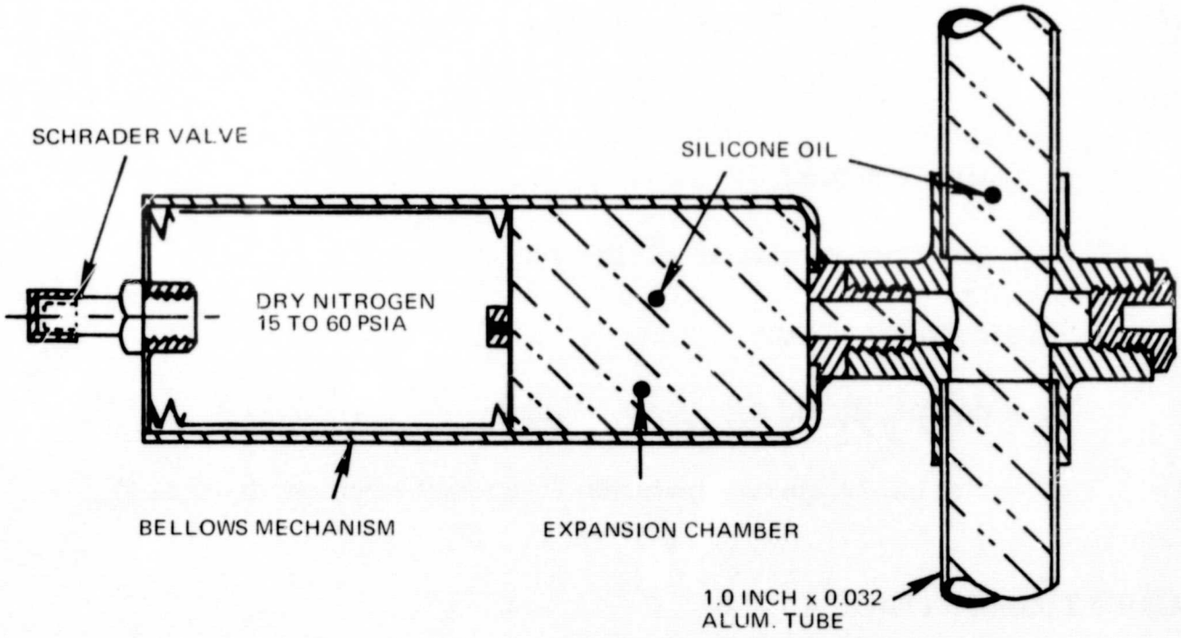

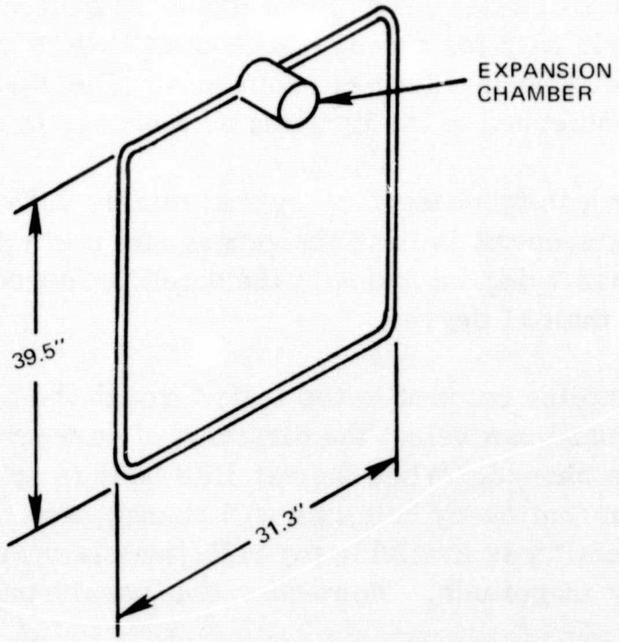

Figure 6. Liquid-Filled Nutation Damper

The damper time constant is computed by:

$$\gamma = \frac{I_2}{FI_d}$$

Where

γ = time constant

I_2 = transverse moment-of-inertia

F = coupling factor

I_d = damper liquid moment-of-inertia

ϕ = forcing frequency (nutation frequency when earth-locked)

MOMENTUM-CONTROL COILS

The MCC's are used on initial acquisition to obtain the required body rate for earth lockon and, in mission mode, to maintain the required satellite momentum and wheelspeed. The two coils are on the same form with their plane perpendicular to the satellite roll axis. The dipole moments generated are placed perpendicular to the spin axis (as a result of current flow in the momentum coils) so that developed torques lie along the spin axis. The resulting change in momentum is then transferred to the flywheel as a change in satellite spin rate.

Satellite momentum can be changed by approximately 0.15 in.-lb-sec per minute per coil when the spacecraft is near the geographic north pole with roll/yaw attitude error less than 1 degree and with the satellite locked to the earth with a pitch error of less than ±1 degree.

Ground command applies current to the coils through the command distribution unit. Ground command can select the direction of current to give a positive or negative momentum change. When the satellite body is spinning, ground-station switching of coil current every half spin will change system momentum. A reduced torquing capability is available for roll/yaw errors up to ±10 degrees or a pitch error of any magnitude. Momentum coil parameters are:

Dipole moment	10.4 ampere turn meter^2 (a-t-m^2)
Type	single coil
Number of turns	160
Wire gage	30 AWG

Wire resistance	314 ohms
Series resistor	12 ohms
Current	75 milliamperes
Power	1.8 watts
Weight	0.3 pound

ATTITUDE-CONTROL COILS

The QOMAC and MBC coils are wound on the same coil form and are designated the attitude-control-coil assembly. The assembly is mounted on the spacecraft equipment module (Figure 4) with the plane of the coil perpendicular to the spacecraft pitch axis, placing the dipole parallel to the pitch axis. MBC, controlled by the magnetic-bias switch (MBS) by ground command, provides continuous torquing to offset part of the residual magnetic dipole of the spacecraft. MBS is ground-commanded through positions until a setting is found where the total dipole creates a torque that corrects attitude changes caused by orbital regression. QOMAC coil provides torquing to precess the spacecraft spin axis to achieve and maintain the pitch axis normal to the orbit plane.

A current level is applied for a period determined by a ground-commanded program with the direction of current being reversed on a quarter-orbit basis. For the initial attitude maneuver, MBC and the QOMAC coils may be paralleled to place the spin or pitch axis normal to the orbit plane. MBC may also be used as a backup to the QOMAC coil for normal attitude control. A unipolar torque mode is incorporated using the QOMAC coil to correct for solar torquing, which results in north/south declination of the satellite pitch axis. Normal QOMAC cycles consist of quarter-orbit reversals of coil current, starting at a time measured from the ascending node. For the ITOS 1 momentum of 212 in.-lb-sec, the low-torque precession rate is 1.09 degrees per orbit. The dipole moment obtained is 4.2 a-t-m^2.

Using the QOMAC coil, a unipolar program torquing technique was developed to automatically correct the satellite attitude as a result of solar torques of approximately 0.00096 oz-in. The use of a normal QOMAC cycle every five orbits could correct the attitude; however, to correct for other disturbances and possible accumulated errors in unipolar torquing, it seemed more practical to use the programmed unipolar torquing technique for approximately 5.6 minutes per half orbit and a normal QOMAC once or twice a week.

Unipolar torquing is programmed for a selected positive dipole at two equally spaced intervals per orbit. The unipolar torquing can precess the satellite up to 3.8 degrees per day, with a resolution of 0.088 degree per day. The negative dipole is always suppressed during unipolar torquing; the unipolar torquing on time can be varied from 16 seconds to 17.1 minutes, depending on the orbit period.

Figure 7 shows the momentum vector normal drift and the effect of unipolar torquing on the drift.

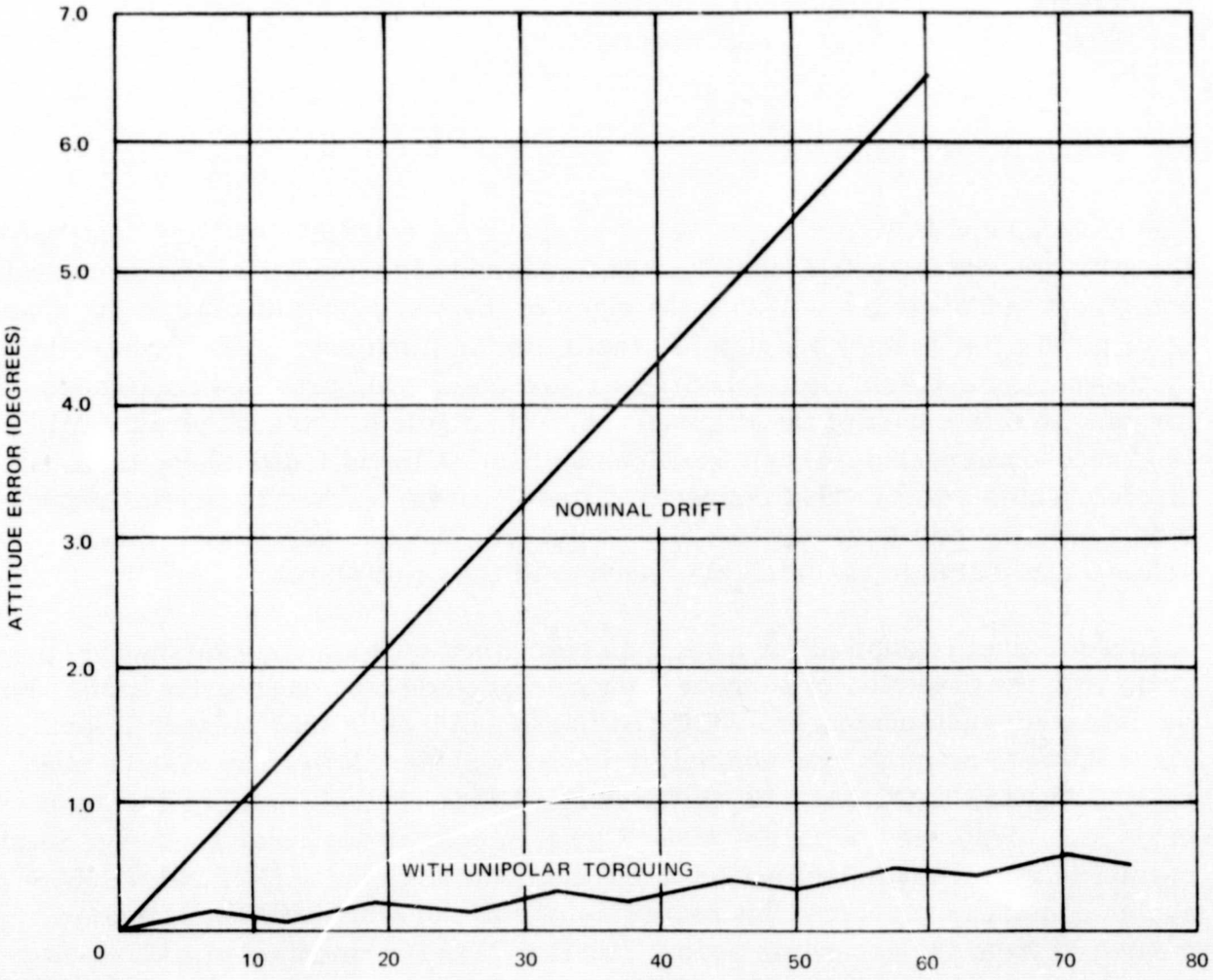

Figure 7. Momentum-Vector Attitude Drift

For satellite turnaround, as required, a high-torque QOMAC mode is provided by paralleling the QOMAC coil with MBC coil for approximately 38 a-t-m^2 at a rate of 5.2 degrees per half orbit.

When the QOMAC coil is disabled, MBC coil remains connected to the QOMAC programmer with a resistor inserted in series, producing a QOMAC backup of 4.8 a-t-m^2. The QOMAC coil parameters are:

Dipole moment	4.2 a-t-m^2
Type	center-tapped
Number of turns	178 per half
Wire gage	31 AWG
Wire resistance	380 ohms

Series resistor	390 ohms
Current	32 milliamperes (at 24.5 volts)
Power (including series resistance)	0.78 watt
Weight	0.50 pound

The MBC parameters are:

Type	single coil
Number of turns	251
Wire gage	25 AWG
Wire resistance	132 ohms
Weight	2.1 pounds

Table 2 lists the MBC operating parameters, giving the MBS switching effect on the MBC dipole. MBC is provided with ±181 milliamperes at -24.5 volts in the high-torque mode and is capable of developing a maximum dipole moment of ±33.8 a-t-m^2.

Table 2

MBC Operating Parameters

MBS Switch Position	Current (ma)	Power (watts)	Total Resistance (ohms)	Dipole Moment (a-t-m^2)
1	0.54	0.013	45,430	0.1
2	1.1	0.026	22,730	0.2
3	1.6	0.040	15,130	0.3
4	2.2	0.052	11,130	0.4
5	2.7	0.065	9220	0.5
6	3.2	0.078	7630	0.6
7	3.8	0.093	6470	0.7
8	4.3	0.10	5750	0.8
9	4.8	0.12	5120	0.9
10	5.4	0.13	4450	1.0
11	181	4.4	132	33.8
11	26	0.64	950	4.8
12,0	OFF	—	—	0.0

MBS is a nonredundant rotary solenoid switch mechanism which controls the current levels and thus the dipole magnitudes of MBC by providing a variable 0 to 181 milliamperes to MBC. Figure 8 shows the magnetic momentum-vector control devices.

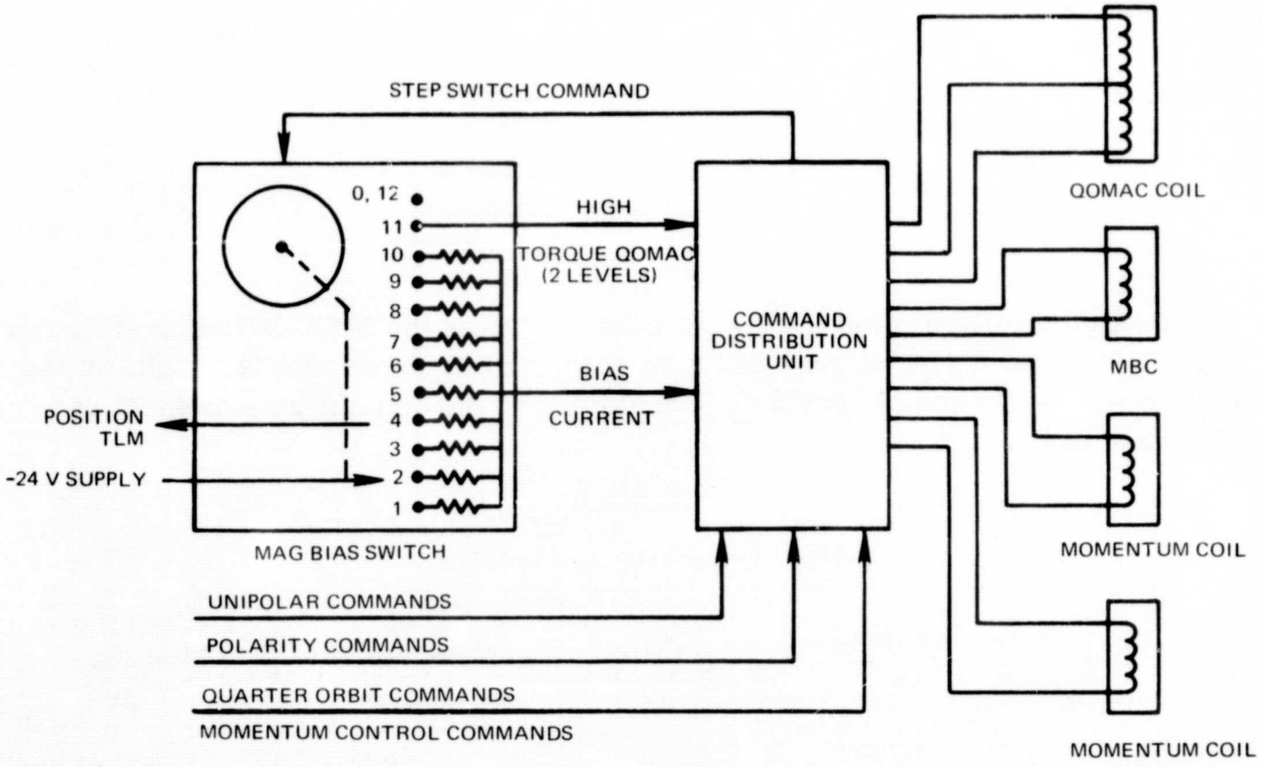

Figure 8. Magnetic Momentum-Vector Control, Simplified Block Diagram

DIGITAL SOLAR-ASPECT SENSOR (DSAS)

DSAS consists of a sensor and its electronics. The primary use of the device is to measure the angle between the spin vector and the satellite sunline in a digital manner. The satellite spin rate for ITOS 1 was also determined by measuring the time between successive readings of trailing edges of the DSAS telemetry readouts.

DSAS has an entrance slit with a field-of-view of 128 degrees. As the satellite rotates, the 128-degree beam generates a solid angle of approximately 3π steradians about the satellite spin axis. Figure 9 shows that the sunlight falls upon the entrance slit and strikes a reticle having a 7-bit gray-coded pattern; from zero to seven photocells are illuminated, depending on the angle of incidence of the sun rays. The outputs of the seven cells are amplified, stored, and updated. When a trigger pulse is received from a command photocell, the stored data is read out serially. DSAS has a resolution of 1.0 degree and an accuracy of ± 0.5 degree.

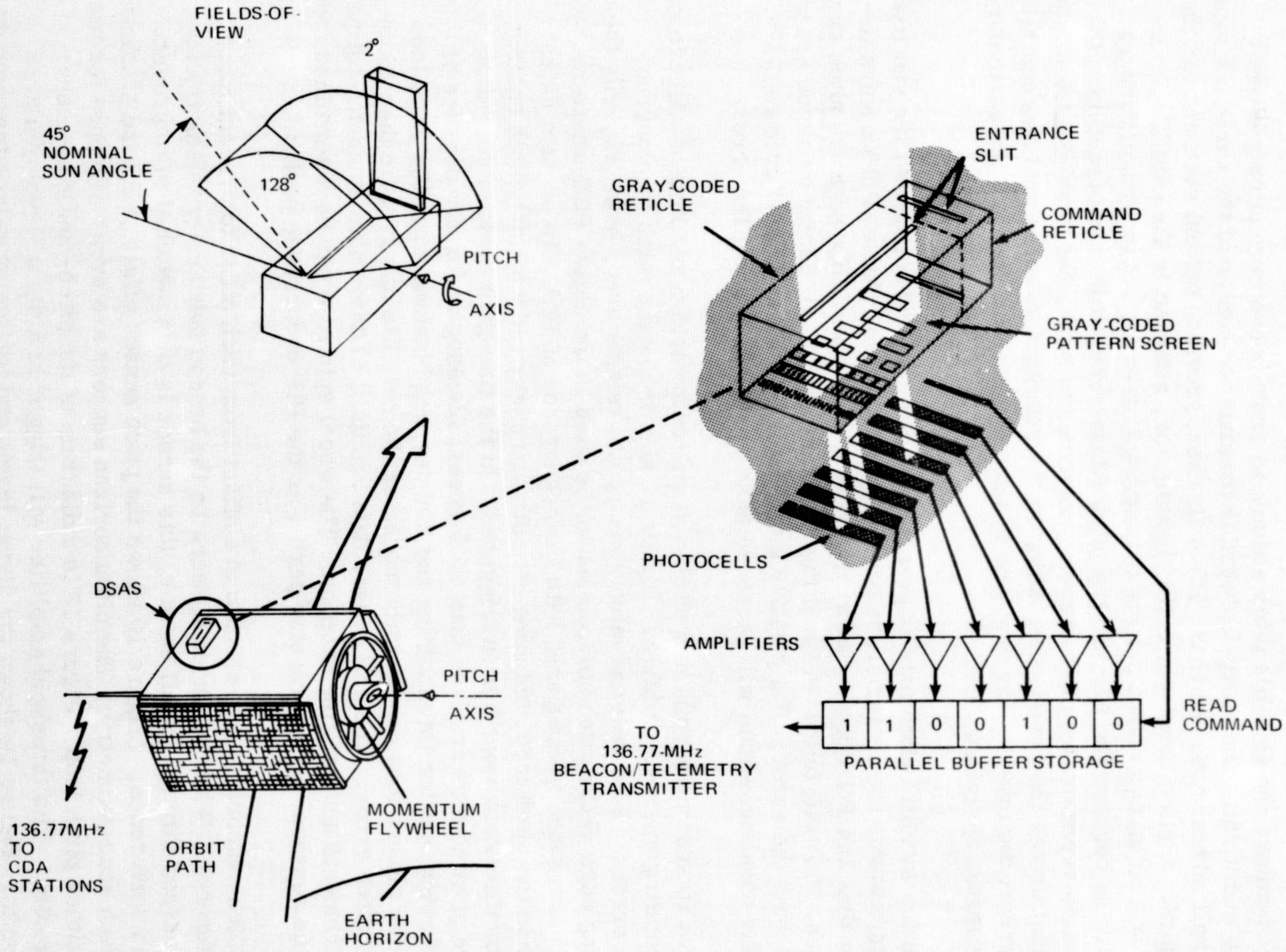

Figure 9. Digital Solar-Aspect Sensor

PITCH-CONTROL ELECTRONICS (PCE)

PCE monitors the satellite pitch attitude to provide one revolution per orbit while maintaining the earth-facing side towards the center of the earth. A pitch and roll mirror attached to the MWA flywheel provides optical scanning for the sensors. A pitch index-pulse (PIP) generator, attached to the satellite, generates a pulse equivalent in time to a zero-pitch error. Any time difference occurring between the PIP and the pitch sensor-scan path's intersection with the earth represents a pitch error. The error is converted to an electrical signal that drives the motor, increasing or decreasing flywheel speed as required to correct the error. The yaw axis is thus kept pointing towards the earth during mission operation.

When the satellite pitch axis is perpendicular to the orbit plane and the yaw axis points towards the center of the earth, the pitch sensor pulse (PSP) occurs the same time the PIP occurs, indicating zero-pitch error. If a negative pitch error occurs, PSP will follow PIP and the resultant signal will decrease motor speed to correct the error. If a positive pitch error occurs, PSP will precede PIP and the resultant signal will increase motor speed to correct the error.

Figure 10 shows the roll- and pitch-sensor configuration and line-of-sight from the rotating mirrors on MWA. Figure 11 shows how the pitch loop corrects pitch errors. Both roll and pitch sensors are telemetered; however, only the leading edge of the pitch horizon sensor is used in the active PCE where its time occurrence is compared with the occurrence of PIP. To prevent earth noise in the pitch loop, blanking circuits are energized when the pitch horizon-sensor threshold amplifier is triggered. In the fine-gain mode of operation where pitch errors are less than 15 degrees, blanking is for 330 degrees of wheel rotation after thresholding and 200 degrees blanking when the pitch loop is in the closed-loop coarse gain mode, or the satellite has greater than 15 degrees pitch error. The roll sensor data are used to determine magnetic-torquing requirements and existing nutation. The wheel spin rate can be determined from horizon sensors' earth-crossing period or the PIP occurrence period.

The pitch sensors' fields-of-view are offset from each other to prevent moon interference. When the moon appears on the beacon subcarrier telemetry to have passed through the off sensor, this sensor is then switched in to prevent moon interference. (Figure 10 shows the pitch sensor offset.) Figure 12 shows the pitch scan geometry. The pitch horizon sensors are cross-strapped for use with either pitch loop. Figure 13 is a diagram of the pitch- and roll-sensor electronics. The threshold amplifier will trigger at a signal level of 160 ±8 millivolts. Figure 14 shows the signal levels and telemetry values for temperatures from 200 to 280°K. The specified pitch- and roll-sensor noise levels are

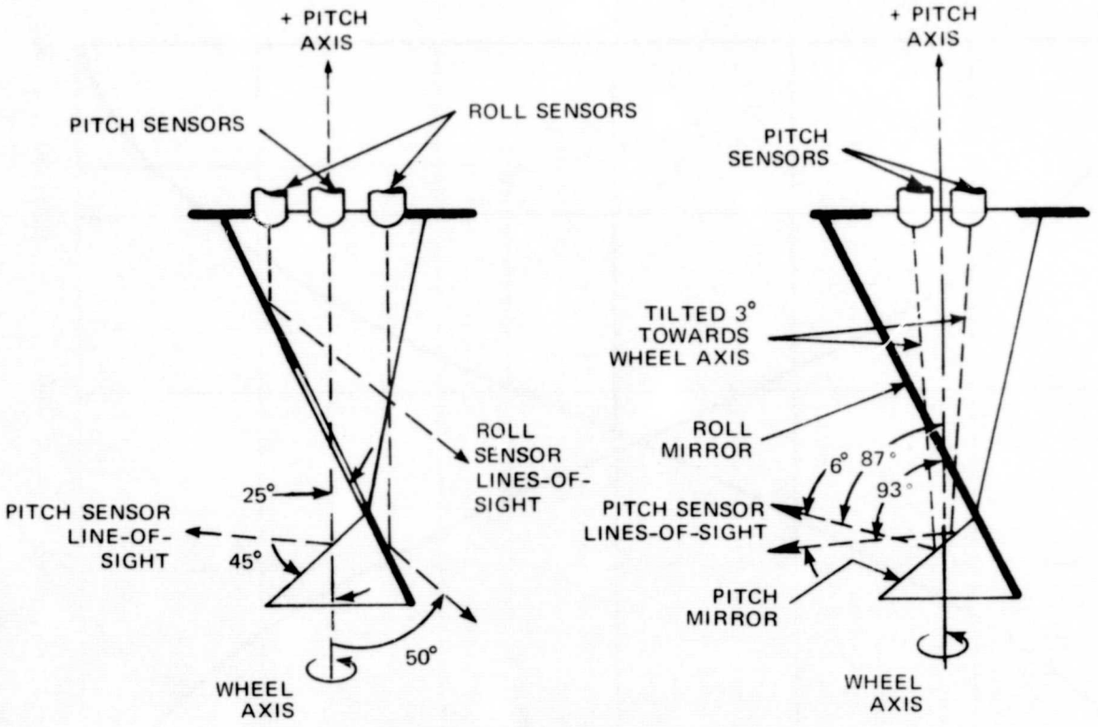

Figure 10. Attitude-Sensor Configuration

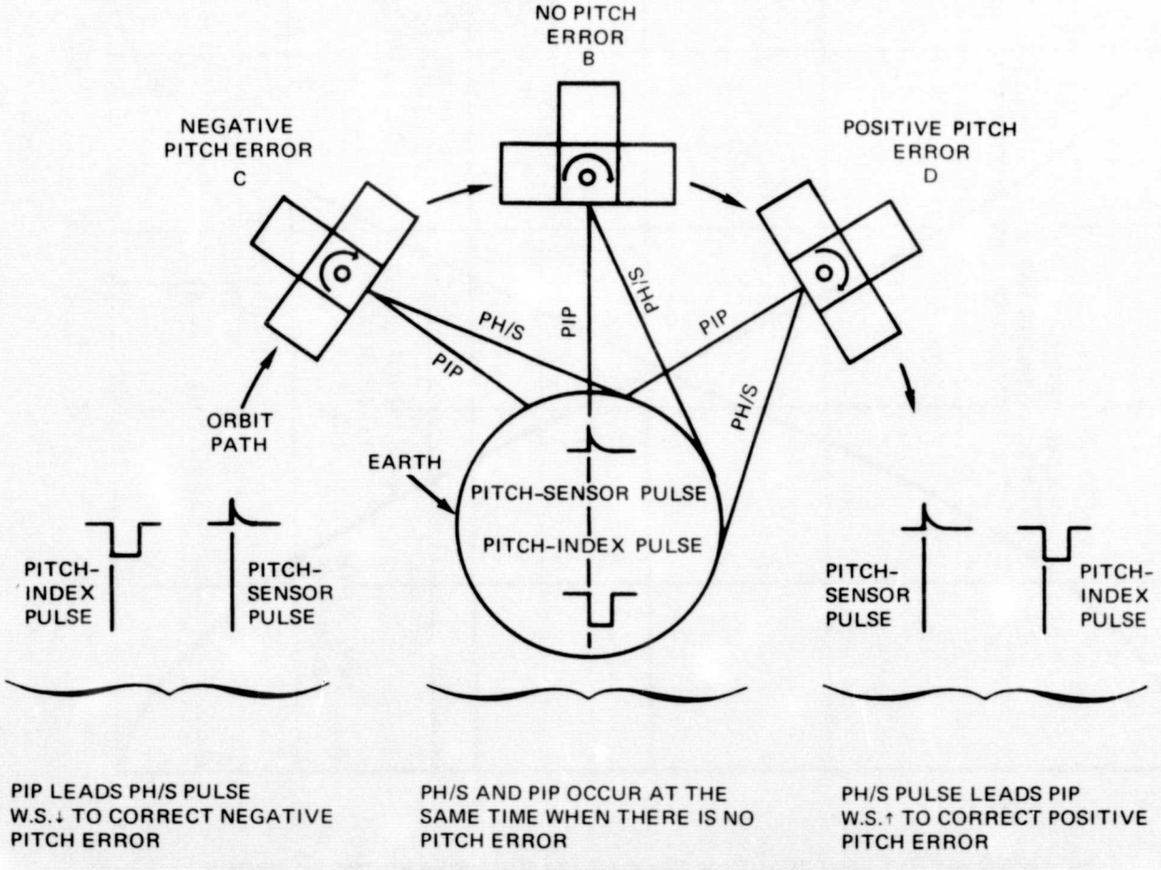

Figure 11. Closed-Loop Pitch-Error Correction

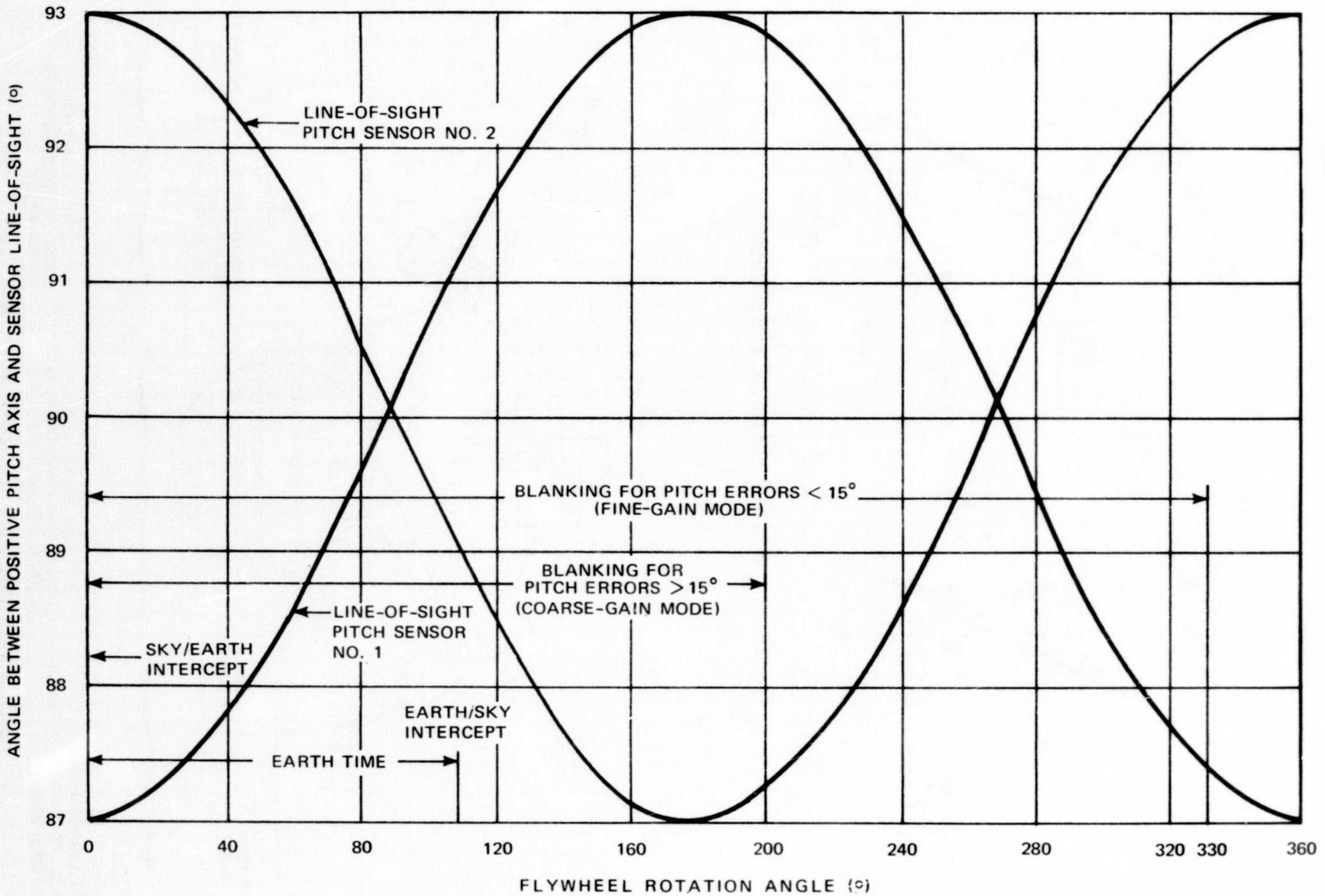

Figure 12. Pitch-Sensor Scan Geometry

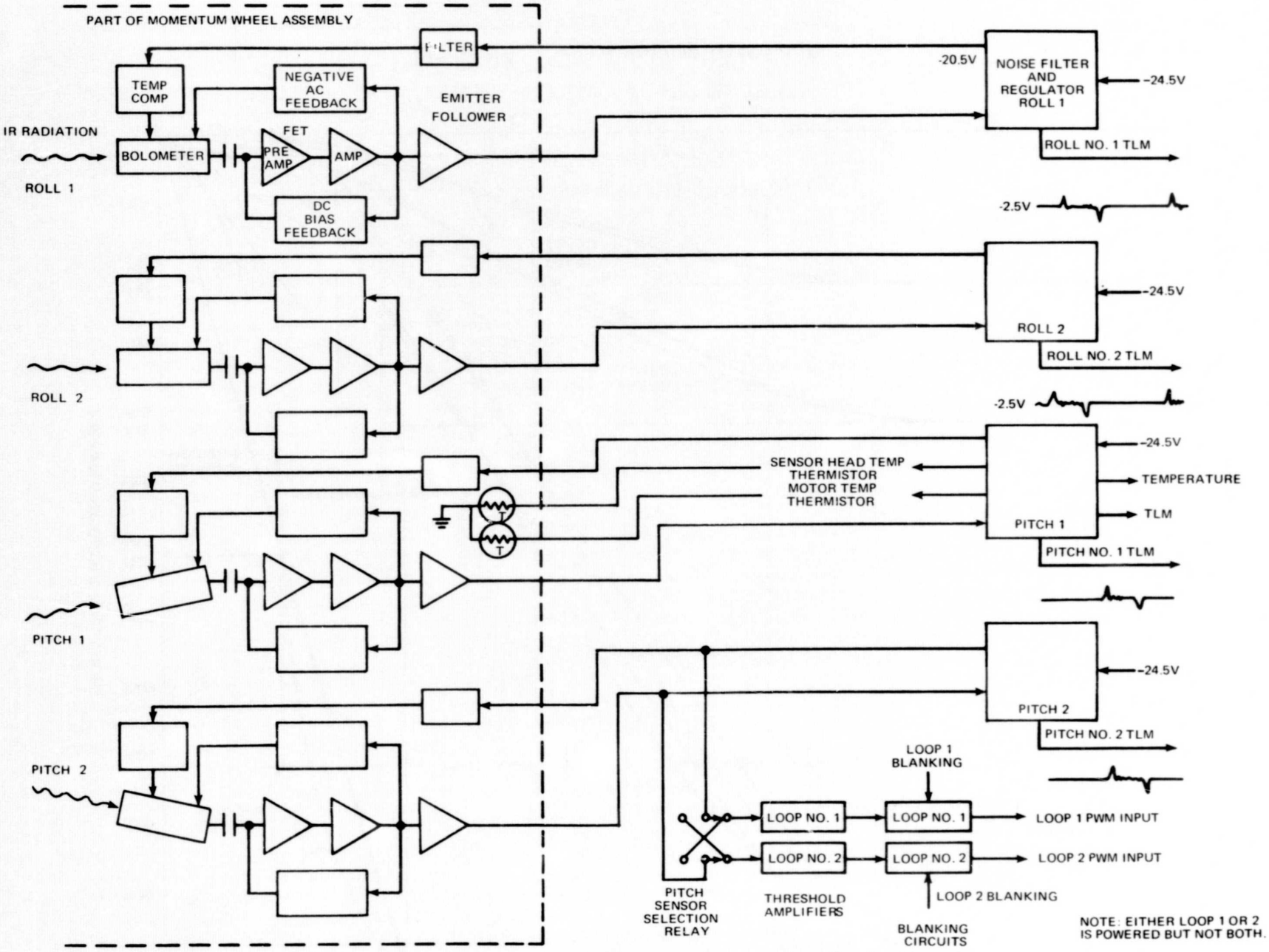

Figure 13. Pitch- and Roll-Sensor Electronics Block Diagram

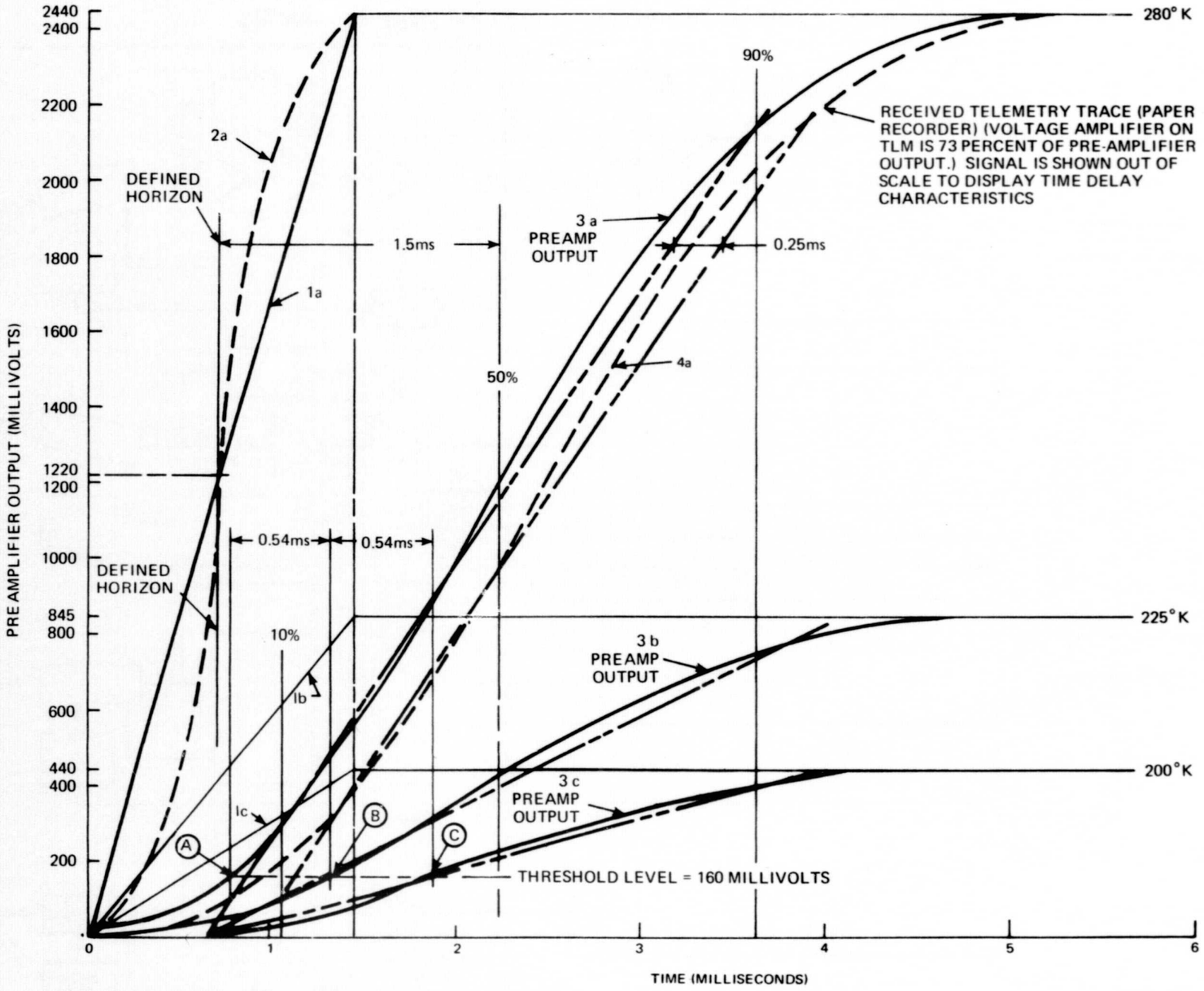

Figure 14. Sensor Preamplifier Output

30 and 33 millivolts, respectively. Both horizon sensors have the same characteristics. Figure 15 shows the infrared bolometer; Figure 16 shows the earth scan lines for the pitch and roll sensors. Figure 17 shows the electronics-measured signal response. Figure 18 shows the pitch-offset-versus-orbit altitude.

MOMENTUM-WHEEL ASSEMBLY (MWA)

Figure 19 is a cross section of MWA (Figure 5 shows MWA and its block diagram interface with the PCE). Each MWA motor has four brushes riding on the commutator, consisting of 50 percent carbon and 50 percent silver. Telemetry monitors the wear on one of the four brushes in each motor to permit calculation of the amount of brush material remaining. Figures 20 and 21 show the brush- and strain-gage configurations, respectively. Figure 22 is an approximate configuration of the ITOS 1 brushes in motors 1 and 2 before launch. PIP, an electromagnetic pickup, originates in the motor encoder. The PIP occurrence time is compared to the time the pitch-horizon sensor pulse occurs. The difference in time of pulsing changes the motor current, which changes wheelspeed and therefore momentum interchange to adjust the pitch within ±1 degree.

Figure 23 shows the pitch attitude-control correction technique. The encoder also supplies a magnetic pickup pulse for each degree of wheel movement. This signal is conditioned and applied to the summing amplifier for motor damping. In 1 second at a wheelspeed of 150 rpm, 900 pulses are obtained for motor damping. The 16-pole wave-wound dc torque motor contains a single bearing, and suitable P-10 oil lubrication for bearing and brush operation. Tables 3 and 4 list the mechanical and electrical characteristics of the motor; Figure 24 shows the torque-speed characteristics of the motor. Exclusive of the power amplifier, the motor requires 3.44 watts at the design point.

DYNAMICS SUBSYSTEM TESTING

An essentially zero-torque dynamic-suspension fixture (single-axis) was used to simulate the ITOS 1 capability to perform pitch capture. Digital computer runs simulated the tests, and the tests and simulations were compared. (Tests were run in vacuum and in air.) The test fixture was well-justified, showing computer-simulator input errors which may have precluded capture. Figure 25 shows the dynamic-suspension fixture with the electrical test model spacecraft installed. With the exception of the 1 g-field and the inability to simulate magnetic torquing, an inspace situation was simulated as nearly as possible. Commands and all possible switching situations were exercised to determine if there was noise interference or onboard disturbance torques which could cause a loss

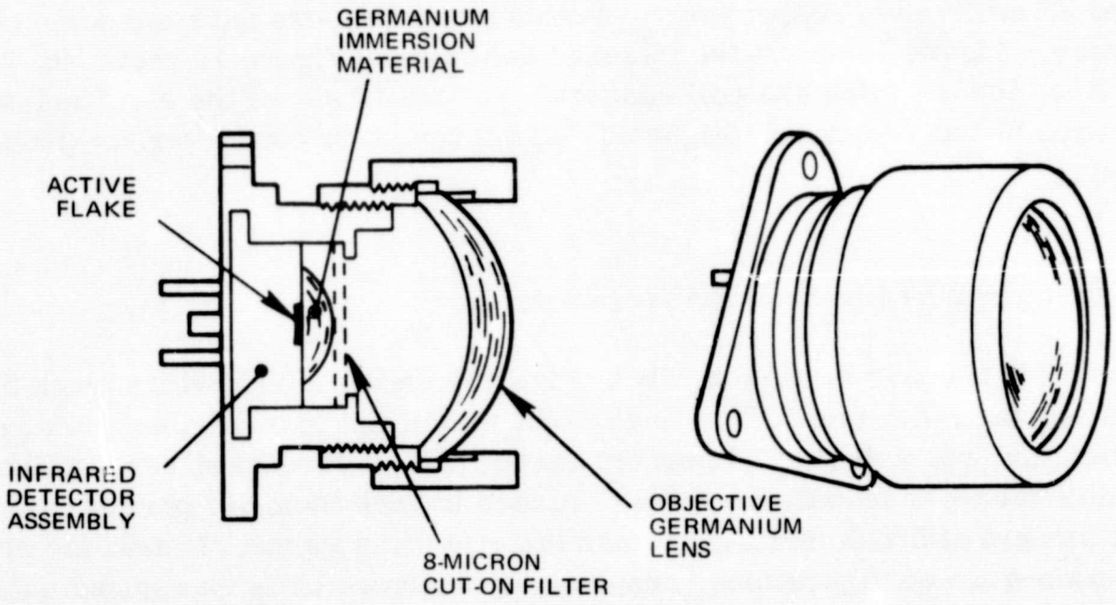

Figure 15. Infrared Bolometer

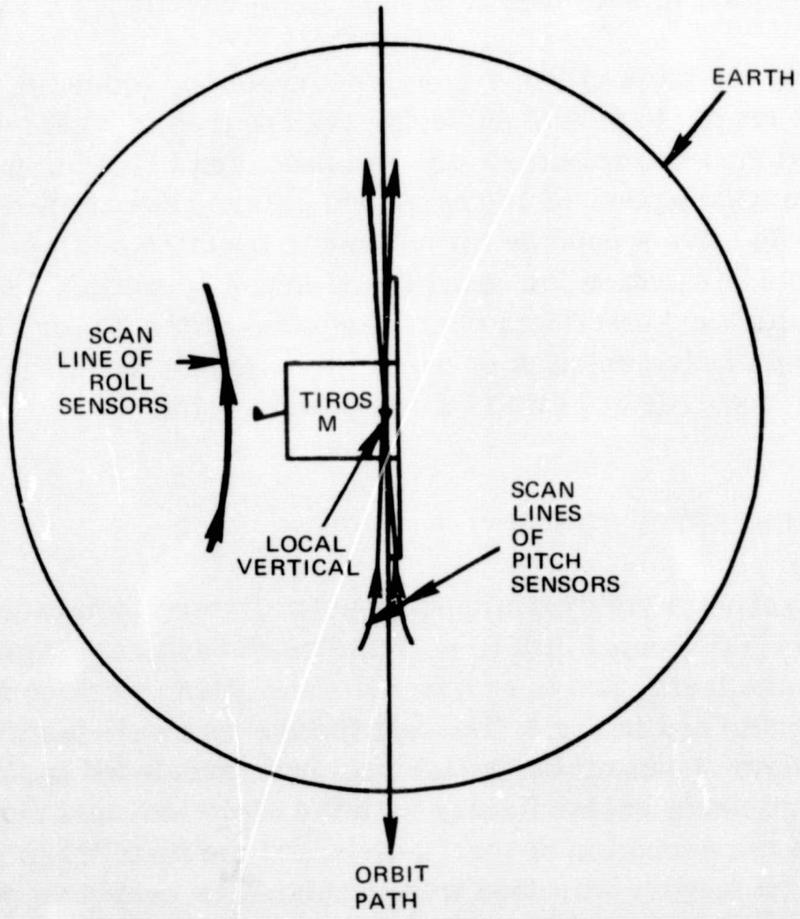

Figure 16. Attitude-Sensor Scan Lines

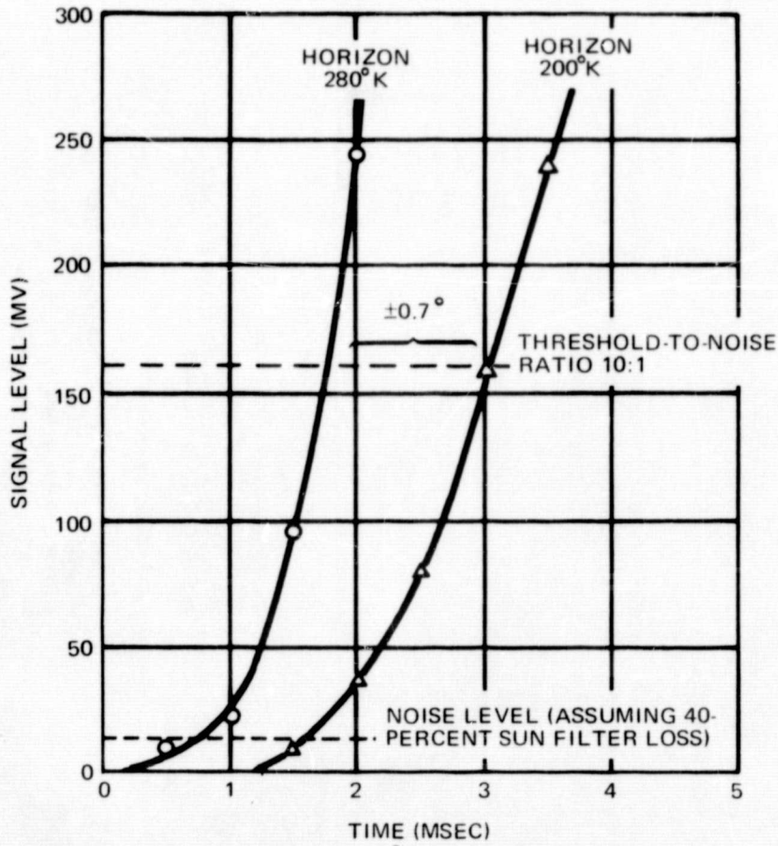

Figure 17. Sensor Electronics-Measured Signal Response

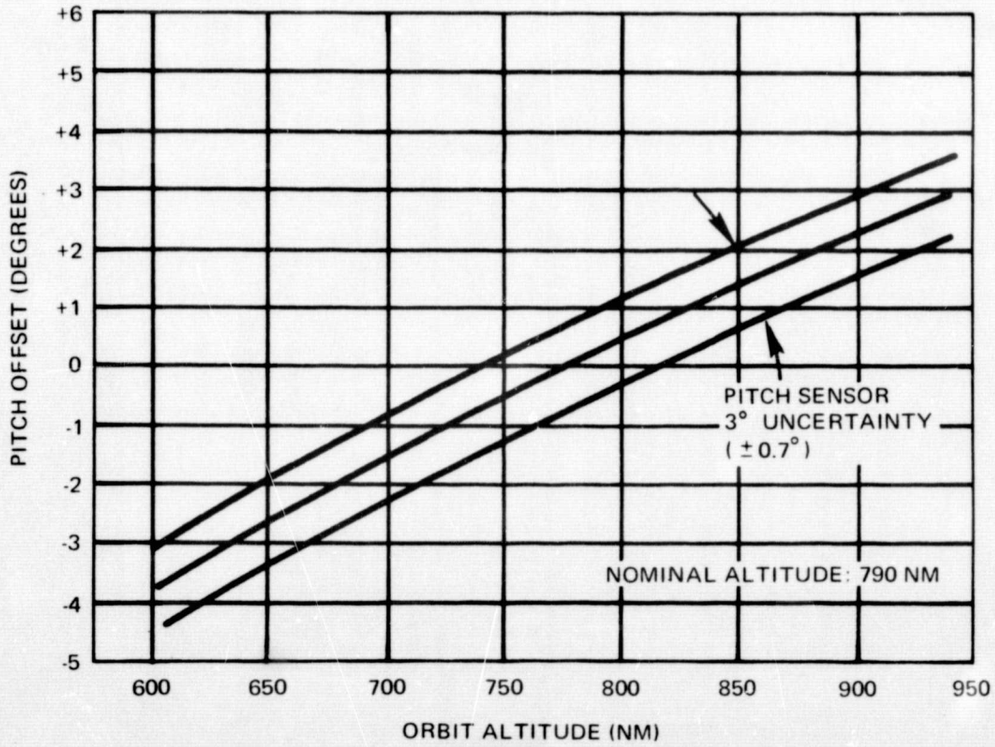

Figure 18. Pitch-Offset-Versus-Orbit Altitude

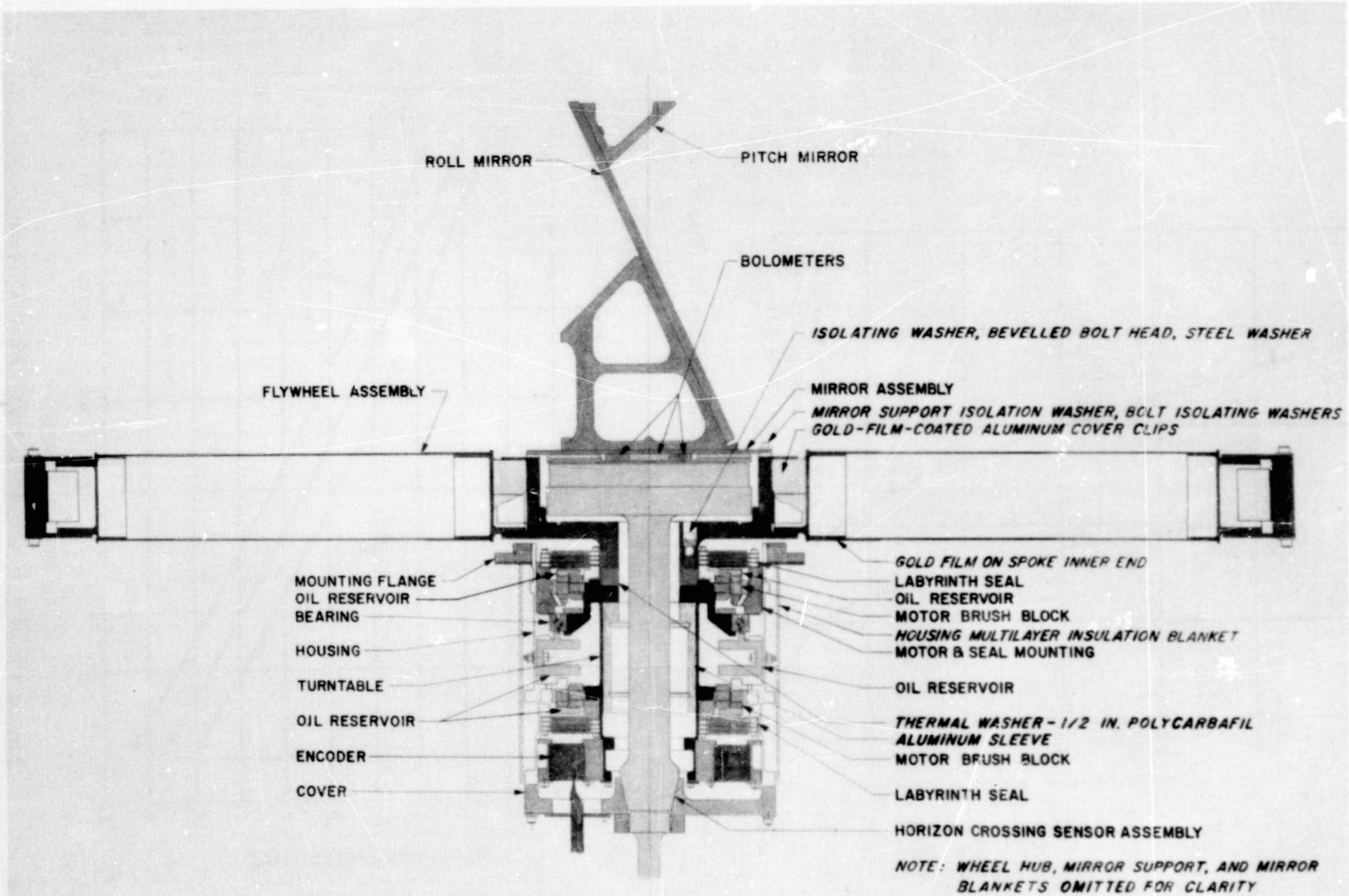

Figure 19. Momentum-Wheel-Assembly Cross Section

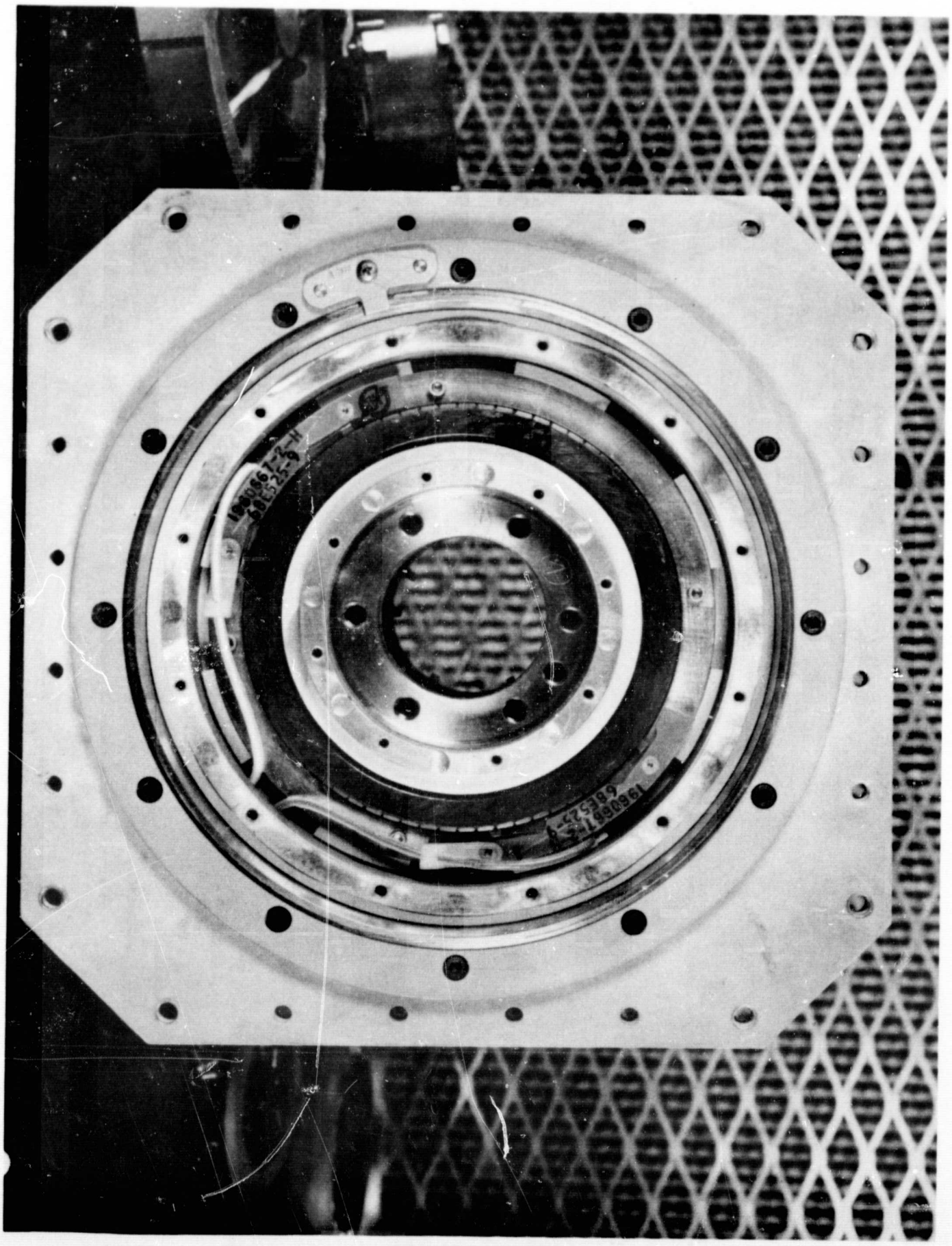

Figure 20. MWA Motor 1 Wheel, Side View

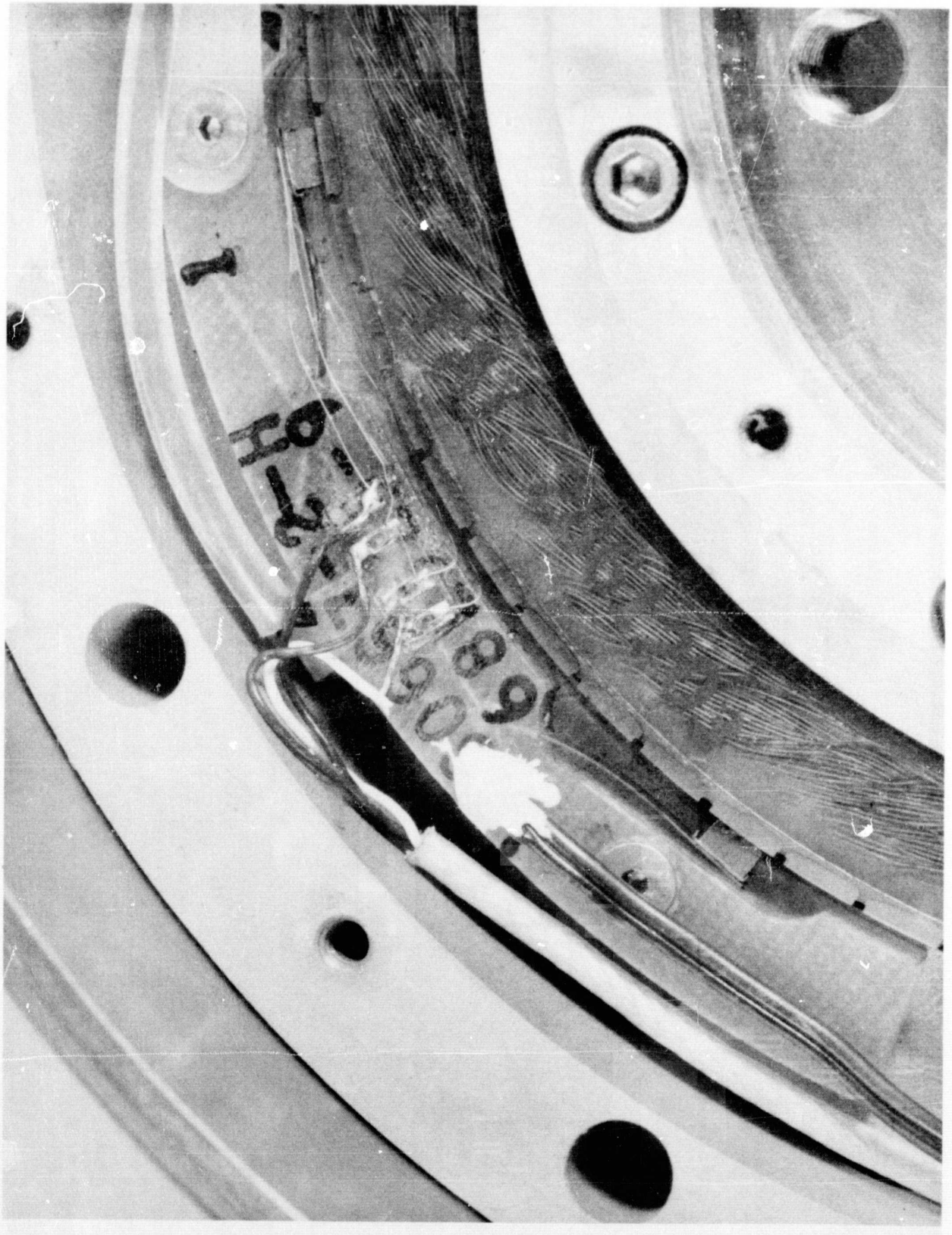

Figure 21. Strain-Gage Mounting on Brush

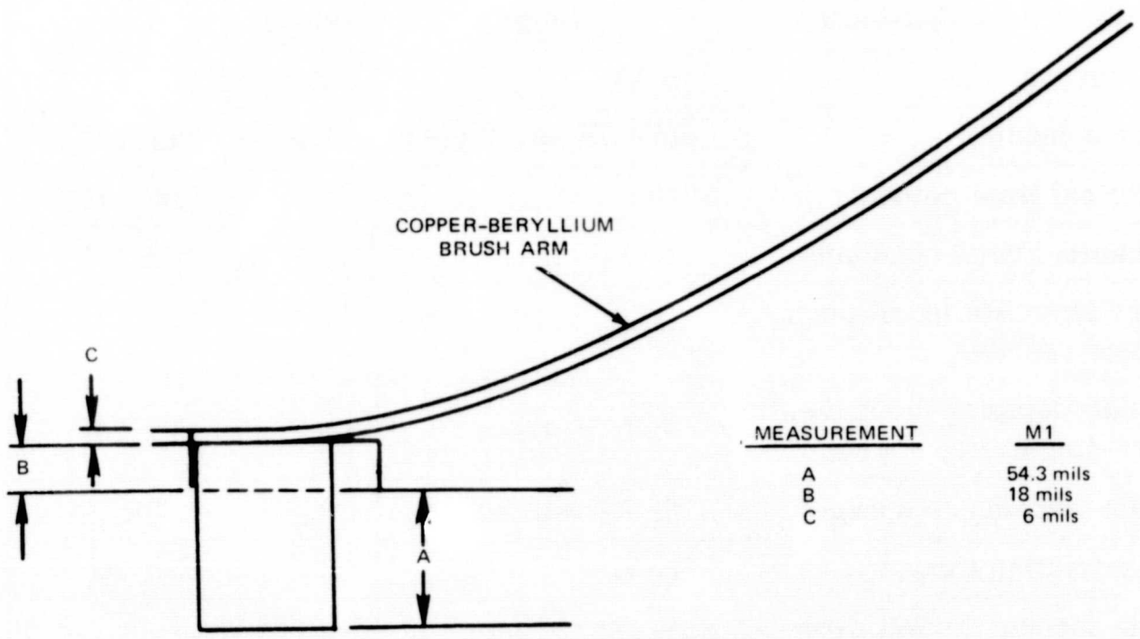

MEASUREMENT	M1	M2
A	54.3 mils	62 mils
B	18 mils	18 mils
C	6 mils	6 mils

Figure 22. Brush Measurements

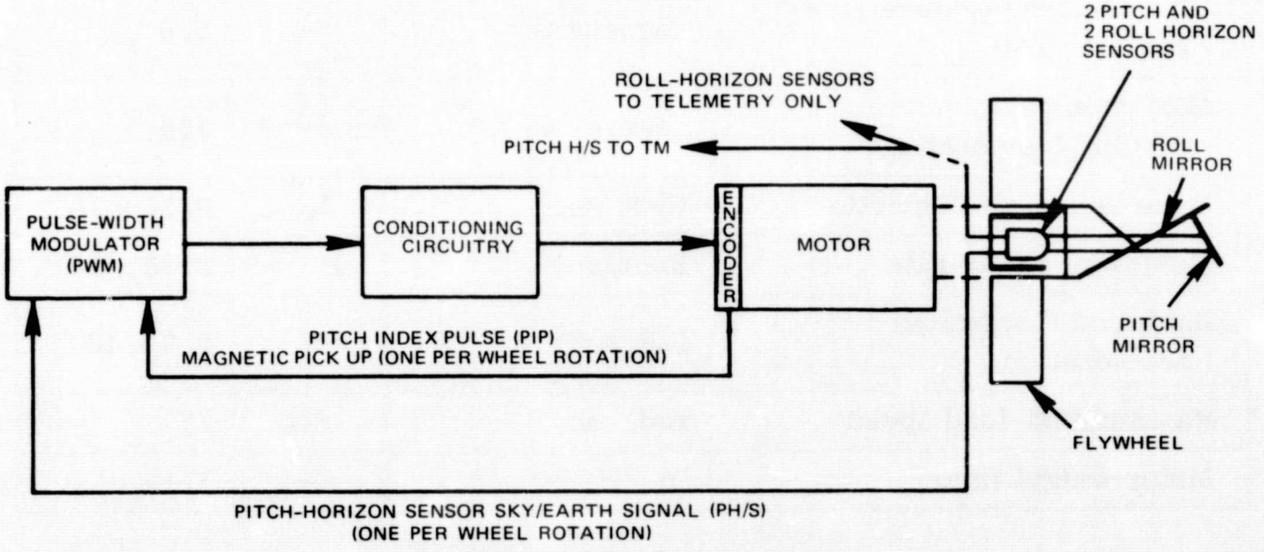

Figure 23. Pitch-Control Subsystem

Table 3

MWA-Motor Mechanical Characteristics
(motor-torque constant = 0.21 in. -lb/v)

Motor Size Constants	Units	Symbol	Value
Peak torque	lb-ft	T_P	1.0
Motor constant	lb-ft/amp/ $\sqrt{\text{ohm}}$	K_M	95×10^{-3}
Electrical time constant	sec	γE	0.6×10^{-3}
Mechanical time constant	sec	γM	27×10^{-3}
Power input stalled at peak torque (25° C)	watts	P_P	110
Viscous-damping coefficients: zero-impedance source	lb-ft/rad/sec	F_O	13×10^{-3}
Infinite impedance source	lb-ft/rad/sec	F_I	0.7×10^{-3}
Motor friction torque	lb-ft	T_F	25×10^{-3}
Ripple torque, average-to-peak	percent	T_R	5
Ripple cycles per revolution	cycles/rev	—	71
Ultimate temperature rise per rms watt	degrees C	—	3.0
Maximum permissible winding temperature	degrees C	—	105
Rotor moment-of-inertia	lb-ft/sec^2	J_M	0.35×10^{-3}
Maximum power rate	lb-ft/sec^2	P	2.88×10^{-3}
Maximum theoretical acceleration	rad/sec^2	∞M	2.9×10^{-3}
Maximum no-load speed	rad/sec	ωNL	77
Motor weight (max)	lb	—	1.13

Table 4

MWA-Motor Electrical Characteristics

Winding Constants	Units	Tolerance	Symbol	D
Resistance, dc (25° C)	ohms	±12.5 percent	R_M	32.1
Volts at peak torque (25° C)	volts	nominal	V_P	57.8
Amps at peak torque	amps	rated	I_P	1.850
Torque sensitivity	lb-ft/amp	±10 percent	K_T	0.55
Back emf	v/rad/sec	±10 percent	K_B	0.74
Inductance	Henries	±30 percent	L_M	0.02

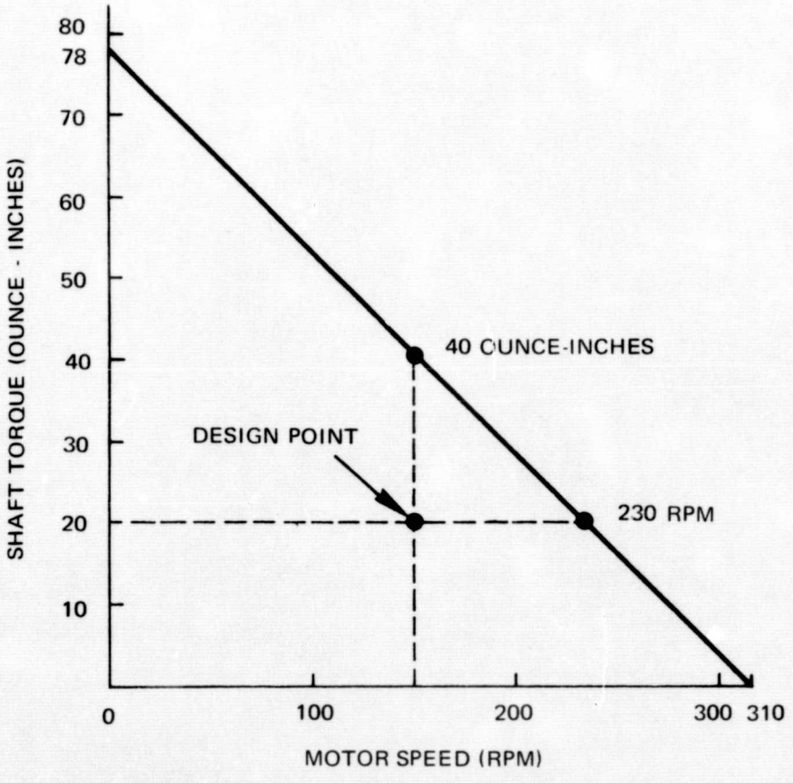

Figure 24. Torque and Speed Characteristics at Power-Amplifier Voltage for Inland Torque Motor of -24 Volts

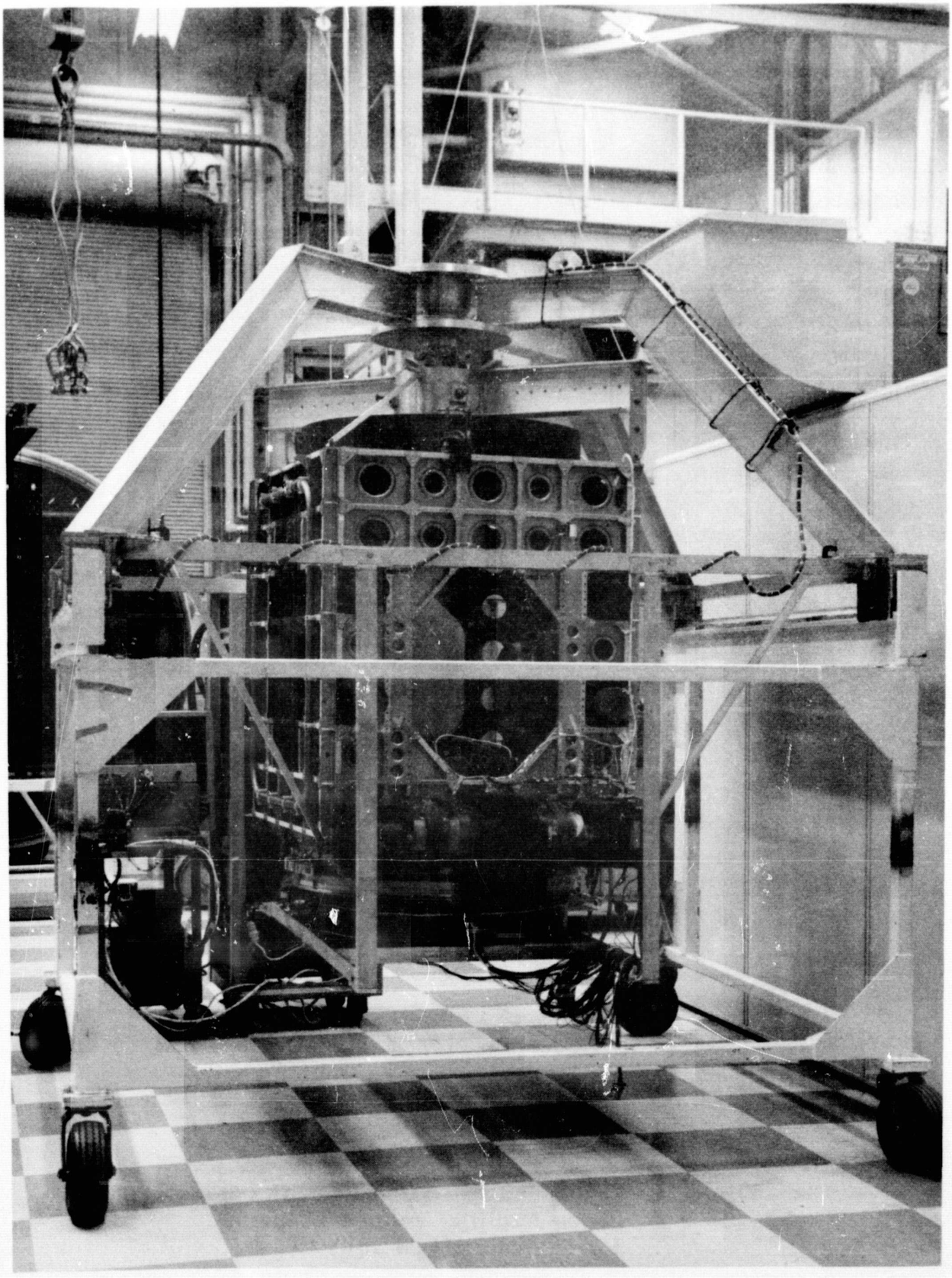

Figure 25. Dynamic-Suspension Rig

of pitchlock. All telemetry and test points were monitored for many initial capture conditions until testing was successfully accomplished. Figure 26 shows a typical pitch-loop capture run.

Table 5 contains single-axis capture data obtained during the dynamic-suspension testing. Table 6 summarizes the three-axis pitch-loop computer simulation. Table 7 contains the inertia values used for the computer study. Table 8 contains the operational power requirements.

Table 5

Single-Axis Capture Data

Initial Momentum (in. -lb-sec)	Initial Pitch Error (deg)	Time to Capture (sec)	Final MWA Speed (rpm)
212	117	120	140
212	262	170	140
263	211	270	170
203	-127	110	134
211	199	160	144
212	304	210	150
181	-112	170	128

The dynamic subsystem element weights are:

	Pounds
Momentum-wheel assembly	41.7
Pitch-control electronics	7.1
Attitude-control-coil assembly (QOMAC and MBC)	2.6
Momentum-control coils (both)	0.6
Nutation dampers	14.5
Magnetic bias switch	0.8
Digital solar-aspect sensor	1.7
Separation connector and bracket	0.3
Total	69.3

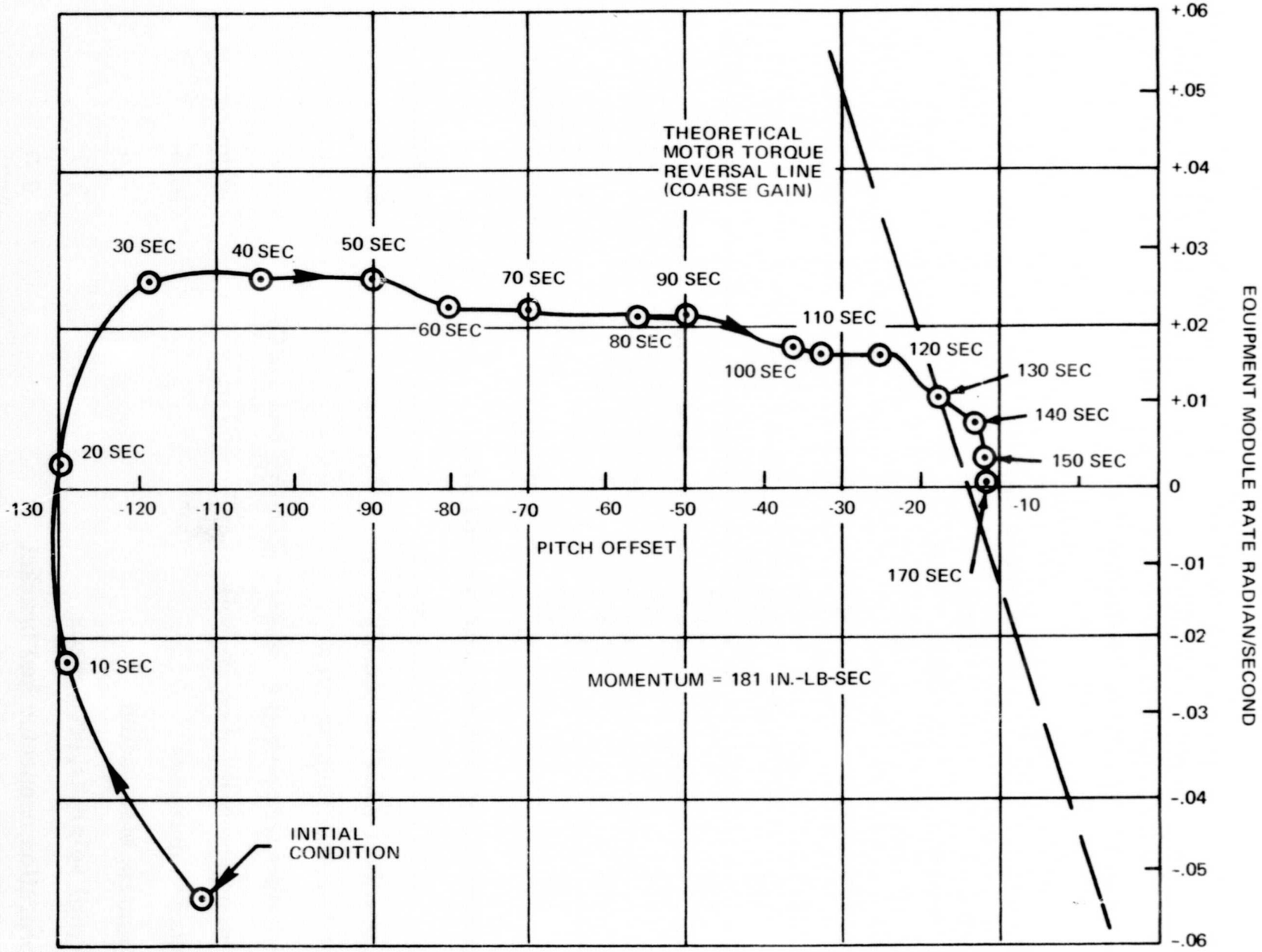

Figure 26. Pitch Capture Phase-Plane Plot

Table 6

Pitch-Loop Computer Simulation

Pitch Sensor (*)	Roll Angle (deg)	Momentum (in.-lb-sec)	Motor Supply Voltage	Friction Load (in.-oz)	Gain Mode	Initial Nutation Angle (deg)	Maximum Nutation Angle After Capture (deg)	Capture Time (sec)	Damping Time Constant (min)	Damping Time Constant + Nutation Danger Time Constant
87	+3	199	35	20	C	1			148.4	1.22
87	+3	199			F				99.1	0.82
87	+3	199			C				79.1	0.65
93	-3	270			F				48.5	0.54
93	-3	270			F				88.1	0.97
93	-3	270			C				32.8	0.36
87	+1	201			C				74.4	0.61
87	+3	201			C				194.5	1.60
87	+5	201			C				-313.2	-2.58
93	-3	223			F				91.0	0.83
93	-5	223			F				84.6	0.78
93	-10	223			F				75.7	0.69
87	+3	270			C				208.3	2.3
93	-3	199			F				46.5	0.38
87	+3	199				0	0.34	228	102.9	0.85
87	+3	212					0.70	180	83.4	0.73
93	-3	212					0.88	315	52.6	0.46
93	-3	270					0.58	310	34.8	0.38
87	+3	199	26.5				0.34	228		
87	+3	212	26.5				0.70	180		
93	-3	212	26.5				0.41	288	52.7	0.46
93	-3	270	26.5				0.07	340		
87	+3	199	35	8			0.25	254	102.7	0.85
87	+3	212	35	8			0.81	190	83.4	
93	-3	212	35	8			0.37	396		
93	-3	270	35	8			0.57	307	35.1	0.39
87	+3	199	26.5	8		0	0.25	254		
87	+3	212	26.5	8		0	0.81	190		
93	-3	212	26.5	8		0	0.62	422		
93	-3	270	26.5	8		0	0.47	490		
87	+3	199	35	20		0.25	0.43	227	102.3	0.84
87	+3	199	35	20		0.25	0.56	227	102.7	0.85
87	+3	199				0.25	0.39	227	102.9	0.85
87	+3	199				0.25	0.11	227		
93	-3	270				1	0.95	310	34.8	0.38
93	-3	270					0.63	313	34.9	0.39
93	-3	270					1.46	311	34.9	0.39

Table 6 (continued)

Run No.	Pitch Sensor (*)	Roll Angle (deg)	Momentum (in.-lb-sec)	Motor Supply Voltage	Friction Load (in.-oz)	Gain Mode	Initial Nutation Angle (deg)	Maximum Nutation Angle After Capture (deg)	Capture Time (sec)	Damping Time Constant (min)	Damping Time Constant + Nutation Danger Time Constant
38	93	-3	270					1.58	310	34.4	0.38
39	87	+3	201			C				169.4	1.40
40	87	+3	201			C				173.4	1.43
41	87	+3	201			C				167.8	1.39
42	87	+3	201			C				186.0	1.53
43	87	+3	201			C				185.0	1.52
44	87	+3	201			C				141.4	1.16
45	93	-3	223			F				80.6	0.74
46	93	-3	223			F				89.3	0.82
47	93	-3	223			F				84.7	0.78
48	93	-3	223			F				81.2	0.74
49	93	-3	223			F				89.5	0.82
50	93	-3	223			F				85.8	0.79
51	93	+5	201			C				394.7	3.35
52	93	+12	201			C				37.6	0.31
53	87	+3	270			C				126.2	1.4
54	87	+3	270			C				208.7	2.3
55	87	+3	270			C				137.5	1.52
56	87	+5	270			C				-288.4	-3.2
57	93	-3	199			C				42.7	0.34
58	86.6	+3	201			C				144.2	1.19
59	86.6	+3	270			C				165.3	1.85
60	93.5	-3	223			F				129.6	1.19
61	87	+3	212				0	1.41	149	83.5	0.73
62	93	-3	212				0	1.44	275	52.7	0.46
63	87	+3	199				0.25	1.15	165	103.1	0.85

Table 7

Inertia Values Used in Computer Study

Inertia (Spacecraft Axis)	Maximum (lb-in.-sec^2)	Nominal (lb-in.-sec^2)	Minimum (lb-in.-sec^2)
Yaw (I_{11})	1326	1302	1278
Roll (I_{22})	1042	1023	1004
Pitch (I_{33})	1168	1147	1126
Yaw-roll (I_{12})	12.2	5.8	-0.6
Yaw-pitch (I_{13})	81.6	78.8	76.0
Roll-pitch (I_{23})	-5.0	-7.8	-10.6

Table 8

Operational Power Requirements

Item	Power at -24.5 Volts (watts)	Operation Time	Equivalent Continuous Drain (watts)
Pitch-axis control loop*	8.4	continuous	8.6
Magnetic bias coil	0.013 to 0.13	continuous	0.013 to 0.13
Momentum coil	1.8 per coil	**	**
QOMAC coil	0.78	1/5 orbit/orbit (23 min)	0.16
Total (continuous maximum)			8.99

*Power from regulated (-24.5 volts) and unregulated (-36 volts) supplies
**As required for adjustment

Table 9 lists the random roll-error contributions. Table 10 lists the maximum principal-point roll-error contributions.

Table 9

Random Roll-Error Contributions*

Attitude Deviations	Roll Error (degrees)	
	Single Sample	10 Samples (4-sec average)
Transverse momentum (tape recorder—worst case)	0.042	0.042
Flywheel unbalance	0.00052	0.00016
Bearing-free motion	0.027	0.009
Roll horizon sensor (noise and ground-data processing)	*0.553	0.175
3σ tolerance (RSS value)	0.556	0.180

*High frequency with respect to 10 minutes of roll determination; best slope fit

Bias roll-error contributions* are:

Attitude Deviations	Roll Error (deg)
Roll-sensor misalignment	0.152
Roll-mirror misalignment	0.152
Principal moment-of-inertia misalignment	0.0195
Roll horizon sensor (horizon variations, radiance changes)	0.162
3σ tolerance (RSS value)	0.280

Pitch-error contributions are:

Attitude Deviations	Pitch Error (deg)
Alignment (RSS value)	±0.1
Horizon index-pulse phasing	±0.1

*During 10 minutes of roll determination; best slope fit

Table 10

Maximum Principal-Point* Roll-Error Contributions

Item	Attitude Deviation	Maximum Roll Error (deg)
a	Least square fit of 10 minutes of random data with 3σ tolerance of 0.180 degree, maximum error for 10 average samples taken every half minute	0.223
b	Primary sensor mounting surface misalignment	0.100
c	Transverse momentum (tape recorder, worst case)	0.042
d		
e	Flywheel unbalance	0.00052
f	Solar torque (cyclic)	0.018
g	Gravity-gradient torque	0.059
h	Roll/yaw residual dipole (1 a-t-m^2 along transverse axis)	0.034
i	3σ tolerance (RSS-value) for items a through h	0.266
j	Residual magnetic dipole (0.05 a-t-m^2 along pitch axis), draft amassed in four orbits	0.03
k	Solar torque (twice per orbit unipolar torquing)	0.054
l	Vector addition of items j and k	0.062
m	Bias roll error	0.280
o	Maximum principal-point roll-error summation of items i, l, and m)	0.608

*Exclusive of errors within primary sensor optics

Pitch-error contributions are: (continued)

Attitude Deviations	Pitch Error (deg)
Horizon-sensing variation	±0.7
Servo-loop tolerances	±0.28
Momentum variation (±1.3 momentum offset)	±0.075
3σ error (RSS value)	±0.77

Table 11 summarizes the possible disturbances and the effects the disturbances would have on the satellite.

Table 12 contains possible transverse momentum disturbances; Table 13 shows results of a three-orbit computer simulation of uncompensated momentum effects.

As on previous TIROS and TOS satellites, no dynamic test of the magnetic control of the momentum vector was required. Calibration of the several coil and spacecraft magnetic-dipole moments and the spacecraft moments-of-inertia was sufficient to predict the behavior of the momentum vector when these dipoles act against the earth's magnetic field in orbit.

The complete closed-loop dynamic suspension test served to verify computer simulations and to evaluate the performance of the pitch-control system in the presence of electrical and mechanical transients generated by various equipment on the satellite.

FLIGHT ATTITUDE-CONTROL PERFORMANCE OF THE ITOS-1 DYNAMICS SUBSYSTEM

ITOS 1 was launched from WTR on a Delta N-6 long-tank two-stage six-solid launch vehicle. (Figure 4 shows the launch and injection sequence of events to attitude acquisition and stabilization.) The performance of the Delta was within predictions and was essentially as shown in Figure 4. Satellite spinup by the Delta was 4.3 rpm which was within the expected range of 3.16 to 5.04 rpm. Table 14 contains predicted and actual satellite performance values. Values through function 4 were predicted using an ITOS 1 stability plot with closed and open solar panels (Figure 26). The plot was prepared before launch using the predicted inertia values shown in Figure 26. After approximately 80 degrees of yaw-left maneuver and after the clockwise spinup, as viewed from Delta, engine-section separation was commanded by the Delta timer, and the wheel came up to 115 rpm; high-torque QOMAC was then commanded. QOMAC was commanded

Table 11

Summary of Disturbances and Effects

Source of Disturbance	Axis of Torque	Effect of Disturbance on Satellite
1. Residual magnetic dipole		
a. 1 a-t-m^2 along yaw axis	(1) Pitch	(1) Sinusoidal modulation of momentum, ±0.15 percent peak change in momentum, ±0.009 degree peak-pitch error, zero average over an orbit
	(2) Roll	(2) Slow precession of pitch axis around a cone, one complete cycle per orbit, maximum excursion of 0.034 degree
b. 1 a-t-m^2 along roll axis	(1) Pitch	(1) Sinusoidal modulation of momentum, ±0.3 percent peak change in momentum, ±0.017 degree peak pitch error, zero average over an orbit
	(2) Yaw	(2) Slow precession of pitch axis around a cone, one complete cycle per orbit, maximum excursion of 0.034 degree
c. 0.05 a-t-m^2 along pitch axis (resolution of MBC coil)	$\pm\hat{e}$	Net drift of ±0.086 degree per day about the $\hat{b}$ axis
2. Solar pressure	(1) $\hat{\ell}\hat{b}$ plane	(1) Slow precession of momentum vector in response to torque, which is normal to a plane defined by the spacecraft pitch (spin) axis and the sunline; magnitude and direction is function of sun angle and season

Disturbance Torque in 10^{-4} inch-pounds

Time of Year	Sun Angle (deg)		
	30	45	60
Summer Solstice	$+0.4\hat{\ell} - 0.49\hat{b}$	$+0.32\hat{\ell} - 0.38\hat{b}$	$+0.23\hat{\ell} - 0.27\hat{b}$
Winter Solstice	$-0.25\hat{\ell} - 0.58\hat{b}$	$-0.20\hat{\ell} - 0.46\hat{b}$	$-0.15\hat{\ell} - 0.33\hat{b}$

Table 11 (continued)

Source of Disturbance	Axis of Torque	Effect of Disturbance on Satellite
2. Solar pressure (continued)		Maximum potential ℓ precession of 1.35 degrees per day is corrected by unipolar torquing. Maximum potential b precession of +0.93 degree per day is corrected by magnetic bias torquing.
	(2) $\hat{\ell}\hat{b}$ plane	(2) Sinusoidal modulation of attitude angles, magnitude is function of sun angle Sun Angle (deg) / Peak-to-Peak Variations (deg) 30 / 0.027 45 / 0.018 60 / 0.009
	(3) Pitch	(3) Sinusoidal modulation of momentum, zero average per orbit, peak change is function of sun angle Sun Angle (deg) / Momentum Change (max percent) 30 / 0.037 45 / 0.020 60 / 0.027
3. Magnetic hysteresis and eddy-current losses	Pitch	Slow decay of momentum; 1 percent per week maximum
4. Gravity gradient	Roll	Sinusoidal precession at orbital frequency, zero average per orbit; peak change in attitude is 0.059 degree
	Pitch	Slow decay of momentum; 2.8 percent per week nominal. Occasional momentum control is required
5. Internal rotating components (uncompensated transverse momentum)	—	Residual offset caused by continuously running components is 0.04 degree. Maximum half-cone nutation angle with anticipated payload duty cycles is 0.042 degree

Table 12

Transverse Momentum Disturbances

Component	Momentum (in. -lb-sec)	Operation
Two radiometers	0.14	Continuous (two simultaneously)
Two SR recorders	Record: 0.0025 Playback: 0.04	One records continuously for a half orbit or a full orbit; both playback simultaneously every third orbit.
One incremental tape recorder	0.002	Playback for 1 minute once per orbit
AVCS recorder*	0.02	Records for 10.25 seconds every 260 seconds, 11 times per orbit Playback every third orbit

*Usually, one of the two AVCS recorders is operated; the redundant unit is reserved for backup.

on orbit 0002; by orbit 0004, the roll/yaw angle was reduced until the pitch axis was nearly normal to the orbit plane. Referring to Figure 26 and following the 4.3-rpm spinup to the zero-wheel speed, or I_3 line (panels closed), shows that the 4.3-rpm spinup provided an ITOS-1 total-system momentum of approximately 305 in. -lb-sec. As the wheel came up to 115 rpm with panels closed, the satellite passed through an unstable region in approximately 11 seconds. The requirement for gyroscopic stability as the wheel speeded up to 115 rpm was to satisfy the following equation:

$$W_3 (I_3 - I_1) + W_f I_f > 0$$

Table 13

Three-Orbit Computer Simulation of Uncompensated Momentum Effects*

Orbit	Disturbance	Maximum Nutation Angle (deg)	Jitter (deg/sec)
1	AVCS recorder, 2×10^{-2} in.-lb-sec 10.25 sec on, 249.75 sec off, 11 cycles	0.056	0.010
2	AVCS recorder, 2×10^{-2} in.-lb-sec 10.25 sec on, 249.75 sec off, 11 cycles	0.028	0.005
3	AVCS recorder, 2×10^{-2} in.-lb-sec 10.25 sec on, 249.75 sec off, 11 cycles SR recorder playback 4×10^{-2} in.-lb-sec for 9 minutes AVCS recorder playback 2×10^{-2} in.-lb-sec for 6 minutes (during SR playback)	0.042	0.008
Completion of orbit 3		0.018	0.003

*Initial nutation angle = 0.056 degree

Where

W_3 = equipment module spin rate about the pitch axis

W_f = flywheel spin rate relative to the equipment module

I_3 = spacecraft moment-of-inertia about the spin axis

I_1 = maximum spacecraft moment-of-inertia about a transverse axis

I_f = flywheel moment-of-inertia

The conditions for gyroscopic stability were satisfied.

Table 14

ITOS-1 Dynamics-Subsystem Predicted and Actual Performance

Function	*Predicted Value	*Actual Value
1. Body rate at separation solar panels closed	+3.16 to +5.04 rpm	+4.3 rpm
2. Body rate with wheel at 115 rpm solar panels closed	+2.03 rpm	+2.03 rpm
3. Body rate with wheel at 150 rpm solar panels closed	+1.3 rpm	+1.3 rpm
4. Body rate with wheel at 150 rpm solar panels open	+0.8 rpm	+0.8 rpm
5. Spacecraft body rate when the command to close the pitch loop was sent	-0.1 to +0.5 rpm	+0.22 rpm
6. Time to lock on earth after the command to close the pitch loop	Within 11 minutes	<1 minute
7. Aligns and maintains attitude about pitch axis to an earth reference	±1 degree	±1 degree
8. Aligns and maintains momentum vector about orbit normal	±1 degree	±1 degree
9. Pitch jitter Roll jitter	0.05 degree 0.05 degree	0.005 degree max 0.005 degree max
10. Half-cone nutation angle and nutation period	0.3 degree, 37.5 sec	0.025 degree, 32.5 sec at 150 rpm and 33.0 sec at 135 rpm

*In volts unless otherwise specified

Table 14 (continued)

Function	*Predicted Value	*Actual Value
11. Momentum decay rate to decrease wheel-speed from 150 rpm to 135 rpm without using MCC	176 orbits	176 orbits (482 to 658)
12. Frequency of MCC torquing to maintain WS 133 to 137 rpm	Torque during one pass every 31 orbits	Torque during one pass every 31 orbits
13. Frequency of MCC torquing to maintain WS 148 to 152 rpm	Torque during one pass every 31 orbits	Torque during one pass every 31 orbits
14. Pitch attitude error at 135 rpm	-0.6 degree	-0.6 degree or less
15. High-torque QOMAC performance	5.2-degree precession per half orbit. QOMAC and MBC in parallel (34.944 a-t-m^2), MBS position 11	3.233 degrees/cycle
16. Frequency and rate-of-torquing high QOMAC	3.233 degrees/cycle orbit #2 only	Orbit #2 only as predicted
17. Low-torque QOMAC performance	1.2 degrees precession per orbit. QOMAC coil only (3.85 a-t-m^2) 0.55 degree granularity	Performed as expected on orbits 118, 245, 274, 415, 1133, at 0.55 degree/cycle
18. Frequency and rate-of-torquing-low QOMAC	0.55 degree/cycle	Not used since orbit 415 and 1133 for moon-conflict prevention; performed as in #17
19. Magnetic-bias performance—as backup for QOMAC	0.36-degree to 3.6-degree precession per day; 0.36-degree granularity MBS positions 1 to 10 (0.1 to 1 a-t-m^2)	Performed as predicted at 0.666 degree/cycle

*In volts unless otherwise specified

Table 14 (continued)

Function	*Predicted Value	*Actual Value
20. Frequency and rate-of-torquing of MBC coil	Approximately a weekly change; use is continuous	MBS used to change torque current as required
21. Unipolar torque performance	0.064-degree to 4.1-degree precession per day; 0.064-degree granularity	At turnover to NOAA 15 min after ascending node, PW was 80 sec on orbit 600 and 19 min on orbit 800 AAN PW = 144 sec
22. Frequency and rate-of-torquing of unipolar torque	Use continuously and change weekly.	A 0.1-minute error accumulates, requiring reset every 15 to 20 orbits.
23. Permanent magnet with N-S pole along spin axis for magnetic bias effect	0.7 a-t-m^2	0.57 a-t-m^2 was considered ideal. The effectiveness is approx. 0.7 a-t-m^2.
24. Pitch loop #1 Open loop coarse Open loop normal Closed loop fine Closed loop coarse Emergency mode	Operated 115 rpm 150 rpm 150 rpm 150 rpm Not operated	 115 rpm 150 rpm 150 rpm 150 rpm Not operated
25. Pitch loop #2 Open loop coarse Open loop normal Closed loop fine Closed loop coarse Emergency mode	Operated orbits 66 to 217 Not operated Not operated 150 rpm Not operated Not operated	 150 rpm
26. DSAS	Provide sun angle and spacecraft body rate	Performed as expected
27. Separation switches	Provide power to selected pitch-loop motor at separation	Performed as expected

*In volts unless otherwise specified

Table 14 (continued)

Function	*Predicted Value	*Actual Value
28. Pitch horizon sensors (PHS)		
PHS #1 S/E beacon T/M	0.338 to 1.78	1 to 1.6
PHS #1 S/E SR T/M	0.338 to 1.78	1 to 1.6
PHS #2 S/E beacon T/M	0.338 to 1.78	1 to 1.6
PHS #2 S/E SR T/M	0.338 to 1.78	1 to 1.6
PHS #1 E/S beacon T/M	0.338 to 1.78	1 to 1.6
PHS #1 E/S SR T/M	0.338 to 1.78	1 to 1.6
PHS #2 E/S beacon T/M	0.338 to 1.78	1 to 1.6
PHS #2 E/S SR T/M	0.338 to 1.78	1 to 1.6
PHS noise amplitude	<330 mv	<300 mv
29. Pitch-index pulse amplitude	2.2	≃2
30. Roll horizon sensors (RHS)		
RHS #1 S/E beacon T/M	0.338 to 1.78	1 to 1.6
RHS #1 S/E SR T/M	0.338 to 1.78	1 to 1.6
RHS #2 S/E beacon T/M	0.338 to 1.78	1 to 1.6
RHS #2 S/E SR T/M	0.338 to 1.78	1 to 1.6
RHS #1 E/S beacon T/M	0.338 to 1.78	1 to 1.6
RHS #1 E/S SR T/M	0.338 to 1.78	1 to 1.6
RHS #2 E/S beacon T/M	0.338 to 1.78	1 to 1.6
RHS #2 E/S SR T/M	0.338 to 1.78	1 to 1.6
RHS noise amplitude	<330 mv	<300 mv

*In volts unless otherwise specified

Upon reaching 115 rpm, some of the satellite body momentum was transferred to the wheel. The satellite body rate decreased to 2.03 rpm; the total system momentum remained the same. Figure 27 shows the momentum interchange as the wheel was commanded to 150 rpm (panels closed). The panels were opened on orbit five, increasing the satellite moment-of-inertia (Figure 27). The increase in the satellite moment-of-inertia decreased the body spin rate to 0.8 rpm. The total system momentum remained the same. Based on the 4.3-rpm spinup by the Delta, performance was as expected.

CDA stations at Wallops Island, Virginia; and Gilmore Creek, Alaska; commanded by MCC's to reduce the body spin rate from 0.8 to 0.2 rpm by orbit 42, when earth lockon was commanded. The satellite body rate was so low that lockon occurred in approximately 1 minute. During MCC torquing, the MWA bearing temperature reading was approximately 8° C; therefore, equipment was turned on in an effort to raise the temperature because higher temperatures help prevent brush wear. Because a higher temperature did not lessen brush wear on motor 2, a decision was made to install heaters on future ITOS MWA's that will employ brush motors.

Opening the solar panels and rotating the wheel to 150 rpm before separation could dynamically prevent the long MCC torquing situation, and provide the 212 in.-lb-sec required for ITOS-1 mission-mode operation. The Delta would not have to fire roll jets to spin ITOS. Optimum momentum for lockon would be possible in the second orbit. The momentum coils would be used as they now are to maintain desired system momentum and wheelspeed. The Delta timer could provide a nominal satellite roll rate of 3 rpm. The correct momentum for lockon would be provided at separation and, when the panels open and the wheel is at 150 rpm, the satellite spin rate would be near zero and earth-lock could be commanded. MCC torquing would be required only during mission mode to maintain wheelspeed.

MWA heater elements, installed to supply heat during acquisition and standby periods when equipment is turned off, should provide proper temperature to reduce brush wear. Figure 28 is a plot of wheelspeed showing 6 MCC torquing intervals and the time for wheelspeed to drift from 150 to 135 rpm without MCC torquing. Torquing maintains the desired wheelspeed and system momentum during mission mode, with the wheel at 150 to 135 rpm. Table 14 shows the frequency of momentum-coil use and the time required for correction. System-momentum corrections during one orbit in about 31 orbits reestablished the desired momentum.

Table 14 also shows predicted spacecraft performance; actual performance after launch was well within expectations.

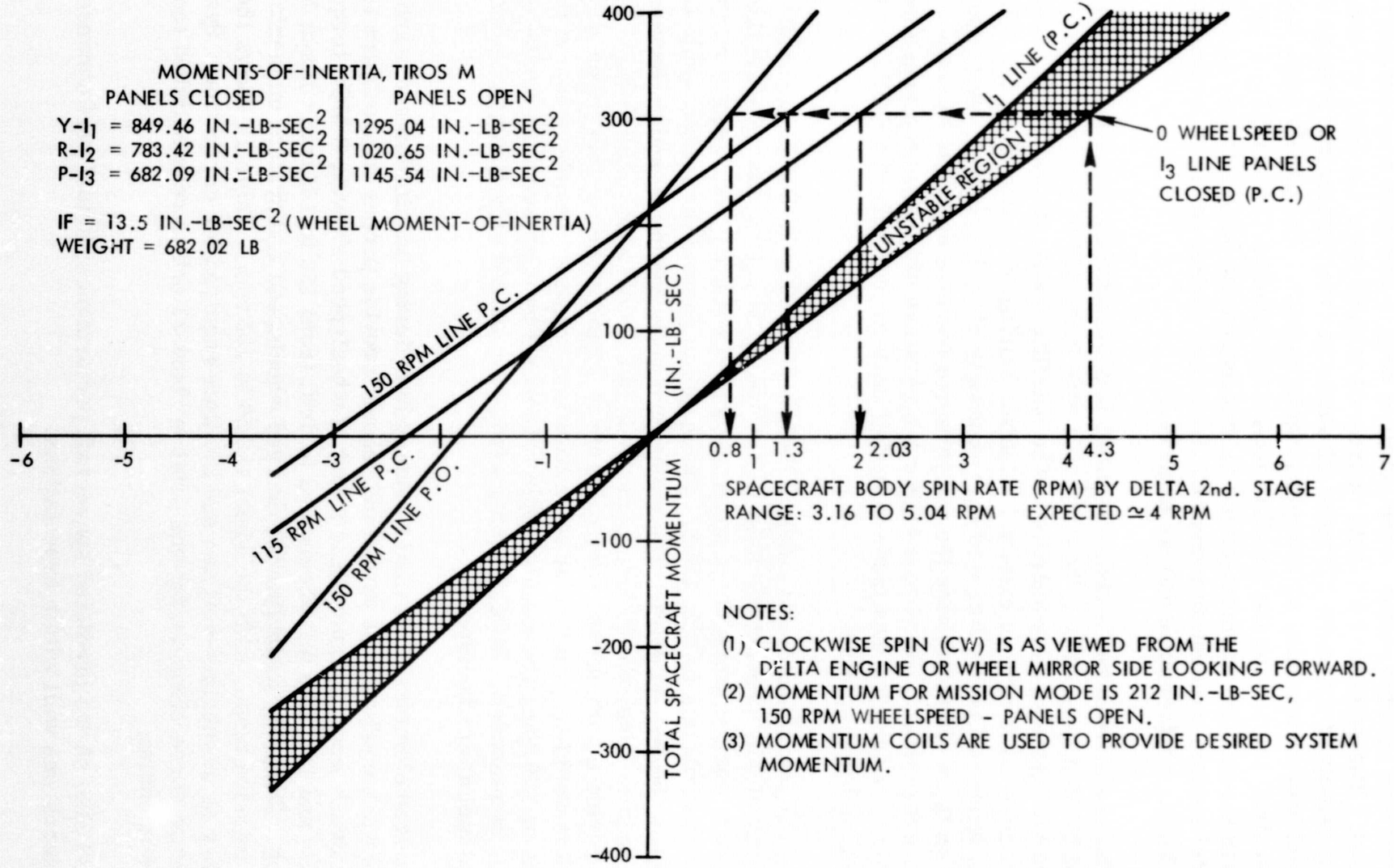

Figure 27. ITOS-1 Stability Plot

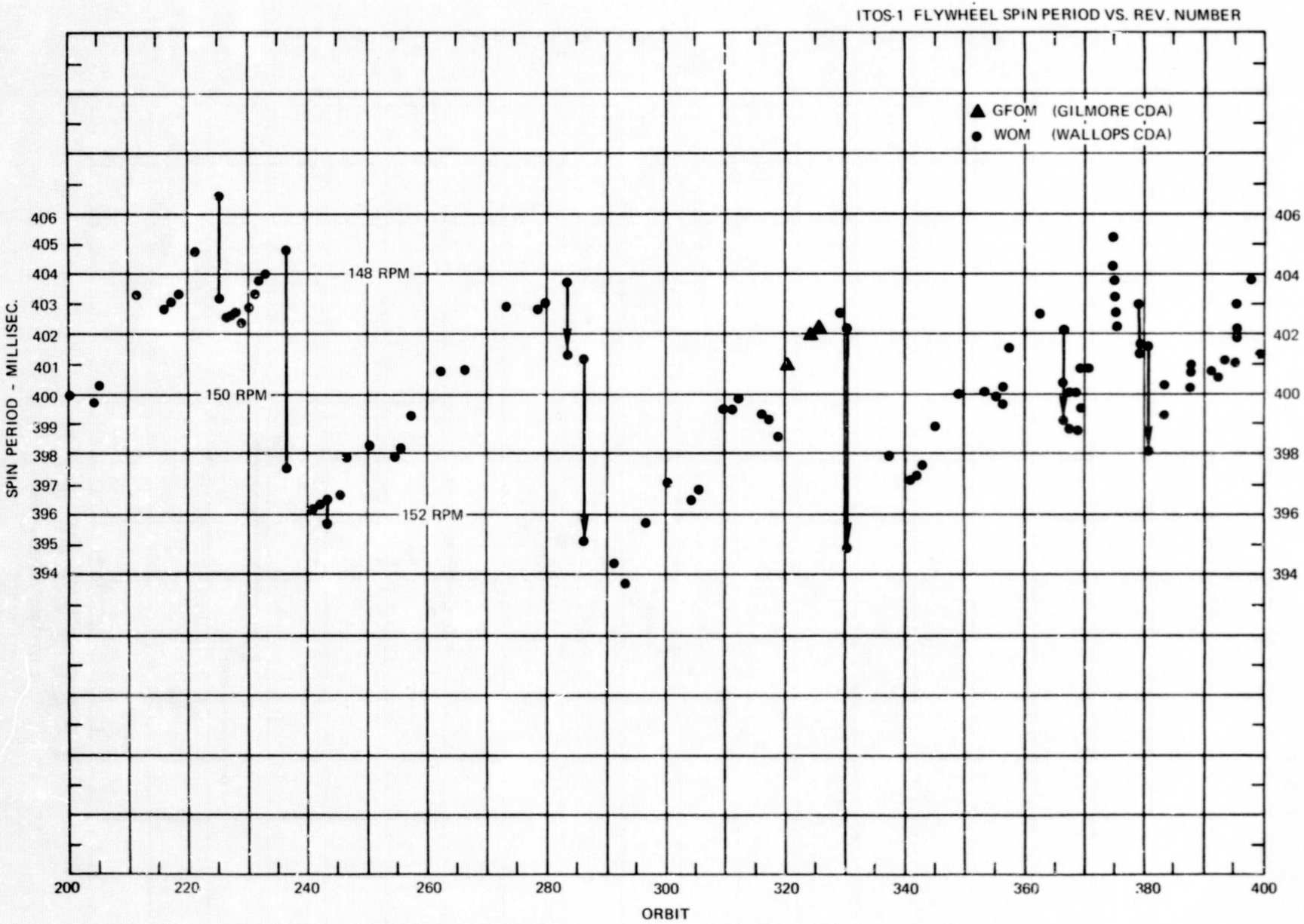

Figure 28. Momentum-Control-Coil Torquing (sheet 1 of 6)

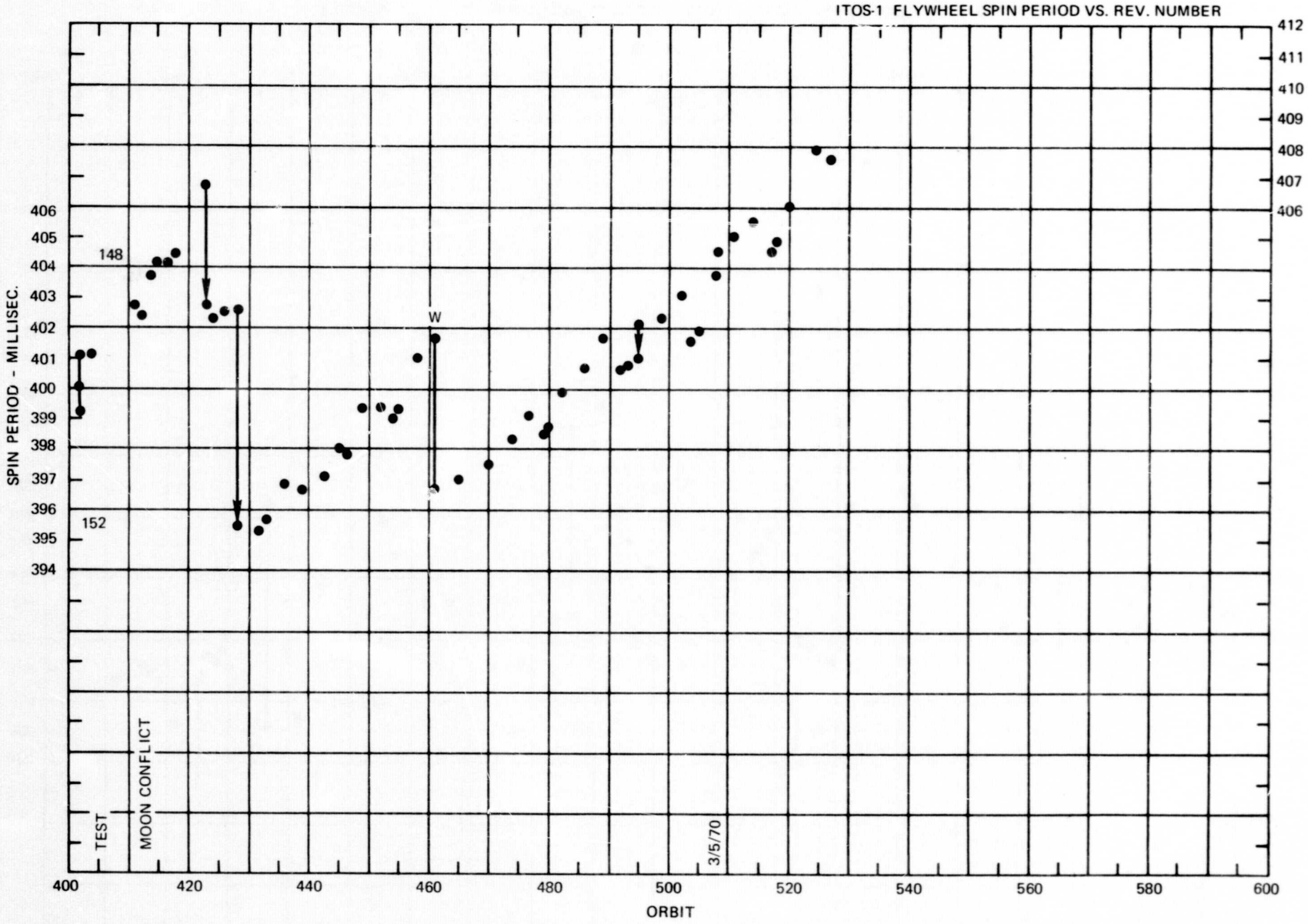

Figure 28. Momentum-Control-Coil Torquing (sheet 2 of 6)

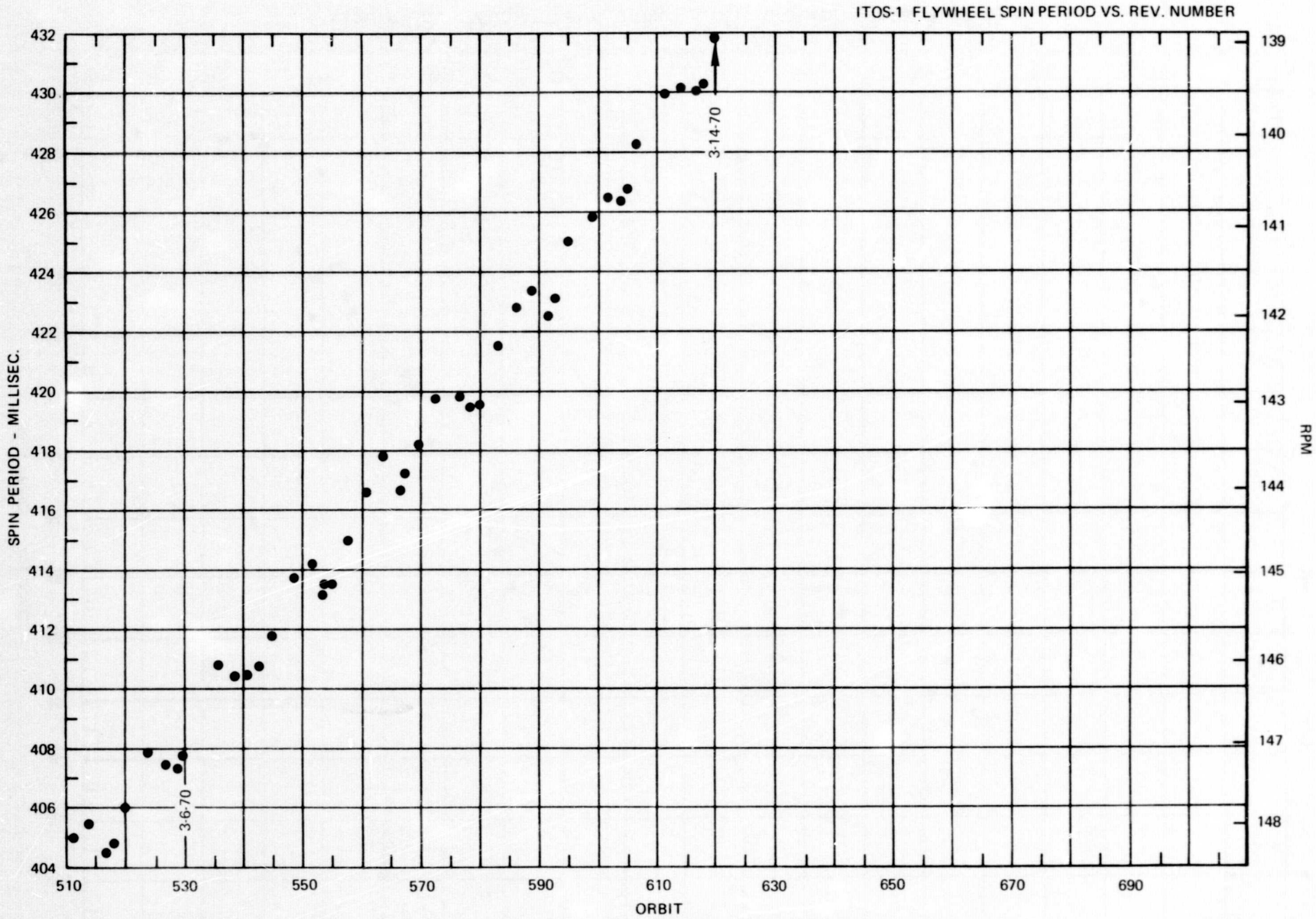

Figure 28. Momentum-Control-Coil Torquing (sheet 3 of 6)

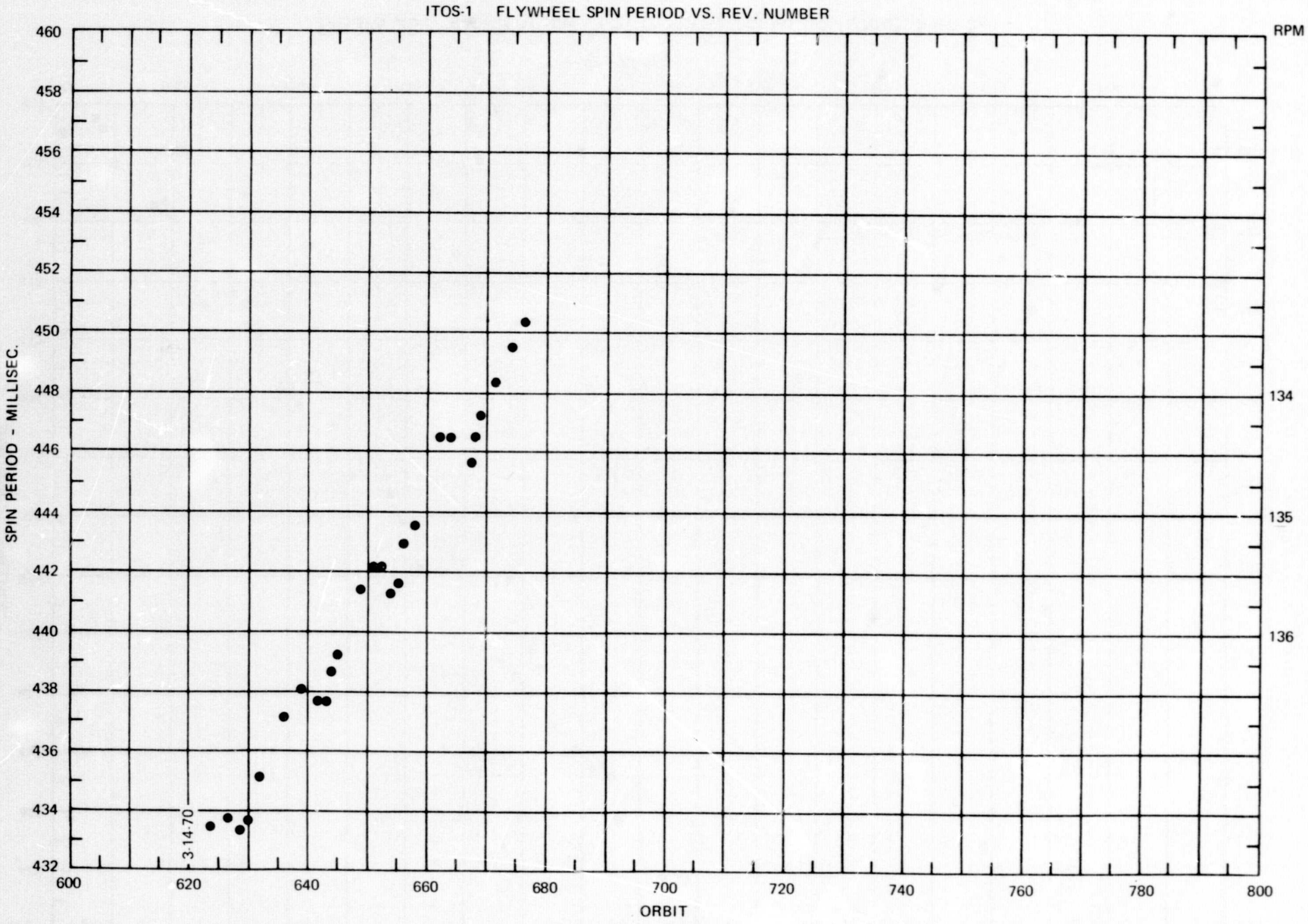

Figure 28. Momentum-Control-Coil Torquing (sheet 4 of 6)

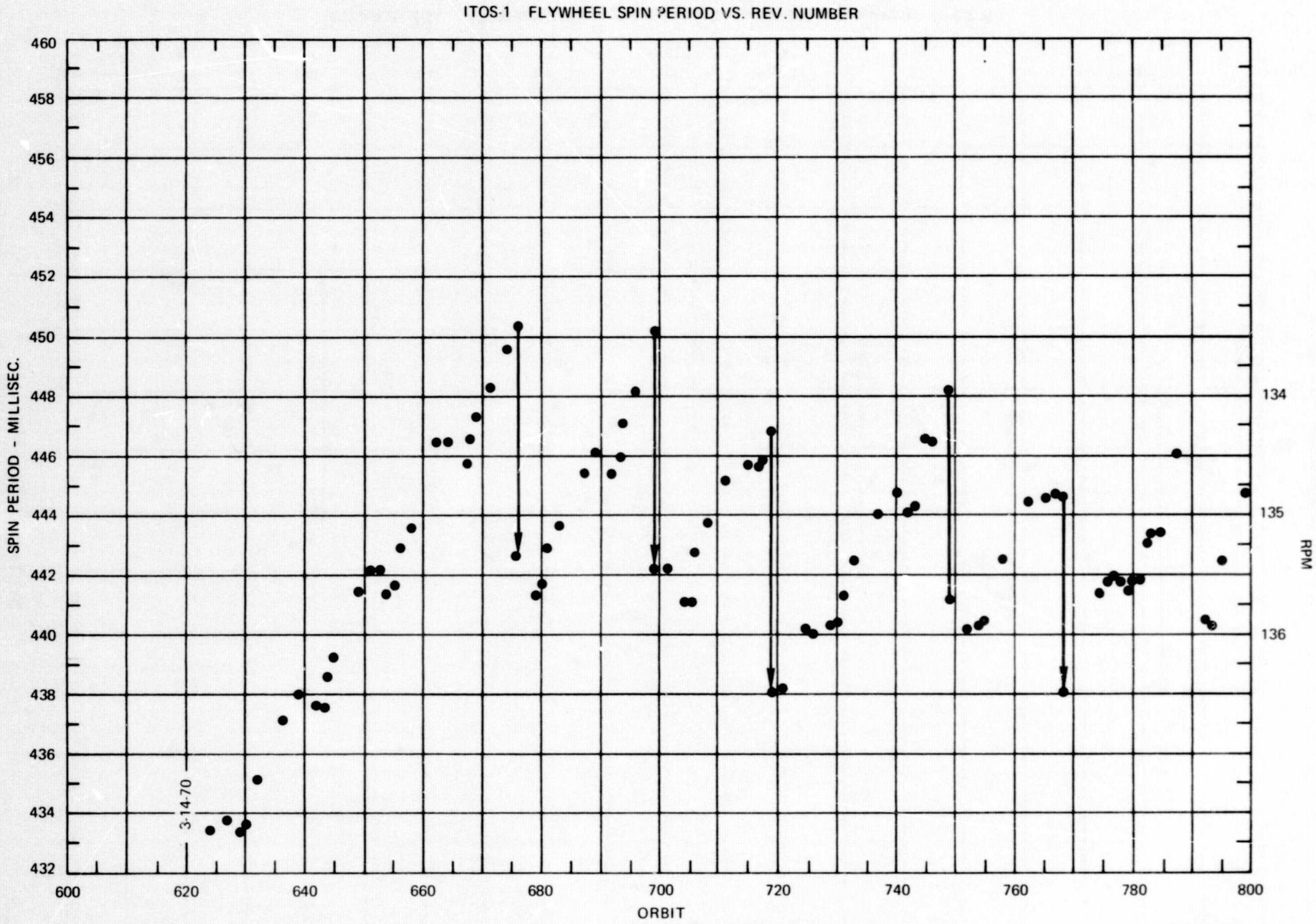

Figure 28. Momentum-Control-Coil Torquing (sheet 5 of 6)

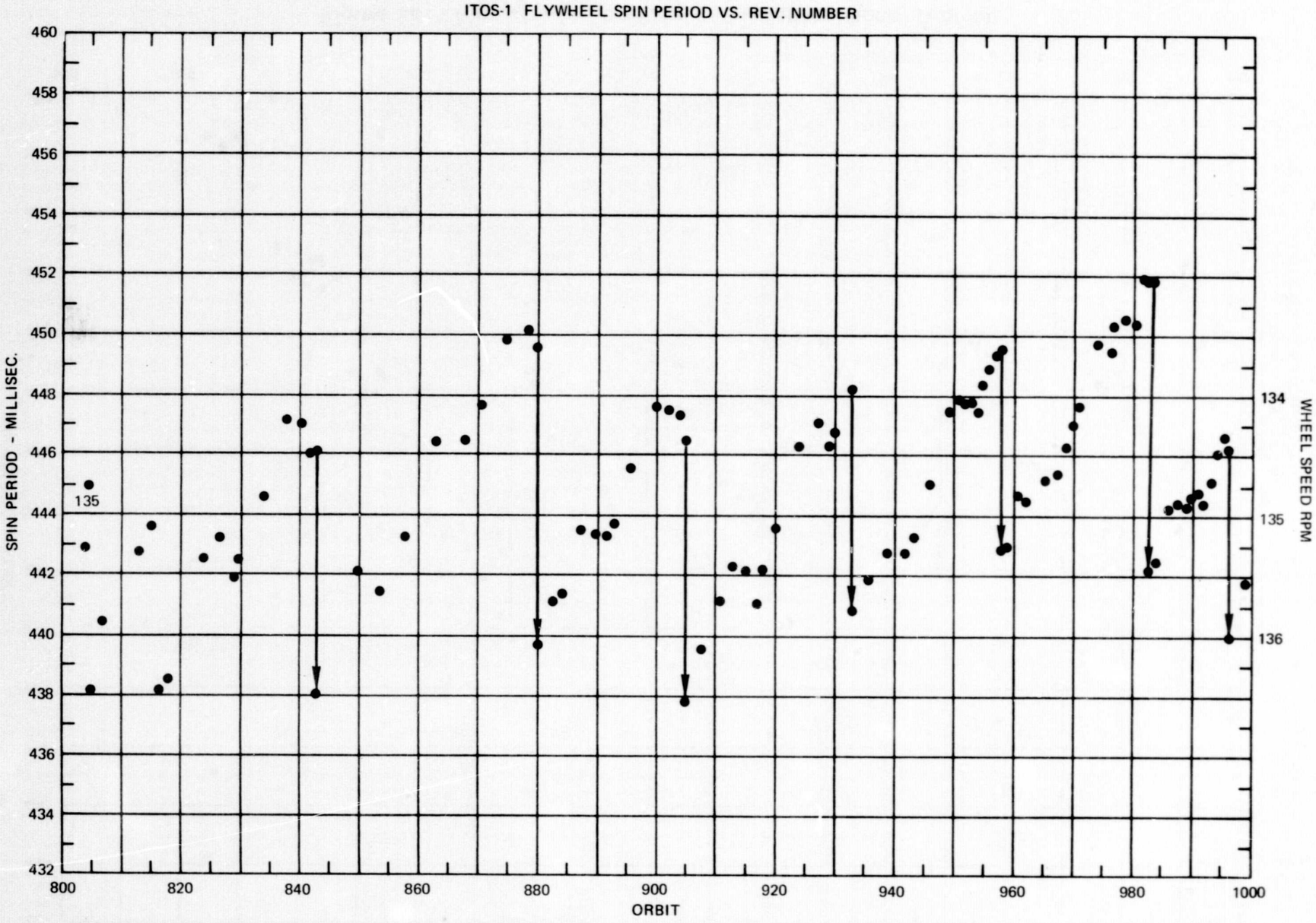

Figure 28. Momentum-Control-Coil Torquing (sheet 6 of 6)

Before the previously mentioned motor-2 brush problem, pitch-loop 2 performed successfully from orbit 66 to orbit 217. The brush-wear problem resulted in the decision to switch back to motor 1.

The switching was smooth, and there was negligible nutation and wheelspeed change. The pitch loop is not cross-strapped to motor 1; therefore, the only remaining pitch-loop redundancy is the pitch-loop 2 horizon sensor cross-strapping to pitch-loop 1. A brushless motor system is scheduled to go on ITOS D, eliminating the brushes, strain gages, and the requirement for heater elements.

The evaluation of the attitude-control system is limited because the computer is unable to accurately identify the sky-earth and earth-sky transitions. Because of the high-earth thermal uncertainty, the computer technique is subject to errors; however, effort is being continued in this area. The most accurate technique used to determine roll angle has been the scanning radiometer (SR) data which has also been used to determine nutation angle. The accuracy with the radiometer signal is approximately 0.3 degree. With zero-pitch error, the SR scans the earth's major diameter, perpendicular to the satellite's flight path or roll axis, every 1.25 seconds. The scan lines terminate and the back-scan telemetry starts and stops for a fixed period of the scan time. Shortly after the telemetry stop signal, the trailing edge of a 7-bit sync pulse occurs. The interval between the trailing edge of this pulse and the SR sky-earth crossing determines the satellite roll. The interval for zero roll is approximately 16.28 degrees. Smaller intervals reveal a clockwise roll.

Figure 29, an SR plot prepared by NOAA for orbit 2733, shows a maximum roll of approximately 0.393 degree. The SR plot is for a complete orbit. Figure 30 is a real-time horizon-sensor manual-data plot for a 14-minute period of orbit 701. The plot is based on data obtained from the roll-horizon sensor during 14 minutes of the 115.1-minute orbit. The roll/yaw errors in the 14-minute pass were determined by the plot and some guesswork.

Using the PIP and sky-earth roll sensor pulse acquires approximately 0.7 degree of accuracy. Two CO_2 sensors are to be incorporated on ITOS D to replace the four horizon sensors. Both CO_2 sensors will provide pitch and roll data. The earth-crossing signal will be of narrower spectral interval and narrower bandwidth, making it suitable for use with the computer for around-the-orbit attitude determination and free from moon interference. The computer can be programmed to determine roll angle and nutation from the SR data around the orbit, providing redundancy for this function. Table 14 lists the amplitude values of the typical attitude-sensor data signals. The beacon and SR telemetered data amplitudes are approximately the same. Figure 31 shows the typical beacon data for the roll-sensor pulse and PIP; Figure 32 shows the pitch-sensor pulse data. (Figure 13 shows the sensor-signal levels.)

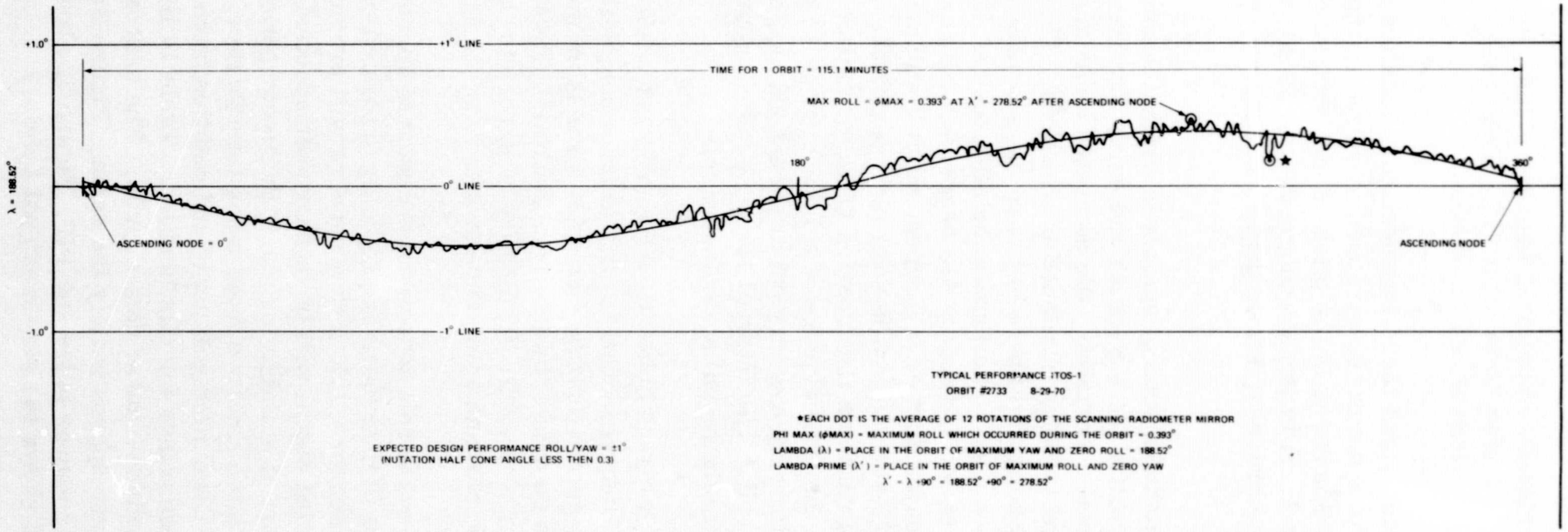

Figure 29. SR Plot of Satellite Roll for Orbit 2733

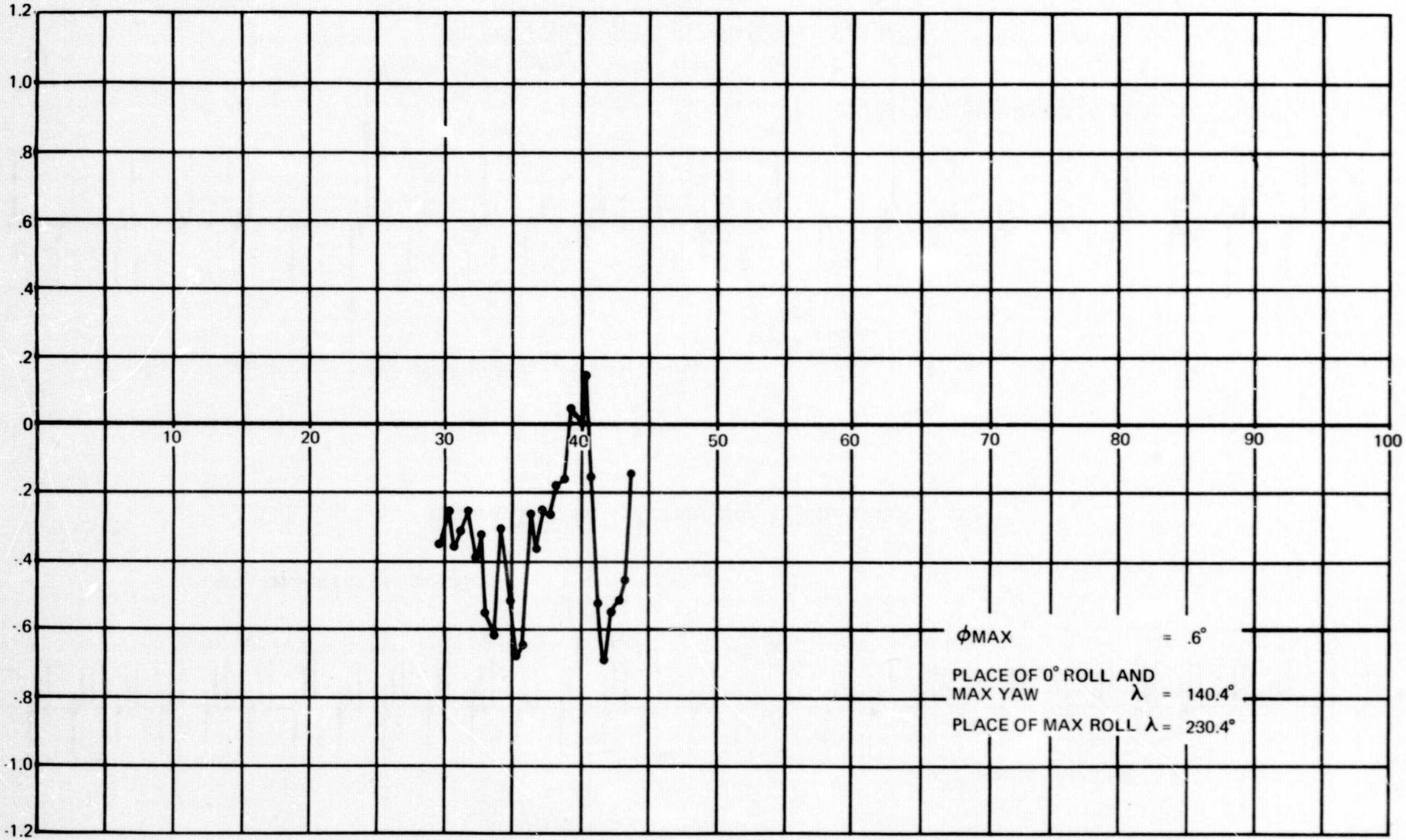

Figure 30. Horizon Sensor Manual Plot of Satellite Roll for Orbit 701

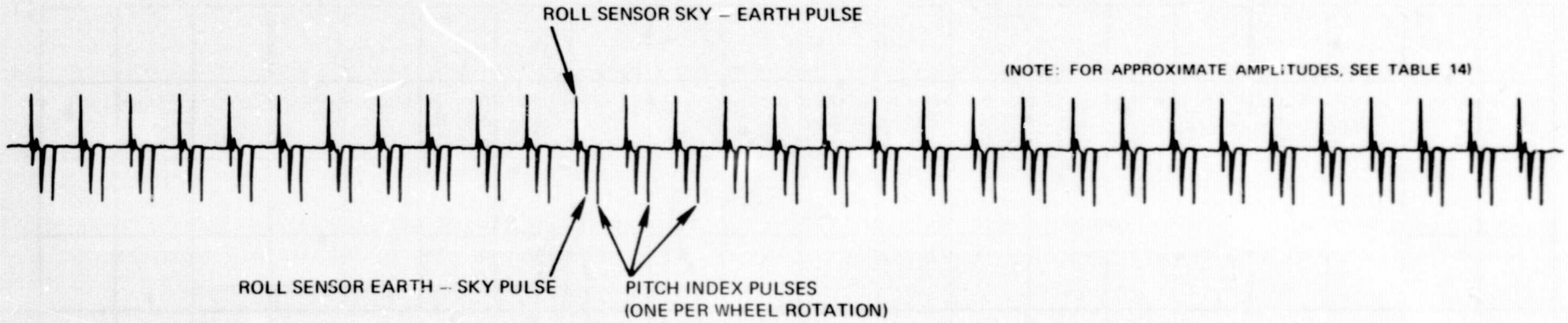

Figure 31. Roll-Sensor and Pitch-Index Pulses

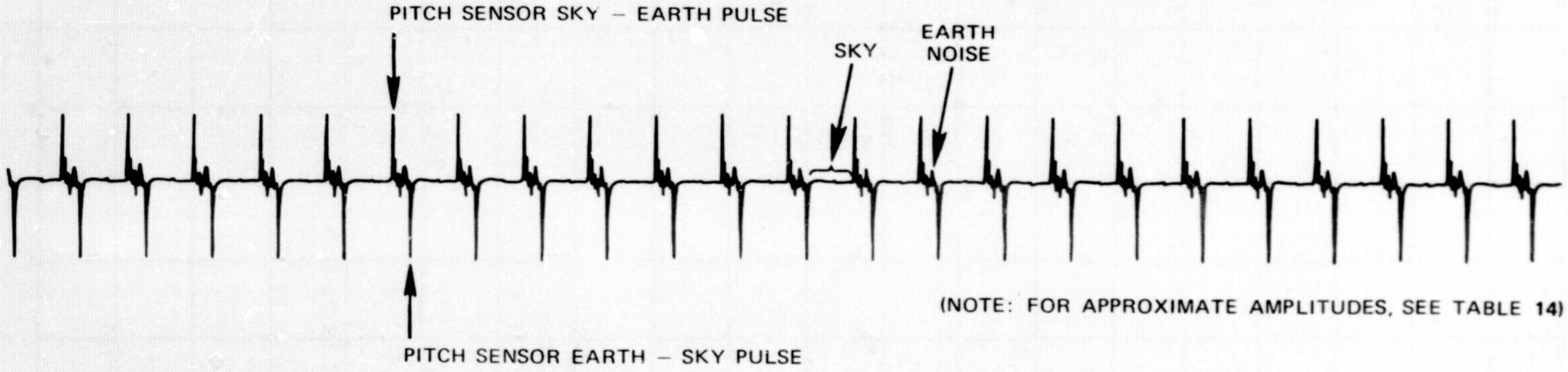

Figure 32. Pitch-Sensor Pulse

ANOMALIES IN ORBIT FROM LAUNCH TO JUNE 15, 1970

Questionable DSAS—Although questionable DSAS burst occurred during the early stages of acquisition, it did not interfere with determining the satellite spin rate or gamma angle. This occurrence probably resulted from gray-scale illumination at extremes of nutation setting during the approximately 10-degree turnaround and while the satellite was nutating and rotating about its pitch axis, resulting in incorrect readout.

Clock error—A unipolar clock-setting error in unipolar torquing caused the satellite roll angle to drift approximately 4 degrees, which resulted in pitch-sensor reception of a moon signal of sufficient energy to cause moon lockon and loss of earth lock on orbit 414. Correcting the programmer, by properly resetting the unipolar torquing every 15 to 20 orbits, eliminated the clock-setting errors and there has been no identified moon lockon since orbit 414 in February 1970. Figure 33 shows scanning radiometer pictures as a result of the moon lockon. The earth was reacquired on orbit 415. The nutation period, approximately 33 seconds, can be determined by counting SR scan lines (1.25 sec/scan line) between nutation peaks.

Brush wear effect—Motor-2 brush wearout, probably caused by carbon dust shorting the commutator-2 segments, placed the load on motor 1, and wheelspeed was allowed to drift down to 135 rpm to decrease the load. (See Table 14.) Lowering the wheelspeed reduced the back electromotive force of motor 1, increasing the torque margin of motor 1, to overcome the drag torque of motor 2. The result of this action lowered the spacecraft momentum but not to the region (115 to 130 rpm) where pitch lock could be lost. Figure 32 is a plot of motor current versus MWA speed for a range of motor terminal voltages. The lower limit of unregulated bus voltage occurs at the end of spacecraft night; therefore, if motor voltage requirements exceed available bus voltage, pitch lock will be lost. Should such a situation occur, wheelspeed and, therefore, system momentum could be further reduced to maintain pitch lock, which reduces the required voltage to run the motor for the same or greater torque generation (Figure 34). The exact limit to which wheelspeed can be reduced without losing pitch lock is questionable; however, the 115-rpm clamp circuit prevents lower speeds.

Inadvertant switching—During a command sequence on orbit 308, the pitch loop was switched from normal to coarse gain, and almost simultaneously, the regulators switched from one to two. The cause of the inadvertent switching is unknown, but the problem did not reoccur during subsequent regulator switching.

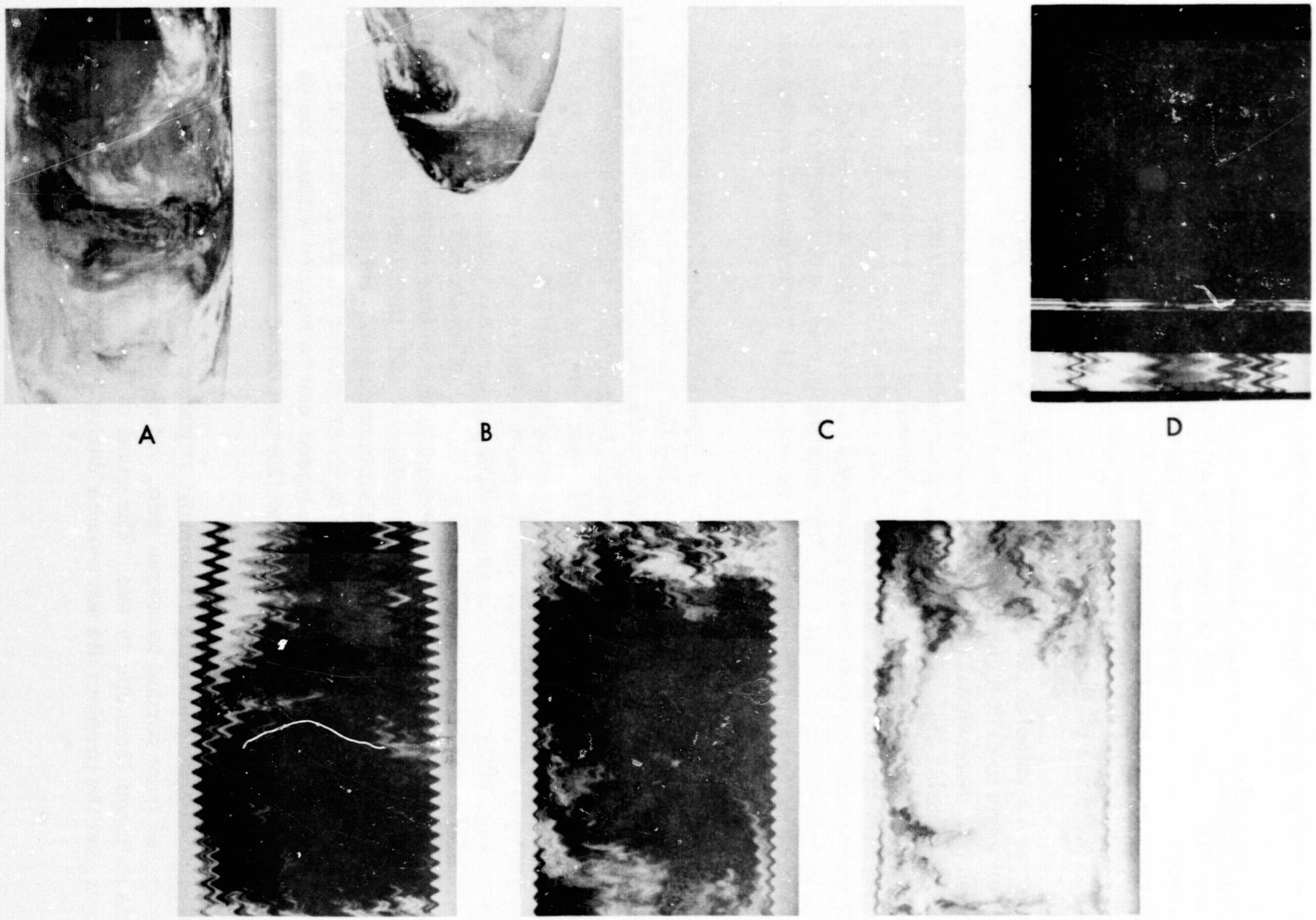

Figure 33. Moon-Conflict SR Pictures

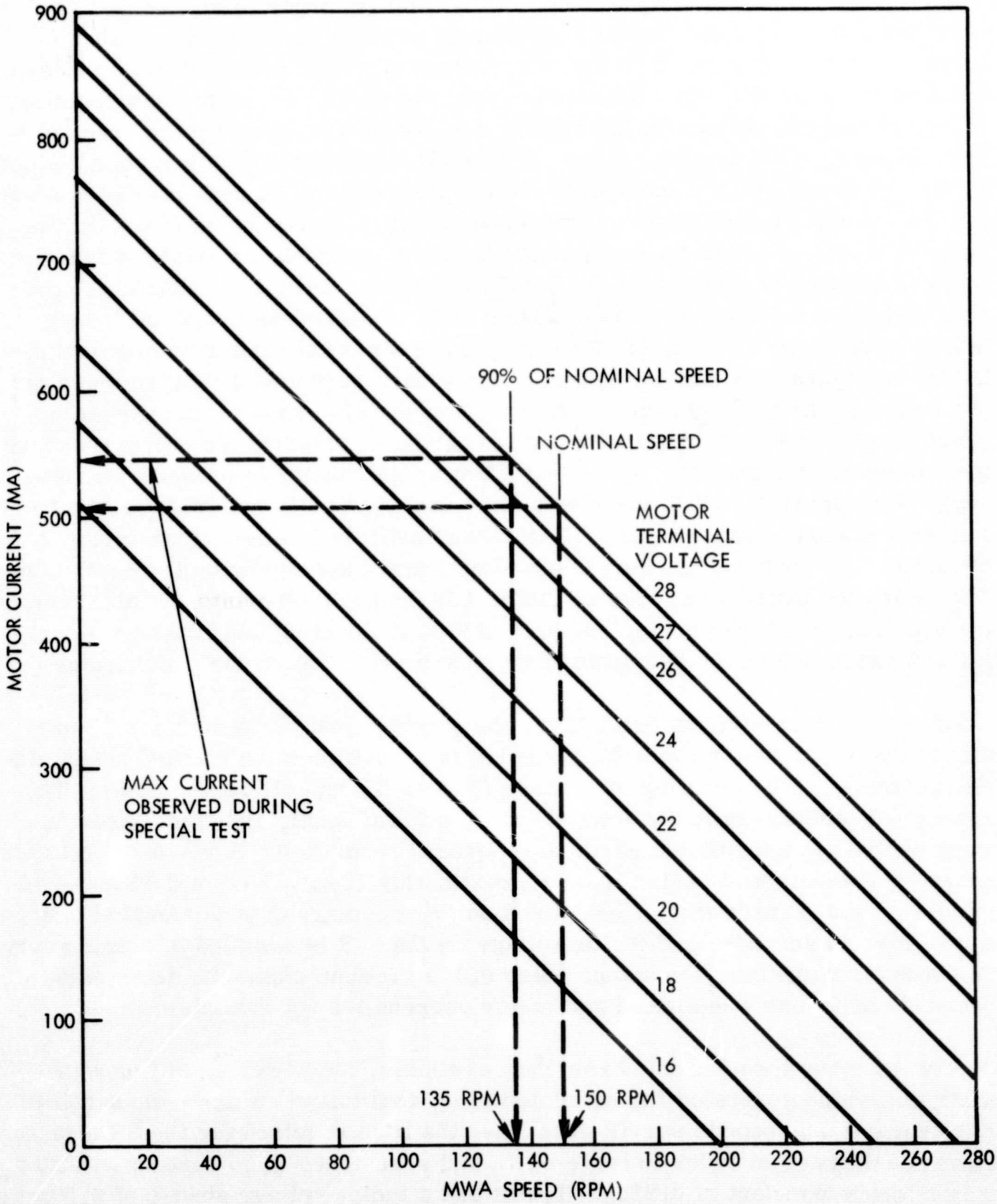

Figure 34. Motor 1 Current versus Speed

Motor-voltage return—During orbit 908 (Figure 35) and until orbit 930, the motor voltages appeared to be returning to normal. During orbit 930, motor-1 voltage began to increase again and motor-2 voltage began to decrease. At about orbit 980 and since then, motor 1 leveled off at about 21 volts and motor 2 at about 4.5 volts. Before orbit 908, the voltage of motor 1 was about 25 volts and motor 2 about 1 volt. This situation caused the previously mentioned decision to reduce the wheelspeed to 135 rpm at the cost of a predicted pitch error of approximately -0.6 degree. No picture or SR data degradation has been noticed. Figure 36 shows MWA wheelspeed-versus-pitch error. A possible explanation for the voltage changes is the shorting, removal of short, and partial shorting again of motor-2 commutator segments by motor-2 brush material. After the motor 2 brushes wore down to the beryllium-copper arm, the metal arm probably dislogged some of the silver-carbon brush material as the metal brush holder wore smooth. (Figures 20 and 21 show the brush-motor and the brush-holder configurations and how the above may have happened.) The voltages did not return to the 25- and 1-volt values, but to the 21- and 4.5-volt values because the carbon-silver brush material redistributed itself but not entirely between the commutator segments. Some beryllium-copper metal is probably wearing away. On August 30, 1970, there was electrical continuity and motor 2 back emf was still available on telemetry. Performance will be interesting when motor-1 brushes wear down and the beryllium-copper arms are riding on the commutator. The estimated brush-wear rate on motor 1 is 3 mils/1000 orbits. With remaining brush of 35.67 mils on September 1, 1970, motor 1 should continue to run for 2.5 years before the beryllium-copper arm will ride on the commutator.

Loss of pitch lock—During orbit 1144, the satellite lost earth-lock for 13 minutes. The moon was in the orbit plane but in a position to be blanked out by the pitch circuits. The attached SR picture (Figure 37) and SR data indicate: The spacecraft pitched, returned toward earth, pitched again, and made 3 revolutions before recapturing the earth on the fourth revolution. A review of SR data shows that wheelspeed varies from approximately 120 to 189 rpm during the 13-minute period (Figure 38). Wheelspeed on SR telemetry data is sampled one time every 20 seconds, and motor voltage on the ITR is sampled one time every 32 seconds; therefore, the actual cause of the problem cannot be determined because continuous wheelspeed and motor current are not available.

One of the many theories is: From data available, the power amplifier was saturated which generated the maximum electrical torque to move the satellite. Estimating 1.25 seconds per SR scan line, the time required for the SR scan to travel 55 degrees in order to leave earth and scan space is 35 seconds. With a motor torque constant of 0.21 in.-lb/volt and a motor voltage change of 6.5 volts, the developed disturbance torque was $6.5 \times 0.21 = 1.305$ in.-lb. This torque would accelerate the satellite whose pitch inertia is determined to be 1128.7 in.-lb-sec^2, at 0.0012 rad/sec^2 ($\alpha = T/I$). The resulting acceleration would move

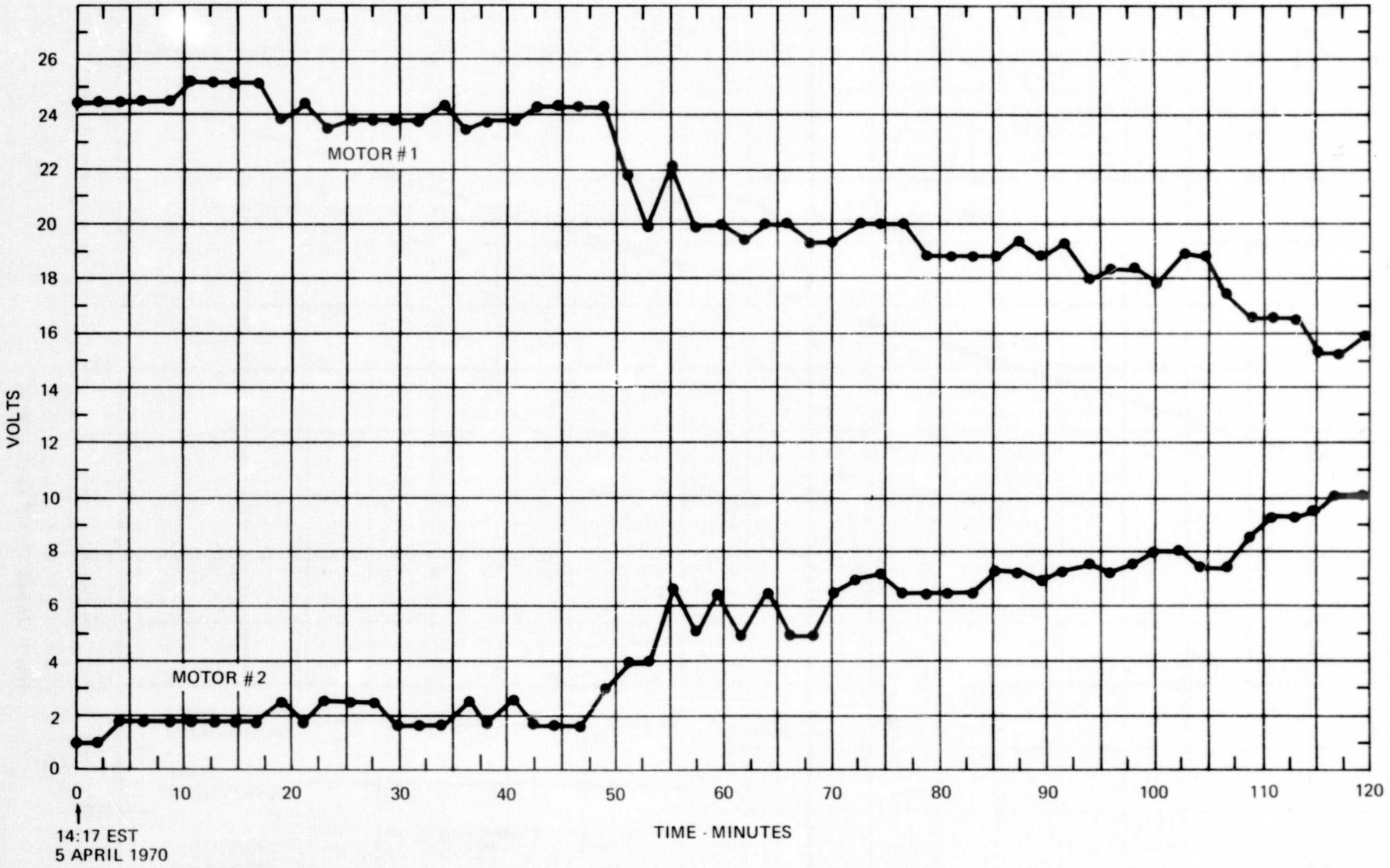

Figure 35. Motor Voltage versus Time

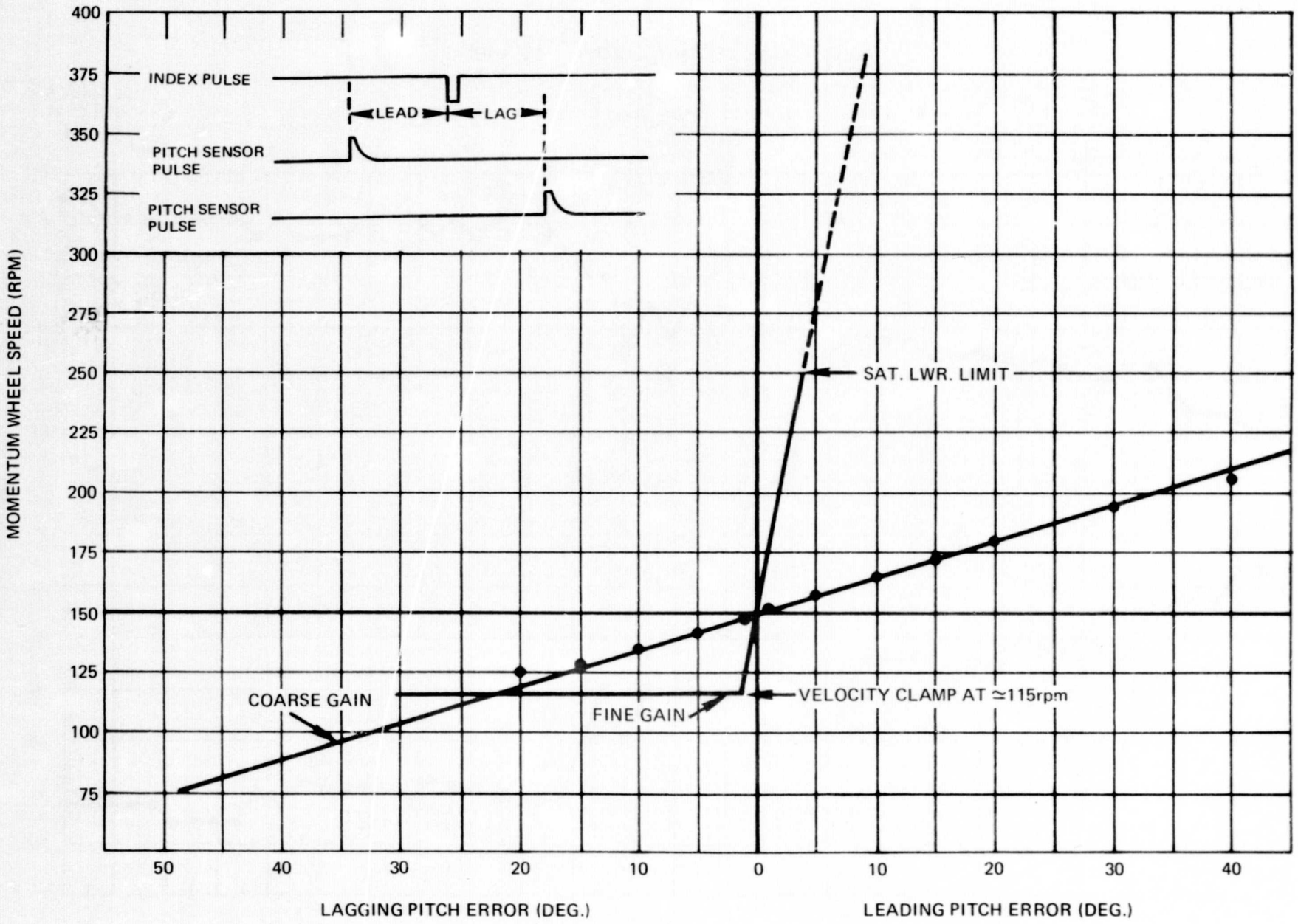

Figure 36. Curves of Nominal Wheelspeed versus Pitch Error

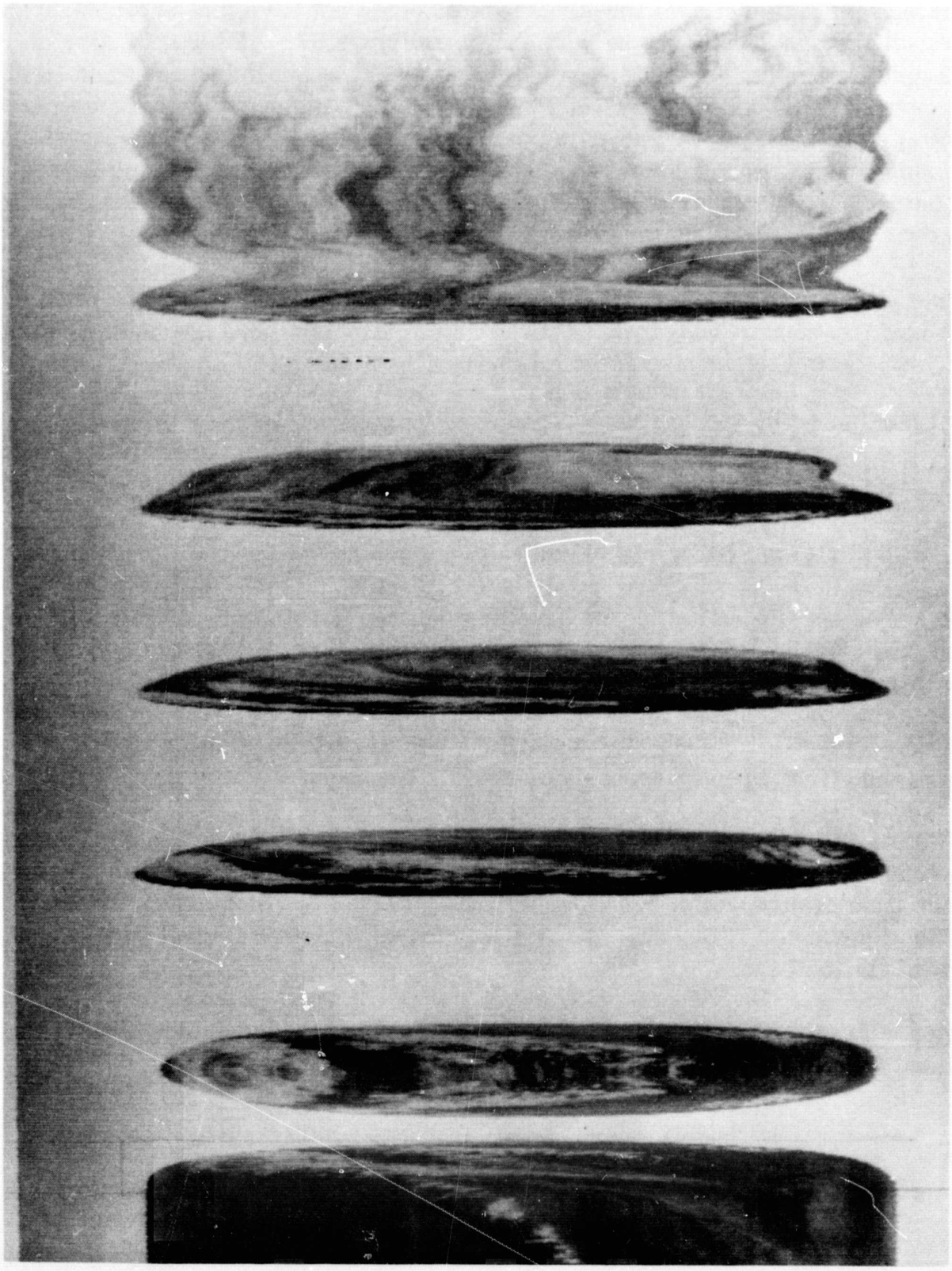

Figure 37. Thirteen-Minute Loss of Pitch-Lock SR Pictures

the satellite a maximum of 0.735 radians, or 42.12 degrees ($\theta = 1/2\ \alpha\ t^2$), showing that the electrical torque generated could not have moved the SR scan lines off the earth in 35 seconds as shown in Figure 37. The exact cause of this disturbance cannot be determined because of the absence of continuous motor current or wheelspeed telemetry; however, the moon could have contributed to the problem during coarse-gain operation. Figure 38 shows the satellite rotations about its pitch axis as wheelspeed and servo gain change from fine to coarse. The SR data (top of Figure 38) show the earth and sky time as seen by the SR.

Power dropout—On orbit 1374, when switching from regulator 1 to 2, pitch and roll horizon-sensor data dropped out for approximately 13.5 seconds. The dropout, not continuous, occurred as follows:

- Four PIP's and no roll-sensor pulses—sensors off for 1.8 sec
- Seven PIP's and roll-sensor pulses—sensors on for 3.2 sec
- Twenty-two PIP's and no roll-sensor pulses—sensors off for 8.5 sec

The sensors are powered by the regulated bus but PIP is not. During this period, the wheelspeed decreased by approximately 21 rpm, but regained speed and mission mode after 13.5 seconds. Investigation shows that the power source causes this performance and that each time the regulators are switched, the attitude sensors drop out, pick up, drop out, and pick up again. Figure 39 shows the effect on wheelspeed of orbit-1374 regulator switching.

TEC data—Plots of motor voltages, calculated motor current, brush wear, bearing temperature, and base-plate temperature from launch on January 23, 1970, to the time of turnover to NOAA on June 15, 1970, are contained in the TOS Evaluation Center (TEC) report. The values were plotted in real time during a ground station pass.

Motor current—The motor current was not on telemetry; therefore, it was calculated as follows:

- *$CEMFm_1 = Vm_1 - Ia_{m1}\ Ra_{m1}$ where:
- $CEMFm_1$ = motor 1 generated voltage when motor 2 was operating

*CEMF = counter electromotive force

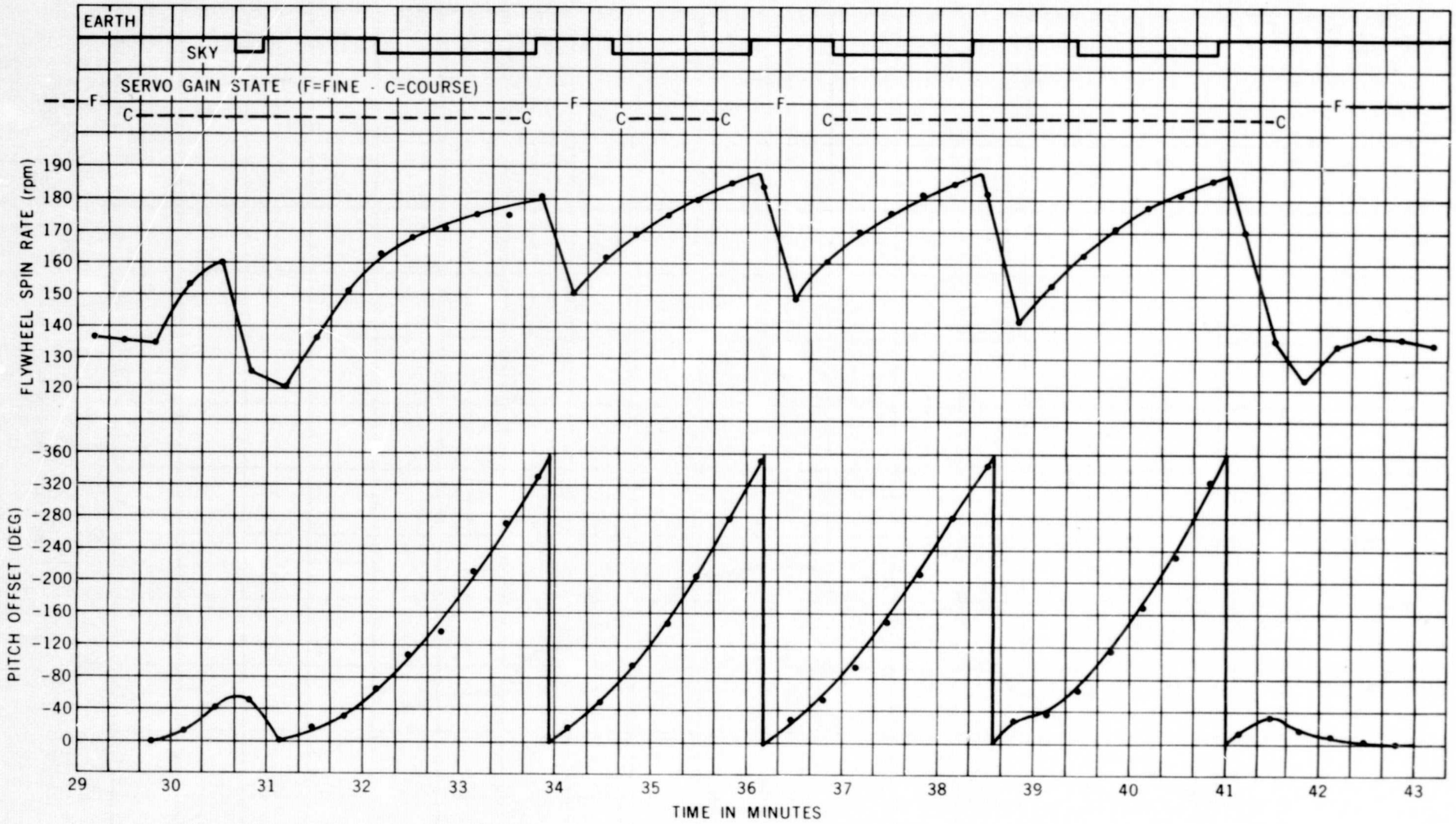

Figure 38. Orbit 1144 Loss of Pitch Lock

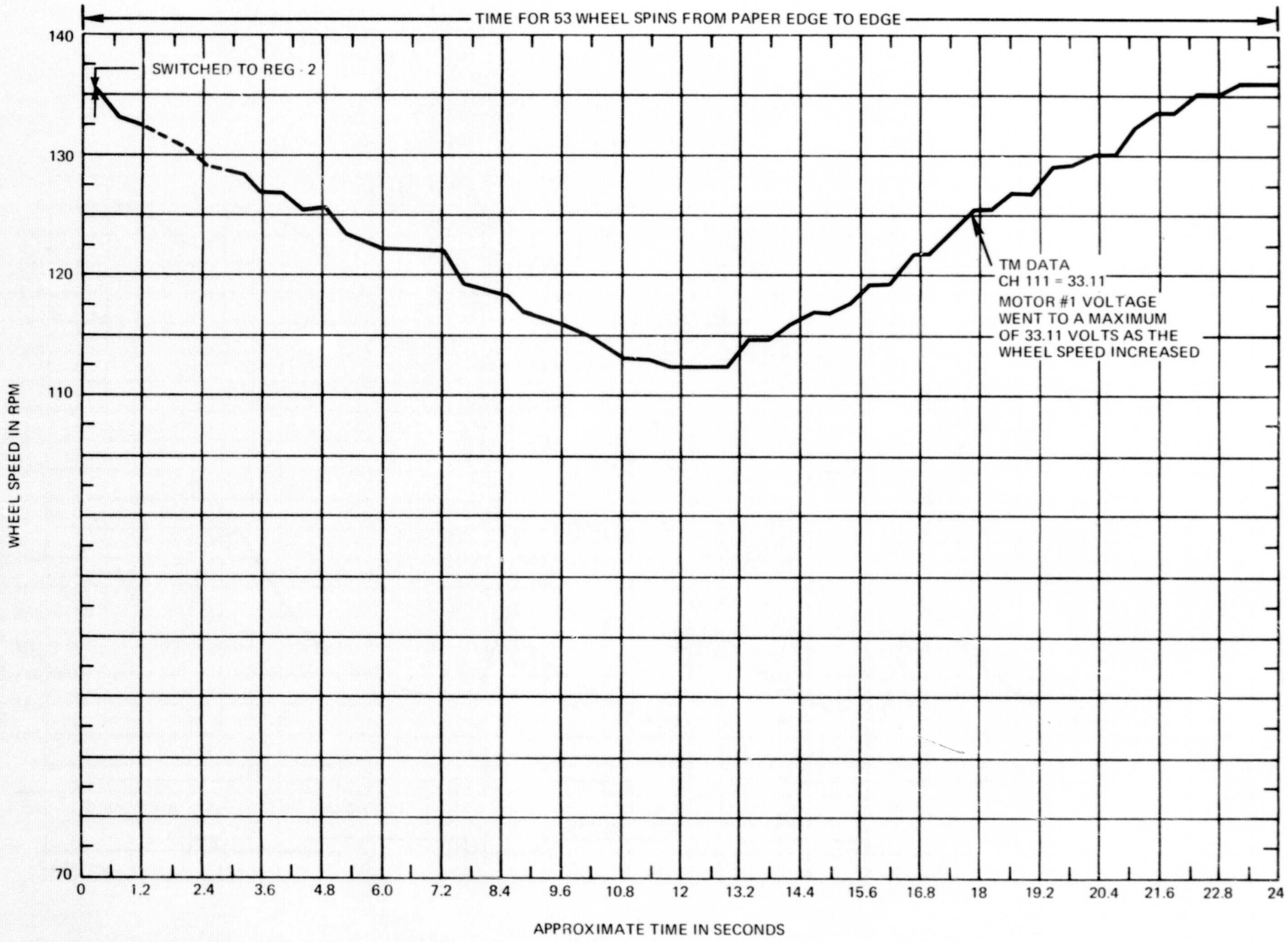

Figure 39. Effect of Regulator Change on Wheelspeed

- Vm_1 = impress voltage to operate motor 1
- Ia_{m1} = current required to operate motor 1
- Ra_{m2} = armature resistance of motor 1

Because of the requirement to reduce wheelspeed, CEMF was obtained from the performance specification which gives CEMF as 0.74 volt per radian per second.

Attitude of satellite—Figure 40 is a polar plot showing typical roll/yaw attitude. Table 15 lists the orbit-by-orbit conditions of the attitude controls. A review

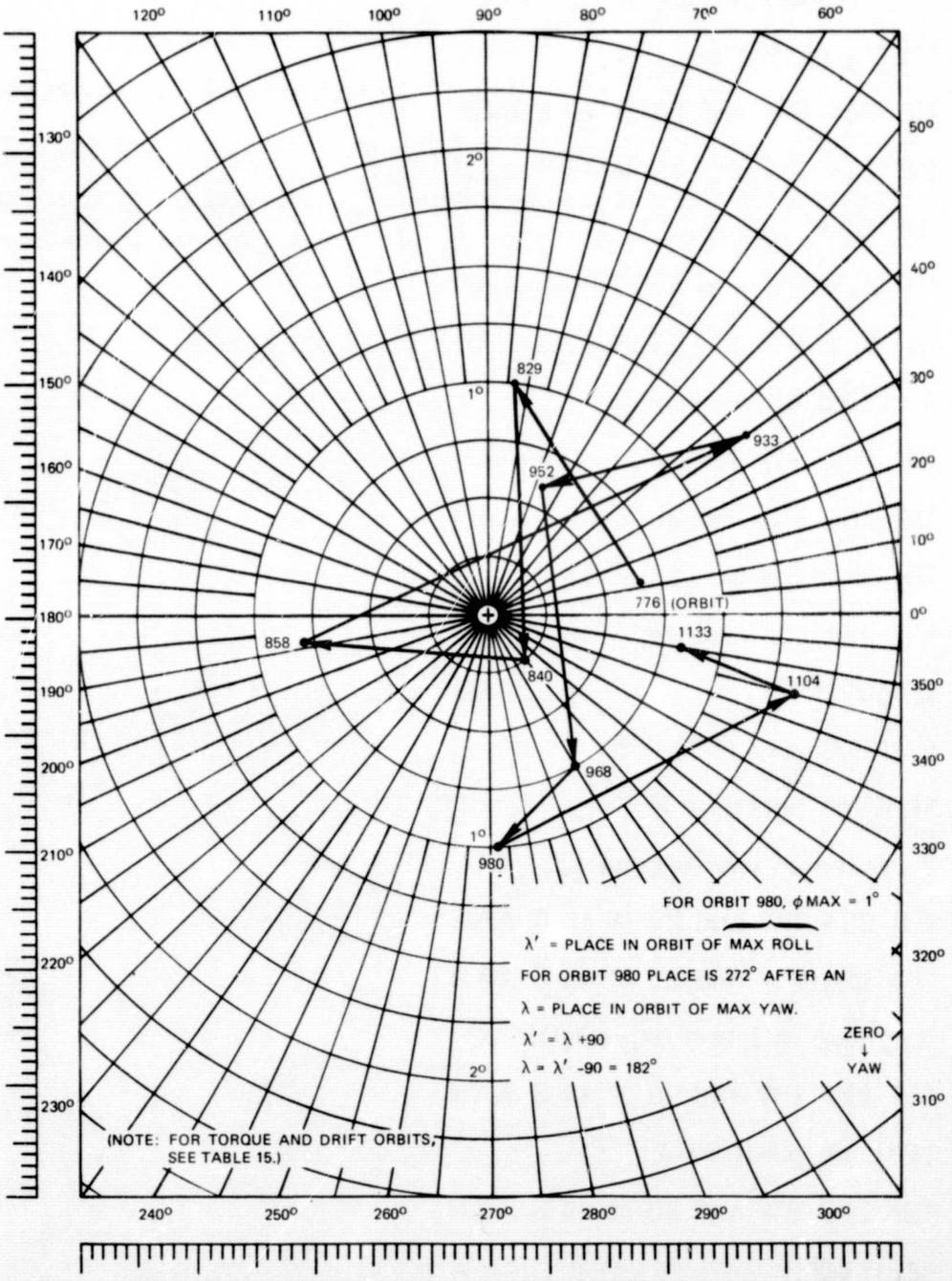

Figure 40. Magnetic-Torque and Drift Effect on Roll Attitude

Table 15

Magnetic Torquing

Orbit	Condition
0002	3 cycles of high-torque QOMAC
0036	5 cycles of low-torque QOMAC
0044	4 cycles of low-torque QOMAC
0073	3 cycles of low backup by MBC
0075	MBC positive 4
0091	UP 224 PW and 20 M 40 S AAN
0092	UP 224 PW and 20 M 40 S AAN
0104	UP OFF
0111	UP 224 PW and 20 M 40 S AAN
0116	UP 224 PW and 20 M 40 S AAN, MBC positive 5
0118	3 cycles of low torque
0124	UP 224 PW and 20 M 40 S AAN
0129	UP 224 PW and 20 M 40 S AAN
0139	UP 224 PW and 20 M 40 S AAN
0154	UP 224 PW and 20 M 40 S AAN
0204	QOMAC off
0217	QOMAC on, MBC off
0233	MBC on positive 5
0245	5 cycles of low-torque QOMAC, MBC off
0255	UP 224 PW and 20 M 40 S AAN
0266	UP 224 PW and 20 M 40 S AAN
0274	4 cycles of low-torque QOMAC
0279	UP 224 PW and 20 M 40 S AAN
0295	MBC on positive 5
0311	UP 208 PW and 20 M 00 S AAN
0399	MBC off

NOTE

UP = unipolar torque
PW = pulsewidth (sec)
AAN = after ascending node
S = sec
M = min

Table 15 (continued)

Orbit	Condition
0402	MBC negative
0415	6 cycles of low-torque QOMAC
0417	MBC positive 3
0420	UP 224 PW and 20 M 40 S AAN
0433	QOMAC off
0467	UP 112 PW and 17 M 51 S AAN
0492	UP 208 PW and 19 M 00 S AAN
0520	MBC off, UP 208 PW and 19 M 00 S AAN
0533	MBC +3, UP 160 PW and 21 M 24 S AAN
0580	UP 160 PW and 21 M 24 S AAN
0592	QOMAC off
0607	UP 144 PW and 21 M AAN, MBC +2
0632	UP 144 PW and 21 M AAN
0668	UP 144 PW and 20 M AAN
0708	UP 144 PW and 19 M AAN
0730	UP 144 PW and 19 M AAN
0781	UP 144 PW and 19 M AAN
0783	MBC off
0829	QOMAC off
0843	UP 128 PW and 18 M AAN
0858	MBC +2
0875	UP 128 PW and 18 M AAN
0917	UP 128 PW and 18 M AAN
0924	UP 128 PW and 18 M AAN
0933	UP 128 PW and 18 M AAN, MBC off
0939	UP 128 PW and 18 M AAN
0949	QOMAC off

Table 15 (continued)

Orbit	Condition
0968	UP 112 PW and 17 M AAN, MBC +1
0980	UP 112 PW and 17 M AAN
1002	UP 112 PW and 17 M AAN
1008	UP 112 PW and 17 M AAN
1046	UP 112 PW and 17 M AAN
1062	UP 112 PW and 17 M AAN
1077	UP 112 PW and 17 M AAN
1091	UP 112 PW and 17 M AAN
1104	MBC negative 1
1106	UP 112 PW and 17 M AAN
1121	UP 112 PW and 17 M AAN
1133	2 cycles of low torque for moon conflict, MBC off
1137	UP 112 PW and 17 M AAN
1162	UP 112 PW and 17 M AAN
1184	UP 112 PW and 17 M AAN
1199	UP 112 PW and 17 M AAN
1211	UP 112 PW and 17 M AAN
1224	UP 112 PW and 17 M AAN
1236	UP 112 PW and 17 M AAN
1249	UP 112 PW and 17 M AAN
1261	UP 112 PW and 17 M AAN
1274	UP 112 PW and 17 M AAN
1288	MBC positive 1
1303	UP 112 PW and 17 M AAN
1318	UP 112 PW and 17 M AAN
1337	UP 112 PW and 17 M AAN
1355	UP 112 PW and 17 M AAN, MBC off

Table 15 (continued)

Orbit	Condition
1375	UP 112 PW and 17 M AAN
1382	MBC on +1
1389	UP 112 PW and 17 M AAN
1405	UP 112 PW and 17 M AAN, 115.2 period
1424	UP 112 PW and 17 M AAN, 115.2 period
1451	UP 112 PW and 17 M AAN, 115.2 period
1481	UP 112 PW and 17 M AAN, 115.2 period
1505	UP 112 PW and 17 M AAN, 115.2 period
1518	UP 112 PW and 17 M AAN, 115.2 period
1534	UP 112 PW and 17 M AAN, 114.9 period
1537	UP 112 PW and 14 M 30 S AAN
1538	UP 112 PW and 14 M 30 S AAN
1543	UP 112 PW and 17 M AAN
1556	UP 112 PW and 17 M AAN
1568	UP 112 PW and 17 M AAN
1587	UP 112 PW and 14 M AAN
1606	UP 112 PW and 17 M AAN
1617	QOMAC off
1625	UP 96 PW and 14 M AAN
1643	UP 96 PW and 14 M AAN
1663	UP 112 PW and 14 M AAN
1684	UP 96 PW and 10 M AAN
1688	UP 96 PW and 16 M AAN, 115.2 period
1705	UP 96 PW and 16 M AAN, 115.2 period
1709	UP 96 PW and 14 M AAN, 114.9 period
1717	UP 96 PW and 14 M AAN
1721	UP 96 PW and 14 M AAN

Table 15 (continued)

Orbit	Condition
1724	UP 96 PW and 14 M AAN
1744	UP 96 PW and 14 M AAN
1755	QOMAC off
1762	MBC negative 1
1775	UP 80 PW and 5 M AAN, error
1784	UP 80 PW and 15 M AAN
1788	UP 80 PW and 15 M AAN, MBC off

of the plot and table gives the required torquing and the maximum roll (phi (ϕ) max), which occurs at lamba prime (λ'), the point of zero yaw. Lambda (λ) is displaced 90 degrees from the point of maximum roll and is the point of maximum yaw. The points of λ and λ' are identified on the polar plot.

CONCLUSIONS

The single-axis capture and momentum interchange have been almost perfectly demonstrated by ITOS 1 in orbit, and in testing before launch.

The inherent gyroscopic stability of ITOS 1 precludes the tumbling hazards of neutral momentum systems and uses the vast experience in magnetic control of the angular momentum vector of spin-stabilized spacecraft. The simplicity of the ITOS-1 system and the redundancy of all critical components form the basis for long operational life expectancy. Environmental tests of MWA and the closed-loop dynamic-suspension testing of the pitch-control system duplicated the respective orbital conditions except for the motor-2 brush wear. Redundancy corrected this problem. Improvements will be incorporated on the MWA by installing heaters to reduce brush wear on the ITOS-A/NOAA-1 satellite. In the future, the use of the brushless motor, an earth-splitting technique using CO_2 sensors, and an active on-board roll-yaw control will provide the optimum in attitude control for ITOS satellites.

REFERENCES

1. TIROS-M Spacecraft (ITOS-1) Final Engineering Report. NAS5-10306-AED R-3318F. April 23, 1970

2. J. E. Keigler. "Precision Attitude Control for the Improved TIROS." Spacecraft Systems Engineering RCA/AED. Princeton, New Jersey

3. ITOS Night-Day Meteorological Satellite. U.S. Government Printing Office, Washington, D.C. TOS Project/Goddard Space Flight Center. Greenbelt, Maryland

4. J. R. Beaird. "TOS Checkout Center ITOS-1 Attitude Control Report January 23, 1970 - June 15, 1970." July 31, 1970

5. Attitude Sensor - Roll Sensor and Pitch Index, Pulse and Pitch Sensor Data from TOS Evaluation Center. Figures 30, 31, and 32

6. Scanning Radiometer Attitude Data from NOAA. Figure 29

7. W. Lindorfer and L. Muhlfelder. "Attitude and Spin Control for TIROS Wheel." RCA/AED. Princeton, New Jersey

8. Harold Perkel. "Stabilite - A Three-Axis Attitude Control System Utilizing a Single Reaction Wheel." RCA/AED. Princeton, New Jersey

9. Flywheel Stabilized Magnetically Torqued Attitude Control System for Meteorological Satellite Study Programs. NAS5-3886. RCA/AED. December 4, 1964